Mega-reservoir regulation: A comparative study on downstream responses of the Yangtze and Yellow rivers

Xiao Wu[1,2]*, Yao Yue[3]*, Alistair G.L. Borthwick[4,5], Louise J. Slater[6], Jaia Syvitski[7], Naishuang Bi[1,2], Zuosheng Yang[1], Houjie Wang[1,2]*

[1] College of Marine Geosciences, Key Laboratory of Submarine Geosciences and Prospecting Technology, Ocean University of China, 238 Songling Road, Qingdao 266100, China

[2] Laboratory for Marine Geology, Qingdao National Laboratory for Marine Science and Technology (QNLM), Qingdao 266061, China

[3] State Key Laboratory of Water Resources Engineering and Management, Wuhan University, Wuhan, 430072, China

[4] Institute for Infrastructure and Environment, School of Engineering, The University of Edinburgh, The King's Buildings, Edinburgh EH9 3JL, UK

[5] School of Engineering, Mathematics and Computing, University of Plymouth, Drake Circus, Plymouth PL4 8AA, UK

[6] School of Geography and the Environment, University of Oxford, Oxford, OX1 3QY, UK

[7] Community Surface Dynamics Modeling System, INSTAAR, University of Colorado, Boulder, CO 80309-0545, USA

***Corresponding author:**

Xiao Wu, Email: wuxiao@ouc.edu.cn, Tel: 86-532-66782950

Yao Yue, Email: yueyao@whu.edu.cn, Tel: 86-027-68772310

Houjie Wang, Email: hjwang@mail.ouc.edu.cn, Tel: 86-532-66782950

Manuscript submitted to *Earth-Science Reviews*

Abstract:

Large reservoirs can considerably alter the water-sediment dynamics and morphology of alluvial rivers. Here we review the effects of two mega reservoirs operated with different regulation modes. The Three Gorges Reservoir (TGR) on the Yangtze River has a typical anti-seasonal regulation mode, while the Xiaolangdi Reservoir (XLDR) on the Yellow River undergoes a swift drawdown process shortly before the flood season through the Water and Sediment Regulation Scheme (WSRS). We examine the influence of these regulation schemes on downstream water-sediment dynamics and find that vast sedimentation occurred in both the TGR (128.4 Mt/yr) and XLDR (210.2 Mt/yr). The two rivers have experienced different changes in downstream sediment transport capacity, with coincident flood and sediment peaks in the Yangtze River but with sediment peaks lagging behind flood flow peaks in the Yellow River. On the Yangtze River, highly unsaturated flows from the TGR led to widespread incision downstream, while on the Yellow River, such flows did not induce significant erosion in the first two years following impoundment. The low annual runoff and high sediment yield of the Yellow River mean that riverbed erosion occurred mainly when the water discharge and sediment transport capacity were enhanced by the WSRS. In both rivers, the riverbed eroded and coarsened downstream of the mega dams, lowering the dry season water level. The increase in channel roughness maintained or even raised flood season water levels, potentially increasing flood risk. Sediment budgets reveal that the river segments downstream of the dams switched from sediment sinks to sources due to riverbed incision. Despite new supply from downstream reaches, sediment deficits arising from dam interception and other human activities within the drainage basins have posed significant challenges to the sustainability of the Yangtze and Yellow river deltas, resulting in lower accumulation rates or even transition from progradation to degradation in subaqueous areas. In contrast to the anti-seasonal regulation mode of the TGR, the WSRS of the XLDR has proven very effective at mitigating reservoir sedimentation and has boosted the quantity of sediment reaching the sea, facilitating delta stability and coastal sediment replenishment.

Keywords: Reservoir regulation; Water-sediment dynamics; Sediment budget; Channel adjustment; Reservoir sedimentation; Delta evolution

Contents

1. Introduction……...4

2. Background……...6

2.1. Overview of the Yangtze and Yellow rivers……..6

2.2. Overview of the Three Gorges Dam and the Xiaolangdi Dam…….……7

2.3. Operation of TGR and XLDR……8

3. Data and Methods……10

3.1. Gauged datasets……...…10

3.2. Reservoir sedimentation……...10

3.3. Channel deposition/erosion…….…10

3.4. Sediment transport capacity of the Yangtze River and the Yellow River……12

4. Sedimentation in, and outflows from, the TGR and the XLDR……13

4.1. Reservoir sedimentation……13

4.2. Outflows from the TGR and the XLDR……..15

5. Reservoir regulation impact on downstream water discharge and sediment transport……..17

5.1. Downstream water transport impacted by reservoir regulation……...17

5.2. Impact of reservoir regulation on downstream sediment delivery……...18

5.3. Changes in downstream sediment transport capacity……..20

6. Impact of reservoir regulation on downstream channel evolution……21

6.1. Channel scouring downstream of the reservoirs……..21

6.2. Coarsening of sediment along the downstream riverbed……24

6.3. Spatial pattern of channel erosion intensity coupled with riverbed coarsening……..25

7. Water level change with modified channel roughness after TGR and XLDR regulation……26

8. Sediment budget of the Yangtze River and the Yellow River affected by regulation of TGR and XLDR……..27

8.1. Sediment budget of the Yangtze River downstream of the TGR……28

8.2. Sediment budget of the Yellow River downstream of the XLDR……...29

9. Delta evolution under the impact of reservoir regulation……...31

9.1. Evolution of the Yangtze River delta after closure of the TGR……...32

9.2. Evolution of the Yellow River delta under impact of the WSRS……34

10. Implications of the TGR and XLDR regulation modes for global reservoirs…….36

10.1. Implication for mitigating reservoir sedimentation……...36

10.2. Implication for flood prevention in the downstream river……38

10.3. Implication for sediment-starved deltas……39

11. Summary and conclusions……40

Acknowledgements……42

Data Availability……..43

References……44

1. Introduction

Rivers play a vital role in the development of human society (Macklin and Lewin, 2015; Wang et al., 2022). Since the emergence of civilization, humans depended on rivers for food, transport, and energy generation (Nicolás Ruiz et al., 2021; Wang et al., 2022). As industry, agriculture, and human population have evolved, anthropogenic demands on river systems have increased, altering fluvial hydrodynamics, biogeochemistry, and river ecology (Kingsford, 2000; Milliman et al., 2009; Fan et al., 2015; Munoz et al., 2018). A better understanding of the complex interactions between human activities and rivers is urgently needed to ensure river sustainability and mitigate the negative impacts of human interference.

Dam construction is one of the most powerful human interventions that can affect a river system by impounding large quantities of water and sediment, fragmenting the system, and altering its hydrodynamics (Best, 2019; Grill et al., 2019; Belletti et al., 2020). By 2020, more than 58,000 large dams (each of height exceeding 15 m) had been constructed, with an estimated cumulative storage capacity of 7000-8300 km^3, accounting for one-sixth of the total annual water discharge to the oceans (Vörösmarty et al., 2003; Chao et al., 2008; Mulligan et al., 2020). Large dams and reservoirs impact on the water-sediment dynamics of their river-estuary continua downstream. Reservoirs homogenize (regulate) intra-year discharge by storing water during wet seasons and releasing it during dry seasons (Poff et al., 2007; Chai et al., 2020). Dams slow down river flow, causing reservoir sedimentations and lowering downstream suspended sediment concentration (Dethier et al., 2022; Syvitski et al., 2022a). The unsaturated outflow tries to achieve a new equilibrium sediment concentration by scouring the downstream riverbed for mobile sediment, thus incising the riverbed (Wang and

116 Kondolf, 2014). Left unchecked, scouring is progressive with its distance lengthening. The
117 effect of reservoirs may even extend to the deltaic area, with the sharp decrease in sediment
118 supply causing erosion of the submerged delta (Syvitski et al., 2009; Yang et al., 2011;
119 Anthony et al., 2014).

120 The most common reservoir regulation mode is anti-seasonal regulation designed for
121 flood control and downstream irrigation (Nishimura et al., 2005). In rivers with high sediment
122 concentration and heavy deposition issues, the regulation mode may be adjusted to maintain
123 reservoir storage capacity and the water-sediment transport capacity of downstream channels
124 (see e.g. Wang et al., 2005). Reservoirs connected to water transfer projects have regulation
125 modes designed according to the downstream water demand curve, an example being
126 Danjiangkou Reservoir, China (Zhang et al., 2009). In more complex river networks, cascade
127 reservoirs are often regulated to achieve multiple objectives across the entire basin (Zhang et
128 al., 2015; Jiang et al., 2022; Xu et al., 2022).

129 Despite the crucial role that reservoir regulation plays in shaping rivers, limited research
130 has examined the response of downstream river-estuary continua to such regulation modes.
131 Notably, the Yangtze River and the Yellow River have undergone intensive regulation after
132 the respective construction of the Three Gorges Reservoir (TGR) and the Xiaolangdi
133 Reservoir (XLDR). The TGR employs an anti-seasonal impoundment strategy, whereas the
134 XLDR prioritizes deposition control in both the reservoir and the downstream channel due to
135 the high suspended sediment content of the river flow. This paper investigates the impacts of
136 the two mega dams on their respective downstream river-estuary systems by analyzing data
137 on water, sediment, and underwater topography, collected before and after reservoir

impoundment. The findings provide valuable guidance for managing river systems and optimizing dam operations.

2. Background

2.1 Overview of the Yangtze and Yellow rivers

The Yangtze and Yellow rivers discharge more than 2.3% of the world's total freshwater and carry approximately 9% of the global sediment load (Yang et al., 2020b; Syvitski et al., 2022a). They originate in the Qinghai-Tibet Plateau and flow eastward until respectively entering the East China Sea and Bohai Sea (Fig. 1a). The Yangtze River basin covers an area of 1.8×10^6 km^2, has a mainstream length of 6,300 km, and supports more than 385 million people. The Yellow River basin covers 0.75×10^6 km^2, has a mainstream length of 5,464 km, and supports 224 million people (Tian and Yang, 2017). The East Asian monsoon dominates climate conditions in both river basins, with more than 70% of annual rainfall occurring in the wet season (Gemmer et al., 2008). However, precipitation is much higher in the Yangtze River basin (1070 mm/yr) than in the Yellow River basin (450 mm/yr), causing the water discharge of the Yangtze River to be several times greater than that of the Yellow River.

The Yangtze River is the 5th largest river worldwide in terms of discharge volume with an average of ~890 km^3/yr, and was 4th largest in terms of sediment load during the 1950s-1980s with an average of ~480 Mt/yr (Milliman and Syvitski, 1992). The Yangtze River basin is divided into upper, middle, and lower sub-basins at Yichang and Hukou, respectively. The upper basin is mountainous, whereas the middle and lower basins consist of vast fluvial flood plains. The mid-lower basin contains three major tributary networks - the Dongting Lake, Hanjiang River and Poyang Lake water systems - that drain into the Yangtze

River (see Fig. S1 in the Supplementary Information). Dongting Lake and Poyang Lake both transport water and act as massive water storage containers that change with the seasonal landscape. Poyang Lake, the largest freshwater lake in China, covers 9% of the Yangtze River basin. It joins the Yangtze at Hukou. Downstream of Hukou, the Yangtze River then flows eastward to the sea without encountering any further large tributaries or lakes.

During the 1950s-1980s, the Yellow River carried on average ~50 km^3 of runoff and over 1,000 Mt of sediment to the sea every year (Milliman and Syvitski, 1992; Wu et al., 2020b). It is divided geomorphologically into three reaches, with divisions at Toudaoguai and Huayuankou (Fig. 1a). The upper and middle reaches generate 55% and 45% of the total runoff in the river basin. However, more than 90% of sediment load comes from the middle reach (Wang et al., 2007) which passes through the highly erodible Loess Plateau, gaining more than 1,200 Mt of sediment load annually. This sediment is heavily deposited in the lower riverbed due to its flat terrain, elevating the channel bed to form an "elevated river" landscape. No large tributaries join the mainstream in the lower reach.

2.2 Overview of the Three Gorges Dam and the Xiaolangdi Dam

The Three Gorges Dam is the world's largest hydroelectric project, with an average annual output of 88.2 billion kW·h. It also acts as a critical water control project, being located on the upper Yangtze River, about 40 km upstream of Yichang. Its crest stands 185 m above mean sea level. The Three Gorges Dam commenced operation in 2003, forming the Three Gorges Reservoir (TGR) with surface area of 1084 km^2 (Guo et al., 2018). The TGR spans 756 km upstream from the dam to Zhutuo, and receives water from several river networks, including the Jialingjiang and Wujiang tributaries (Fig.1b; Tang et al., 2022). It

controls a catchment area of 1.0 $\times 10^6$ km^2, or 56% of the entire Yangtze River basin. At first impoundment in July 2003 the maximum water elevation in the TGR was 135 m. This was later increased to 156 m in October 2006 and 173 m in October 2008 (Li et al., 2021). The water level reached its maximum elevation of 175 m in 2010 and has since fluctuated between 145 m and 175 m (Fig. 1c). The total capacity of the TGR is 39.3 km^3 at its maximum water level of 175 m and includes 22.15 km^3 for flood control.

The Xiaolangdi Dam, completed in October 1999, is a project located on the middle Yellow River, approximately 128 km upstream of Huayuankou (Kong et al., 2022). The dam controls a catchment area of 0.69×10^6 km^2 (about 92% of the Yellow River basin), and was primarily constructed for flood control, ice-jam prevention, and sedimentation reduction, while also providing water supply, irrigation, and power generation (Liang et al., 2016). The Xiaolangdi Reservoir (XLDR) has a surface area of 296 km^2 and extends 130 km upstream from the Dam (Fig. 1d). It has a total capacity of 12.65 km^3 at peak water level of 275 m (Fig. 1e), including 7.55 km^3 for sediment storage, 4.05 km^3 for flood control, and 1.05 km^3 for water and sediment regulation.

2.3 Operation of TGR and XLDR

Operation of the TGR follows an anti-seasonal water-level regulation schedule, whereby water is stored during the flood season and released in the dry season (Bao et al., 2015). This involves (Fig. 2a): a discharge stage (March to May), when the TGR starts to release water stored during the preceding year, causing the water level to drop from 175 m to a minimum of 145 m; a flood control stage (June to September), when the water level is maintained at a low level of 145-160 m; and a storage stage (October to February), during which the TGR retains

204 incoming water, causing the water level to rise gradually to a maximum level of 175 m. By
205 contrast, as shown in Fig. 2b, the water level in the XLDR remains high at between 241 and
206 267 m (near the maximum permitted level of 273 m) from November to the following March.
207 In late March, the XLDR starts to release stored water for downstream irrigation, resulting in
208 an outflow that exceeds the inflow. This causes the water level to decrease gradually until it
209 reaches a low level between 211 and 237 m by July. From late August, the water level rises
210 back until it reaches the maximum permitted elevation by the end of year.

211 The main difference between the regulation modes of the TGR and XLDR is the
212 significant increase in outflow of the XLDR during the pre-flood season, leading to a rapid
213 drop in water level over a short period of 2-3 weeks (from late-June to mid-July, as depicted
214 in Fig. 2b). The Water and Sediment Regulation Scheme (WSRS) of the XLDR consists of
215 separate water and sediment regulation phases. During the water regulation phase (lasting
216 approximately 10 days), clear water (almost free of sediment) is released from the XLDR,
217 mimicking a flood wave of maximum discharge ~4000 m^3/s. This scours the river channel
218 downstream of the dam and maintains the flood control capacity of the XLDR. During the
219 sediment regulation phase which lasts 4-6 days, water retained in the upstream Wanjiazhai
220 and Sanmenxia reservoirs (Fig. 1a) is utilized to expel sediment that would otherwise be
221 deposited in the XLDR, thereby prolonging its working life. The resulting highly turbid water
222 with suspended sediment concentration (SSC) of 60-100 kg/m^3 is then released from the
223 XLDR at a lower water discharge of 2000-3000 m^3/s. Ever since its initiation by the Yellow
224 River Conservancy Committee in July 2002, the WSRS has become a defining feature of
225 anti-seasonal water level regulation in the Yellow River basin, replacing the once natural

seasonal rhythm of water and sediment delivery with impulse events generated by dam-released floods (Wang et al., 2017).

3. Data and Methods

3.1 Gauged datasets

The datasets include long-term daily and yearly hydrographic records from major gauging stations along the Yangtze and Yellow rivers (Table 1). Since 1950, sediment samples and flow discharge data have been collected daily in the Yangtze and Yellow rivers, from which monthly and annual water and sediment fluxes were determined. The resulting hydrographic datasets were released by the Ministry of Water Resources of China and are available from the official websites of the Changjiang Water Resources Commission (CJWRC; http://cjw.gov.cn/) and the Yellow River Conservancy Commission (YRCC; http://www.yrcc.gov.cn/).

3.2 Reservoir sedimentation

Annual reservoir sedimentation in the TGR and XLDR was calculated from sediment fluxes into and out of the reservoirs. Given that the ratio of bed load to total sediment load entering and leaving each the reservoir is very low (0.02-0.3%; Yang et al., 2014), we assume that the suspended load represents total sediment load. The annual and monthly reservoir sedimentation dataset was taken from Liu et al. (2022). Annual and monthly sedimentation estimates for the XLDR were calculated from sediment loads exiting the Sanmenxia Reservoir and the XLDR.

3.3 Channel deposition/erosion

Geomorphological changes to the main channel of the mid-lower Yangtze River and

lower Yellow River have been monitored annually by the CJWRC and YRCC since the 1970s. Based on bathymetric surveys of fixed sections, annual volumes of riverbed change were inferred as follows. Consider the *i*-th reach of a river. The volumetric rate of change of the riverbed material, $\Delta V_{\text{bed-}I}$, (m^3/yr) for a given water or discharge level is approximated by:

$$\Delta V_{\text{bed-}i} = \Delta A_{\text{sectoin-}i} \times I \quad (1)$$

where $\Delta A_{\text{section-I}}$ (m^2/yr) is the annual rate of change of area of the *i*-th cross-section and L_i (m) is the length of the reach. Hence, the total annual rate of change in riverbed material volume, $\Delta V_{\text{bed-}total}$, ($m^3$/yr) for an indicated water level or discharge level is given by:

$$\Delta V_{\text{bed-}total} = \sum_i \Delta V_{\text{bed-I}} \ . \quad (2)$$

Changes in river channel volume have been published annually in bulletins describing the water and sediment load of the Yangtze and Yellow rivers, compiled by the Ministry of Water Resources, China. We calculated sediment deposition/erosion along the river channel by multiplying the volume change by the dry bulk density of sediment (1.3 t/m^3).

For the lower Yellow River, sediment changes induced by channel deposition/erosion were determined using the above method to evaluate the impact of reservoir regulation on channel adjustment. However, the method is not applicable to the mid-lower Yangtze River which has been experiencing heavy in-channel dredging and sand mining activities (Chen et al., 2006). Channel deposition/erosion along the mid-lower Yangtze River was therefore calculated from the following mass balance equation:

$$M_{\text{deposition}} = M_{\text{upstream}} + M_{\text{tributaries}} - M_{\text{downstream}} - M_{\text{outlets}} \quad (3)$$

where $M_{\text{deposition}}$ (t/yr) is the annual mass deposition rate in the river reach; M_{upstream} (t/yr) and $M_{\text{tributaries}}$ (t/yr) are the combined net annual rates of mass sediment influxes from the upstream

section and tributaries; $M_{downstream}$ (t/yr) is the annual mass sediment transport rate in the downstream section; $M_{outlets}$ (t/yr) is the annual mass sediment rate exiting from lateral outlets. Note that a negative value for $M_{deposition}$ indicates erosion. To estimate sediment delivery from small tributaries without gauging stations, we use the sediment transport modulus (i.e., mass sediment yield per unit area of the river basin) of adjacent catchments with similar geographical conditions extracted from the Changjiang Sediment Bulletin (1998-2016).

3.4 Sediment transport capacity of the Yangtze River and the Yellow River

Zhang (1998)'s formula is used to estimate the sediment transport capacity of the Yangtze River:

$$S_* = k_1 \left(\frac{U^3}{gh\,\omega}\right)^{m_1} \quad (4)$$

where S_* is suspended sediment transport capacity (kg/m^3), U is flow velocity averaged over the cross-section (m/s), g is acceleration due to gravity, h is water depth, ω is suspended sediment settling velocity (m/s), and k_1 and m_1 are empirical parameters.

The suspended sediment transport capacity in terms of sediment flux (t/s), Q_*, is given by:

$$Q_* = S_* \cdot Q/1000 \quad (5)$$

where Q is water discharge (m^3/s).

In the lower Yellow River where sediment concentration is extremely high, we adopt the following equation (Zhang and Tu, 2005):

$$Q_* = k_2 \left(\frac{S_{up}}{Q_{up}}\right)^n \left(\frac{BU^4}{\omega_c}\right)^{m_2} \quad (6)$$

where S_{up} is upstream sediment concentration (kg/m^3), Q_{up} is upstream water discharge (m^3/s), B is water surface breadth, ω_c is suspended sediment settling velocity in cluster (m/s), and k_2, n and m_2 are parameters.

4. Sedimentation in, and outflows from, the TGR and the XLDR

Reservoirs trap huge quantities of sediment, reducing global reservoir storage capacity by 0.5-1.0% each year (Kondolf et al., 2014; Schleiss et al., 2016; Patro et al., 2022). Water and sediment efflux from dams is affected by reservoir regulation and sedimentation. Dam interception decelerates the flow of sediment-laden water entering a reservoir reach and reduces sediment-carrying capacity, leading to gradual accumulation of sediment. This results in an annual global economic loss of 13 billion US dollars due to storage loss (Bhattacharyya and Singh, 2019).

4.1 Reservoir sedimentation

4.1.1 Sedimentation in the TGR

From 2003 to 2008, a total of 2617.13 Mt of sediment entered the TGR (Liu et al., 2022), whereas 562.35 Mt of sediment exited the TGR, resulting in net sedimentation of 2054.75 Mt (78.5% of the total sediment input). The annual sedimentation rate in the TGR ranged from 28 Mt/yr to 196 Mt/yr, with a mean of 128.4 Mt/yr (Fig. 3a). This equated to 0.25% loss of TGR storage capacity each year and was dominated by variations in sediment influx to the TGR. From 2003-2012, the sedimentation rate increased from 177 Mt/yr during the initial stage of TGR operation (2003-2005) to 194 Mt/yr during normal operation after 2008. On completion of the Xiangjiaba and Xiluodu reservoirs on the Jinshajiang River in 2013, the mean sediment mass flow entering the TGR decreased from 206.8 Mt/yr during 2003-2012 to 91.6 Mt/yr

312 during 2013-2018 (Fig. 3a). As a result, the mean sedimentation rate during 2013-2018
313 reduced to 75.14 Mt/yr, a decrease of 53.2% compared to the 2003-2012 period. Decreased
314 sediment supply, caused by the upstream cascade of reservoirs, led to a lower observed
315 sedimentation rate in the TGR than originally predicted. However, the observed trapping
316 efficiency (TE, calculated as the ratio of sedimentation to total sediment inflow) during the
317 first decade of TGR operation (2003-2012) was on average 70% higher than predicted (Yang
318 et al., 2014), increasing from 63% in 2003-2005 to 86% in 2008-2012 (Fig. 3a). TE remained
319 relatively high at about 85% during the following 2013-2018 period.

320 About 90% of annual sediment deposition in the TGR occurred during the flood season
321 (Fig. S2a). This seasonality accords with the pattern of sediment influxes, which are highest
322 during the flood season from June to September, dominated by the Asian Monsoon climate
323 (Ren et al., 2021). TE is much higher in the flood season (83%) than in the dry season (76%)
324 (Liu et al., 2022). Intense deposition occurred in the wide valley region below 145 m
325 elevation, making up 90.4% of total sedimentation (Ren et al., 2021) where the longitudinal
326 profile exhibited a disconnected, belt-like deposition pattern (Tang et al., 2021). No deltaic
327 deposition was observed in the first 16 years after impoundment due to the reduced sediment
328 inflow (Liu et al., 2022).

329 4.1.2 Sedimentation in the XLDR

330 From 1999 to 2018, a total of 6121.1 Mt entered and 1916.2 Mt exited the XLDR,
331 leading to net sedimentation of 4205.0 Mt (68.7% of the total sediment input). The annual
332 sedimentation rate in the XLDR ranged from 25 Mt/yr to 687 Mt/yr, with a mean of 210.2
333 Mt/yr during 1999-2018 (Fig. 3b). This sedimentation represents a significant threat to the

XLDR, given the annual loss of storage capacity of 1. 5%. Meanwhile, the annual TE ranged from 5.1% to 100%, with a mean of 78.0%. However, the WSRS reduced the TE from 94.5% (2000-2001, pre-WSRS period) to 76.1% (2002-2018). Since 2002, the WSRS has become the primary tool for managing sedimentation in the XLDR (J. Chen et al., 2012). During 2015-2017, the WSRS ceased operation due to insufficient water storage in the XLDR and so the TE reached a peak of 100% (Fig. 3b), meaning that all sediment entering from the upstream river was trapped behind the dam (Wu et al., 2021a). Excluding these three years, the average TE during the WSRS was 71.0% (Fig. 3b).

Sedimentation in the XLDR, as in the TGR, exhibited significant seasonal variability, with 94% of deposits occurring during the flood season (Fig. S2b). The efficacy of the WSRS in mitigating sedimentation in the XLDR is evident from the monthly distribution of sedimentation which shows that sedimentation during months when the WSRS was in operation was much lower than during other flood months (Fig. S2b). About 95% of reservoir sedimentation occurred within 65 km upstream of the dam. This severe sedimentation caused a shallow deltaic deposit to form, which subsequently prograded downstream towards the dam (Wu et al., 2020a), unlike deposition observed in the TGR.

4.2 Outflows from the TGR and the XLDR

TGR and XLDR hydrographs reveal that peak inflow discharges during the flood season were considerably reduced after reservoir regulations (Fig. 4a,c). Modulation of water levels can reduce outflow by 20,000 m^3/s in the TGR and 3,800 m^3/s in the XLDR. These outflow discharges are generally higher than the inflow discharges during the dry season (Fig. 4a,c), when the reservoirs release stored water to meet downstream water demand. The management

strategy for both reservoirs can be summarized as ‘storing water in the wet season and releasing it in the dry season’. However, operation of the WSRS creates a noticeable difference between the regulation modes of the two reservoirs (Fig. 4).

In late June, the XLDR generates an artificial flood that rapidly increases the peak outflow discharge to ~4000 m^3/s, which is ~3400 m^3/s higher than the corresponding inflow (Fig. 4c). Although the magnitude of such artificial floods is comparable to or even greater than that of natural floods, they start earlier in the year and have a shorter duration. Moreover, the asynchronous delivery of water and sediment during the WSRS differs greatly from the TGR regulation mode (Fig. 4b,d). The two-stage operation of the WSRS results in high outflows with extremely low SSC (usually < 0.01 kg/m^3) during the water regulation period and the release of highly turbid water with reduced river discharge during the sediment regulation period (usually in early July; Fig. 4d). By comparison, the TGR releases exhibit closer correlation between water discharge and SSC (Fig. 4b). Both rivers present declines in sediment outflow and reservoir sedimentation after dam operation, whereas the TE remains relatively stable but fluctuating (Fig. 3). Reservoir sedimentation and sediment outflow mainly depend on sediment inflow (Pearson’s correlation coefficients, r, between sedimentation and inflow in TGR and XLDR are 0.94 and 0.69; r values between sediment outflow and inflow in TGR and XLDR are 0.80 and 0.55, all correlations significant at the 0.01 level). The declines in reservoir sedimentation and sediment outflows in both reservoirs are due to decreasing trend of sediment inflows, caused by cascade reservoirs in the upper Yangtze River (Yan et al., 2021) and large-scale soil-water conservation projects in the upper Yangtze River Basin and the middle Yellow River Basin (Wang et al., 2016; Yue et al., 2016).

5. Reservoir regulation impact on downstream water discharge and sediment transport

5.1 Downstream water transport impacted by reservoir regulation

The modification of outflows from reservoirs affects the hydrology of downstream river reaches (Milliman et al., 2008). After TGR impoundment, the downstream daily water discharge altered significantly (Wang et al., 2020). The anti-seasonal water-level regulation of the TGR led to an average increase of ~2000 m^3/s in daily water discharge from January to April at Yichang, Hankou and Datong, but a decrease of ~6000 m^3/s during July-November (Fig. 5a-c). These changes substantially modified the monthly spatial distributions of water and sediment downstream of the TGR (Fig. S3). Mean runoff during the natural flood season (May-October) at Yichang, Hankou and Datong decreased by 40.5 km^3, 55.1 km^3 and 66.5 km^3, corresponding to an average reduction of 3.8% at these stations, as seasonal runoff became more homogenized in the mid-lower reaches of the Yangtze River (Fig.6a,b; Chai et al., 2020).

Operational times of the WSRS in the Yellow River varied from year to year. Although the WSRS was typically conducted from late June to mid-July, the start and end dates differed greatly (Table S1). For example, the WSRS was implemented between June 19 and July 7 in 2011, but from June 29 to July 9 in 2014. Two WSRS cycles were conducted in 2007 and three in 2010, complicating assessment of their impact on daily flow using average daily discharge data. To examine the effect of the XLDR on downstream daily discharge, we analyze data from 1998 and 2008, during which years the total discharges into the lower river were roughly equivalent. XLDR regulation significantly impacted on the daily water discharge in the Yellow River, as observed at Huayuankou, Gaocun and Lijin stations (Fig.

5d-f). River discharge decreased during the natural flood season (July-October) but increased during the dry season (Fig. 5d-f), controlled by the anti-seasonal regulation of the XLDR. This has led to homogenization of water allocation between flood and dry seasons along the lower Yellow River (Fig. 6c,d; Chai et al., 2020). XLDR regulation also resolved the persistent problem of the lower River drying up (Fig. S3), which had become very severe in the last three decades of the 20th century due to declining precipitation and increased water consumption (Miao et al., 2010). This is evident from hydrological records at Lijin station, where the number of no-flow days was 142 in 1998 but has since fallen to zero due to the XLDR releases in the dry season (Kong et al., 2022). Correspondingly, the contribution of the natural flood season to annual runoff has decreased by 10.9%, from 64.6% to 53.7% (Fig. 6c,d), whereas minimum monthly discharge volumes have increased by 0.1 km^3 at Huayuankou and 0.2 km^3 at Lijin (Fig. S3). Peak discharges at stations downstream of the XLDR exhibited notably different characteristics to those downstream of the TGR, with the former shifted to late June (Fig. 5d-f), at least one month earlier than natural flood events during 1980-1998 (Fig. 6c,d). This shift was due to the artificial release of water in the lower Yellow River, resulting in a slight increase in maximum monthly discharge by 0.1 km^3 at Huayuankou and 0.3 km^3 at Lijin in 2003-2018, compared to the 1990s (Fig. S3). It takes four to six days for the flood wave generated by the WSRS-released water to reach Lijin station located ~800 km downstream of the XLDR (Fig. 5d,f). As a result, the maximum monthly water discharge is observed in late June at Huayuankou and early July at Lijin (Fig. 6c,d).

5.2 Impact of reservoir regulation on downstream sediment delivery

Reservoirs affect sediment delivery by retaining sediment and reducing the amount that

422 reaches the downstream channel (Syvitski et al., 2022a). As shown in Fig. 6a,b, the sediment
423 load at Yichang and Datong has experienced a sharp annual decline since the TGR became
424 operational. Most sedimentation in the TGR occurred during the flood season, accounting for
425 nearly 90% of total annual sediment retention (Fig. S2a) and reducing sediment delivery
426 compared to that in the dry season (Fig. 6a,b). The average sediment load in the flood season
427 decreased by 420.0 Mt at Yichang and 193.5 Mt at Datong, indicating that the influence of the
428 reservoir decreased with downstream distance from the dam. It should be emphasized that
429 these reductions cannot be solely attributed to the dam, given that other environmental factors
430 - such as fluctuations in precipitation, and soil conservation initiatives - have also contributed
431 to the decrease in sediment load (Yang et al., 2014). It is estimated that the TGR was
432 responsible for 79%, 53%, and 44% of the overall sediment reduction at Yichang, Hankou,
433 and Datong stations respectively (Yang et al., 2018). Similar to the TGR, the XLDR also
434 caused a significant decline in sediment load downstream due to sediment interception (Wang
435 et al., 2007). Following initiation of the XLDR operation, the monthly sediment load at
436 Huayuankou and Lijin reduced significantly, particularly during the flood season (Fig. 6c,d).
437 Nonetheless, not all of these reductions can be solely ascribed to the XLDR. By comparing
438 the decrease in sediment load between the pre-dam and post-dam periods at Tongguan Station
439 (~250 km upstream of the XLDR; Fig. 1a) and XLDR, it becomes evident that ~80% of the
440 sediment load decrease in the lower Yellow River is due to natural and anthropogenic factors
441 upstream of the XLDR, such as the water and soil conservation efforts in the Loess Plateau,
442 while the remaining 20% reduction is attributed to the closure of the XLDR.
443 The TGR has resulted in a more uneven pattern of monthly sediment delivery (Li et al.,

2011), with the July-September percentage contribution of sediment load to total annual sediment load increasing by 10.3%. By contrast, operation of the XLDR helped even out the monthly distribution of sediment delivery in the Yellow River (Wu et al., 2021b), decreasing the flood season contribution to annual total sediment delivery from 87.0% in the pre-dam period (1980-1998) to 76.1% in the WSRS decade (2002-2018). The WSRS of the XLDR also caused a shift in the sediment peak in the lower Yellow River from August to July, whereas the maximum sediment load in the middle and lower Yangtze River occurred in July both before and after the dam became operational (Fig. 6).

5.3 Changes in downstream sediment transport capacity

Alternations in the monthly sediment transport patterns of the two rivers can be explained by changes in sediment transport capacity (S_* in kg/m^3, or Q_* in t/s, see Equations 4, 5 and 6), which are determined from the stream energy and the sediment properties. In an idealised river, stream energy can be indicated by the U^3/h parameter in Equation 4, because energy is directly proportional to U^3/h for constant water discharge, cross-section area, water density and g. After the TGR was impounded, U^3/h at Hankou station increased by 11-85% (Fig. 7a), rising faster than the increase in discharge because the stream energy is sensitive to the flow velocity cubed. The difference between the highest and lowest values of U^3/h converged by 73% due to homogenization of the stream energy. However, the value of U^3/h at Huayuankou station of the Yellow River decreased sharply by 69-76% after impoundment of XLDR, with the intra-annual variation being confined within a smaller range.

As mentioned above, Zhang (1998)'s formula (Equation 4), which relates S_* with U^3/h and the sediment settling velocity (ω), is often applied to the Yangtze River. Fig. 7c,d display

466 relative sediment capacity over a typical year. After TGR impoundment, the sediment settling
467 velocity at Hankou station increased by 23% because the median diameter of the suspended
468 sediment was 50% larger than before impoundment (Lai et al., 2017). As a result, Q_{*r}
469 decreased by 2-38% from June to November at Hankou, whereas Q_{*r} increased by 2-33%
470 from December to May due to amplification of U^3/h (49-84%). In the Yellow River, the
471 sediment transport capacity, Q_{*r}, is linked to U^3/H, ω, and the ratio of upstream sediment
472 concentration to water discharge (S_{up}/Q_{up}, in kg·s/m^6, see Equation 6). Fig. 7d demonstrates
473 that after XLDR impoundment, Q_{*r} decreased by 59-86% throughout the year, owing to the
474 substantial decrease in U^3/h. Nonetheless, the Q_{*r} peak appeared in July, one month later than
475 the U^3/h peak after reservoir regulation (because ω in July was 27% smaller than in June).
476 The relatively slower settling velocity in July can be explained by higher SSC which hinders
477 sediment particles from falling. In both rivers, the monthly sediment transport follows
478 changes in monthly sediment transport capacity, indicating that sediment transport capacity
479 controls the sediment transport processes.

480 **6. Impact of reservoir regulation on downstream channel evolution**

481 **6.1 Channel scouring downstream of the reservoirs**

482 Fluctuations in river flow regime and sediment dynamics caused by the operation of
483 reservoirs can greatly alter erosion and accumulation processes in the downstream channel
484 (Graf, 2006; Słowik et al., 2018). Although the main channel of the mid-lower reaches of the
485 Yangtze experienced visible deposition from 1980 to 2002 (Yang et al., 2014), once operation
486 of the TGR commenced in 2003, the main channel downstream of the TGR started to erode,
487 with an average annual erosion rate of 61 Mt/yr (Fig. 8a). Sediment load entering the middle

488 reach of the Yangtze declined from 461.4 Mt/yr in the pre-dam era to 35.7 Mt/yr (or by 92.3%)
489 after impoundment of the TGR. This decrease, combined with changes in water inflow, has
490 resulted in long-distance cumulative scouring along 954.4 km downstream of the TGR (Dai
491 and Liu, 2013; Lai et al., 2017; Yang et al., 2022).

492 This long-distance riverbed erosion of the Yangtze River can be explained by the sharp
493 decrease in sediment concentration (Fig. 8a) that occurred as water flow became starved of
494 sediment due to operation of the TGR, despite relatively small changes in sediment transport
495 capacity (Fig. 7c). Channel erosion was most severe near the TGR and decreased with
496 increasing downstream distance (Yang et al., 2011; Dai and Liu, 2013). The scouring intensity
497 along the ~500 km reach between Yichang and Luoshan (9.05×10^4 t/km/yr) was two to three
498 times higher than in the Luoshan-Datong reach (Yang et al., 2023b). The riverbed incised by
499 an average of ~3.7 m from Yichang to Zhicheng, less than 1.0 m from Jianli to Hankou, and
500 ~0.1 m between Hankou and Datong (Lai et al., 2017), i.e., decreasing progressively with
501 downstream distance from the dam. It should be noted that sand mining and dredging also
502 contributed to lowering the riverbed, but this effect was not included in the estimation of
503 sediment equilibrium in the lateral direction (i.e., Equation 3).

504 After the Yellow River flows through the Loess Plateau, its lower reach is perhaps the
505 muddiest large river in the world (Milliman and Meade, 1983). The high sediment load and
506 gentle slope of the lower Yellow River result in significant deposition on its riverbed. Siltation
507 and artificial levees have also elevated the riverbed, creating perched channels that are 5-8 m
508 higher than the surrounding plains (Y. Chen et al., 2012). Before construction of the XLDR,
509 annual siltation in the lower reach of the Yellow River was estimated to be 77.6×10^6 m^3/yr

from 1980 to 1998, equivalent to 100.9 Mt of sediment (with dry bulk density taken as 1300 kg/m^3; Fig. 8b). In the first two years of the XLDR's operation, before implementation of the WSRS, the lower Yellow River was roughly in an equilibrium state. However, after initiation of the WSRS in 2002, channel scouring rapidly increased, with mean annual erosion of 119.1 Mt/yr (Fig. 8b). Consequently, a total of over 2000 Mt of extra sediment was eroded from the lower riverbed, turning the lower Yellow River from a sediment sink that trapped over 100 Mt/yr to a sediment source of ~120 Mt/yr after the WSRS operation (Fig. 8b). Similar to the mid-lower Yangtze River, the scouring intensity decreased downstream along the main stem of the Yellow River from 34 $\times 10^4$ t /km/yr in the XLDR-Gaocun channel reach to 15 $\times 10^4$ t /km/yr in the Gaocun-Aishan channel reach, and dropped further to 9 $\times 10^4$ t /km/yr between Aishan and Lijin (Bi et al., 2019).

Unlike the TGR, impoundment of the XLDR did not significantly induce channel erosion before the WSRS was initiated. As shown in Fig. 8b, although the SSC of water discharging into the lower Yellow River greatly decreased by 85.8% as soon as the XLDR was impounded, no obvious channel erosion occurred in the first two years of XLDR's operation. During this period, the water energy and sediment transport capacity also decreased significantly (Fig. 9c). Correspondingly, the river channel's capacity continued to decrease in 1999 and 2000 (Fig. 9b), suggesting that the anti-seasonal operation mode of the XLDR did not result in riverbed scouring in the first two years of dam operation. After implementation of the WSRS, the water energy and sediment transport capacity of the bankfull water discharge in the flood season increased by a factor of about three (Fig. 9c), resulting in significant erosion of 129.4 Mt and 294.8 Mt in 2002 and 2003 (Fig. 8b). This led to recovery

of the cross-sectional bankfull area and corresponding bankfull discharge, which reached 82.0% and 83.8% of the 1980s levels, respectively, and a subsequent increase in river channel capacity for discharging water (Fig. 9).

6.2 Coarsening of sediment along the downstream riverbed

Along with channel adjustment, an erodible riverbed downstream of a reservoir is likely to become coarser due to the selective entrainment of relatively fine particles (Brandt, 2000). Fig. 10a demonstrates that this trend has emerged in the mid-lower Yangtze River since operation of the TGR began. The greatest coarsening was observed in the first ~80 km reach downstream of Yichang (Lai et al., 2017; Zhang et al., 2017). The riverbed sediment shifted from mostly sand-sized to predominately gravel-sized particles each of diameter exceeding 30 mm (Yang et al., 2022). This gravel-sand transition appears to have migrated ~70 km downstream by 2021, coinciding with the largest channel incision. Between 100 km and 400 km downstream of Yichang, the bedload coarsened, with the degree of coarsening decreasing progressively with distance downstream (Yang et al., 2023b). The main stem more than 400 km downstream from Yichang presented an overall coarsening trend, superimposed with alternating coarsening and fining (Fig. 10a). Similarly, continuous erosion of the riverbed downstream of the XLDR has led to a coarsening trend in sediment due to removal of fine particles (Wang et al., 2017). After 1999, the main stem of the Yellow River downstream of the XLDR exhibited an overall coarsening trend, with the percentage of fractions finer than 50 μm decreasing at key locations along the river (Cheng et al., 2022). The median grain size of bed sediment increased by a factor ranging from 2 to 5 in the downstream river segments (Fig. 10b). Riverbed sediment near the XLDR was particularly affected by pronounced

554 coarsening, with the median grain size increasing from 0.05 mm to 0.15 mm between 2002
555 and 2019 (Fig. 10b). As with the mid-lower Yangtze River, the degree of coarsening has
556 decreased with downstream distance along the lower Yellow River.

557 **6.3 Spatial pattern of channel erosion intensity coupled with riverbed coarsening**

558 Despite coarsening of riverbed sediment in the mid-lower Yangtze River, the rate of
559 channel erosion has remained relatively high, indicating that armoring was insufficient to
560 reduce erosion over the past two decades (Deng et al., 2022). Due to spatial variations in
561 coarsening, the hotspot of bed scour shifted downstream (Lai et al., 2017). The overall erosion
562 intensity between Yichang and Datong remained relatively stable at about 5.3 $\times 10^4$ t /km/yr
563 allowing for some fluctuation (Fig. 11a). However, erosion intensity in the Yichang-Luoshan
564 reach gradually decreased from 11.5 $\times 10^4$ t /km/yr in 2003 to 9.1 $\times 10^4$ t /km/yr in 2018 (Fig.
565 11a), due to continuous coarsening of the riverbed from sand to gravel to pebbles. Meanwhile,
566 erosion intensity along the channel between Luoshan and Datong increased from ~1.4 $\times 10^4$ t
567 /km/yr to 3.8 $\times 10^4$ t /km/yr (Fig. 11a). This was due to reducing sediment concentration
568 during 2003-2018 (Fig. 8a) and the increasingly unsaturated river flow (Yang et al., 2023b).

569 The lower Yellow River developed an armored riverbed because of coarsening of its
570 sediment through channel erosion (Miao et al., 2016; Wang et al., 2017). The WSRS-released
571 flood discharges, which were generally controlled below 4000 m^3/s for flood security
572 purposes, made it increasingly difficult for the lower reach to experience erosion (Wu et al.,
573 2020a). As shown in Fig. 11b, the erosion intensity of the lower Yellow River exhibited a
574 generally decreasing trend after 2003. During the first six years of the WSRS operation, the
575 erosion intensity was 85.6 $\times 10^4$ t/km/yr. However, from 2008 to 2018, the erosion intensity

decreased by nearly half to 43.3 $\times 10^4$ t /km/yr. Similarly, the erosion efficiency, defined as the ratio of eroded sediment volume to water discharge volume, also decreased significantly from 6.0 to 2.7 due to coarsening of the riverbed sediment (Cheng et al., 2022).

7. Water level change with modified roughness after TGR and XLDR regulation

The response pattern of water level to discharge alters following modification of river channels due to the impoundment of large reservoirs (Brandt, 2000; Pinter et al., 2008; Munoz et al., 2018). Such changes have significant implications for flood control, navigation, and riverine ecology. During the 2003-2016 period, the water level corresponding to low water discharge decreased along the mid-lower Yangtze River, while the flood water level increased, for the same discharge magnitude (Fig. 12).

For example, at Yichang station (where the Yangtze River had a typical low discharge of 6,190 m^3/s), the water level decreased by 4.98 cm/yr during the 2003-2016 period, whereas the flood water level increased by 0.42 m with a discharge magnitude of 46,500 m^3/s. This decrease in water level observed at low discharge was primarily caused by channel erosion (Fig. 8a). Yang et al. (2017) estimated that the part of channel below bankfull water level accounted for 73.2-96.4% of total erosion, whereas the part above bankfull water level experienced little erosion, or even deposition. The rise in flood water level was mainly due to increases in riverbed roughness and floodplain vegetation (Li et al., 2020; Chai et al., 2021). Riverbed incision from 2002 to 2012 caused the median value of the Manning roughness coefficient of the main channel to increase by 21.4% (Fig. 13a). The amplification ratio of Manning's roughness coefficient, defined as the ratio of the pre-impoundment Manning coefficient to that afterwards, was found to grow with increasing discharge magnitude (Fig.

13), causing a more rapid increase in bed roughness during the flood season that led to higher flood water levels. Moreover, the Normalized Difference Vegetation Index (NDVI) of floodplains along the mid-lower Yangtze River increased by 4.4-31.2% over the past decade (Hu et al., 2022). This growth in floodplain vegetation contributed to further increase in the Manning roughness coefficient when the water level was above bankfull stage, and thus affected the conveyance efficiency of the system, reducing flow velocities and raising water levels (Li et al., 2020).

The response pattern of water level to discharge in the lower Yellow River is similar to that in the mid-lower Yangtze River (Fig. 12d and e). With channel erosion induced by the WSRS, the water level decreased significantly at low discharge magnitude. For example, the water levels at Huayuankou and Lijin stations in 2018 for a discharge of 2,000 m^3/s were respectively 1.8 m and 1.3 m lower than in 1981. Dam-induced riverbed incision and coarsening established large dune fields in the lower Yellow River, ultimately changing its roughness structure, flow resistance, and depth (Fig. 13b; J. Chen et al., 2012; Ma et al., 2022). This caused the flood water level to increase by at least 0.4 m for a discharge of >3,800 m^3/s at Lijin station (determined from empirical equations fitted to the curves in Fig. 12e). Although flood flows exceeding 4,000 m^3/s were relatively rare due to reservoir regulation, they nevertheless occasionally occurred. For example, heavy rainfall in October 2021 produced a flood discharge event of over 5,000 m^3/s that lasted for nearly four weeks. In short, the variation in high water level has increased flood pressure in the lower Yellow River, and requires immediate attention.

8. Sediment budget of the Yangtze River and the Yellow River affected by regulation of

620 **TGR and XLDR**

621 Sediment budgets provide a quantitative assessment of the spatiotemporal distribution of
622 sediment sources, sinks, and fluxes within a specific region and time period (Slaymaker,
623 2003). Sediment budget analysis has usually focused on suspended riverine particles, because
624 data are limited on dissolved load and bedload (Richards, 1982). The sediment budget offers a
625 useful tool by which to study the effect of human interventions in drainage basins (Kesel et al.,
626 1992; López-Tarazón et al., 2012). Previous studies have shown that the interception of
627 sediment by reservoirs and the release of sediment-free water from dams can significantly
628 alter the sediment budget of dammed rivers (Kondolf, 1997; Warrick et al., 2015; Piqué et al.,
629 2017).

630 **8.1 Sediment budget of the Yangtze River downstream of the TGR**

631 Following Yang et al. (2014), we conducted a source-to-sink sediment budget for the
632 Yangtze River basin in three periods: 1950-1980 and 1981-2002 (pre-TGR construction), and
633 2003-2018 (post-TGR impoundment). Before TGR construction, sediment from the upper
634 reaches through Zhutuo Station remained steady (300 Mt/yr during 1956-1980 and 312 Mt/yr
635 during 1981-2002). However, sediment supplied by surrounding tributaries to the mainstream
636 decreased from 233 Mt/yr to 138 Mt/yr (Fig. 14a,b). During 1956-1980 and 1981-2002, totals
637 of 517 Mt/yr and 447 Mt/yr of sediment were discharged into the middle Yangtze River, while
638 the Zhutuo-Yichang section transformed from a heavily depositional area of 17 Mt/yr to a
639 weak sediment sink of only 3 Mt/yr. Deposition rates also decreased along the river channel
640 between Yichang and Hankou (from 70 Mt/yr to 57 Mt/yr) and in Dongting Lake (from 142
641 Mt/yr to 83 Mt/yr) during the pre-TGR periods. With the mean sediment load passing through

642 Datong Station to the sea decreasing from 469 Mt/yr to 372 Mt/yr in the pre-TGR periods, the
643 lower reach switched from being a sediment source of 14 Mt/yr to a weak sediment sink of 3
644 Mt/yr (Fig. 14a,b).

645 Due to the construction of upstream cascade reservoirs and implementation of
646 soil-conservation practices, the sediment supply to the TGR region through Zhutuo Station
647 decreased to 121 Mt/yr (Yang et al., 2014; Liu et al., 2022). Sediment replenishment from the
648 tributaries in the TGR also declined by 62%, to 70 Mt/yr (Fig. 14c). Meanwhile, the TGR
649 effectively trapped an average of 128 Mt/yr of sediment. As a result, sediment discharged into
650 the middle Yangtze River through Yichang Station dramatically decreased from 447 Mt/yr to
651 36 Mt/yr. Due to dam-induced channel scouring, the Yichang-Datong river reach changed
652 from a sediment sink to a sediment source (Deng et al., 2022), supplying an average of 41 Mt
653 of sediment per year. Meanwhile, the deposition rate in Dongting Lake decreased from 83
654 Mt/yr to 2 Mt/yr. These changes have caused the sediment discharge from the Datong to the
655 sea to decline by 64%, to 133 Mt/yr after impoundment of the TGR (Fig. 14c).

656 **8.2 Sediment budget of the Yellow River downstream of the XLDR**

657 Prior to construction of the XLDR, the Sanmenxia Reservoir discharged an average of
658 826 Mt/yr of sediment from 1980 to 1993. Most of this sediment (97%) was transported
659 downstream, with only a small portion (3%, 28Mt/yr) being deposited between Sanmenxia
660 Reservoir and XLDR (Fig. 15a). Two minor tributaries downstream of XLDR, the Qinhe and
661 Yiluohe, discharged into the main stem and supplied sediment at rates of 2 Mt/yr and 5 Mt/yr,
662 respectively. Along the river channel, sediment accumulation was 62 Mt/yr between XLDR
663 and Huayuankou and 66 Mt/yr downstream of Huayuankou (Fig. 15a). Water abstraction in

664 the lower reach led to a loss of 16% of sediment passing Huayuankou. Hence, the total annual
665 sediment delivery from the Yellow River to the sea, measured at Lijin station, was 571 Mt/yr
666 before the XLDR was built (Fig. 15a).

667 The sediment load passing the Sanmenxia Reservoir declined by 57% to 326 Mt/yr after
668 construction of the XLDR but prior to implementation of the WSRS (2000-2001). This
669 decrease has been attributed to the construction of upstream reservoirs and implementation of
670 soil-conservation practices in the Loess Plateau (Wang et al., 2007). Almost 95% of the
671 sediment load passing the Sanmenxia Reservoir was trapped by the XLDR, leading to a
672 significant reduction in sediment input to the downstream river channel. From 2000 to 2001, a
673 mere 17 Mt/yr of sediment escaped the dam (Fig. 15b). Correspondingly, the sediment load
674 greatly declined to 75 Mt/yr at Huayuankou. The decreased sediment supply caused the river
675 channel downstream of the XLDR to transition from a sediment sink to a sediment source
676 (Fig. 8b). An estimated 46 Mt/yr of sediment was eroded from the river channel in the
677 XLDR-Huayuankou reach and 22 Mt/yr downstream of Huayuankou. During this period, the
678 sediment load to the sea declined to 18 Mt/yr, a mere 3% of the pre-XLDR level (Fig. 15b).

679 After implementation of the WSRS in 2002, sediment input from the Sanmenxia
680 Reservoir to the XLDR further decreased to 292 Mt/yr (Fig. 15c). However, the WSRS
681 alleviated the severe sedimentation issue in the XLDR. Due to sediment flushing as part of
682 the regulation process, the trapping efficiency of the XLDR then decreased from 95% to 71%
683 (Fig. 3b). Unlike the decline in sediment input from the Sanmenxia Reservoir, the sediment
684 load passing the XLDR rebounded to 85 Mt/yr. Intensified riverbed scouring caused by
685 sediment-free flood water releases during water regulation resulted in an increase in channel

686 erosion downstream of the XLDR, yielding an average erosion rate of 136 Mt/yr (17 Mt/yr
687 between XLDR and Huayuankou and 119 Mt/yr downstream of Huayuankou), equating to a
688 total of 2317 Mt from 2002 to 2018 (Fig. 15c). Downstream channel erosion now provides a
689 major source of sediment from the Yellow River to the sea, outpacing the supply from the
690 upstream Loess Plateau. Therefore, the WSRS significantly boosted the Yellow River's
691 sediment in two ways: (1) reservoir flushing during the Sediment Regulation Period alleviated
692 the sedimentation issue in the XLDR, leading to more sediment transported to the lower
693 Yellow River than expected; (2) artificial flood releases during the Water Regulation Period
694 scoured over 100 Mt/yr along the lower Yellow River to the sea. As a result of the WSRS
695 implementation, the sediment load to the sea through Lijin station increased to 137 Mt/yr, a
696 remarkable 8-fold increase from the pre-WSRS era (2000-2001).

697 **9. Delta evolution under the impact of reservoir regulation**

698 As rivers enter the sea, vast masses of sediment accumulate, forming various types of
699 marine deltas (Wright, 1977). Such deltas are among the most consequential landforms in
700 terms of ecosystem services and societal utility, and nourish more than half a billion people
701 through providing fertile soil and abundant natural resources (Giosan et al., 2014; Syvitski et
702 al., 2022b). Because deltas lie at the interface between rivers and oceans, they are highly
703 dynamic systems controlled by both fluvial and marine processes (Day and Giosan, 2008).
704 Delta progradation can only occur when the river-borne sediment supply is both robust and
705 sustained in order to replenish sediment loss induced by ocean energy and maintain deltaic
706 landforms (Stanley and Warne, 1993; Kim et al., 2009; Anthony et al., 2014; Syvitski et al.,
707 2022b). Owing to sediment deficits caused by dam interception and other human activities,

708 many of the world's deltas have transitioned from progradation to degradation over the past
709 few decades (Blum and Roberts, 2009; Syvitski et al., 2009; Brown and Nicholls, 2015).

710 **9.1 Evolution of the Yangtze River delta after closure of the TGR**

711 The Yangtze River delta, situated on the west coast of the East China Sea, is a
712 funnel-shaped depositional system that formed because of the abundant fluvial sediment
713 supply over the past 5000 years (Hori et al., 2001). Today, the Yangtze delta supports 8% of
714 China's population and contributes to 15% of China's gross domestic product (Xu et al.,
715 2014). Given that the construction of the Yangtze River Economic Belt is one of China's
716 national strategies, the sustainable development of the Yangtze River delta has received
717 considerable attention. As a result, several large-scale engineering projects have been
718 undertaken in recent decades within the Yangtze River mouth to maintain its geomorphologic
719 stability (Luan et al., 2016). These projects have caused significant changes to the estuarine
720 circulation and sediment dynamics, complicating the spatiotemporal evolution of the Yangtze
721 River delta (Dai et al., 2013; Jiang et al., 2013; Luan et al., 2021). Nevertheless, many
722 attempts have been made to identify how the deltaic morphology has responded to the closure
723 of the TGR (e.g., Yang et al., 2011; López-Tarazón et al., 2012; Dai et al., 2014; Luo et al.,
724 2017).

725 The sediment load from the Yangtze River to the sea declined from 372 Mt/yr in the
726 pre-TGR period to 133 Mt/yr in the post-TGR period (Fig. 14), leading to concern that the
727 delta would retreat. Nevertheless, the shoreline of the delta has continued to accrete seaward
728 (Yang et al., 2020a; Leonardi et al., 2021; Yang et al., 2021). For example, the seaward edge
729 of the low marsh area in Eastern Chongming Island, a major component of the subaerial

Yangtze River delta, has advanced seaward at an average rate of 44 m/yr, resulting in an increase in marsh area of 1.8 km^2/yr over the past decade (Fig. 16a). Engineering projects, such as jetties and perpendicular dikes in the Yangtze River estuary, have played a critical role in protecting the subaerial delta (Luan et al., 2016). In eastern Chongming, the seawalls have been relocated 10 km offshore during the past few decades, effectively preventing the subaerial delta from being submerged. Moreover, sediment supply from delta-front and pro-delta erosion has helped maintain the subaerial delta through estuarine regime adjustment (Wei et al., 2019). Engineering projects, such as land reclamation activities in the estuary, along with sea-level rise have also increased both the tidal range and tidal prism, reinforcing sediment supply from subaqueous delta erosion to the intertidal zone (Yang et al., 2020a). Leonardi et al. (2021) concluded that 90% of the deposition in the marsh areas could be attributed to sediment supply from the subaqueous delta and ocean zone. In the landward direction, sediment transport is mainly influenced by tidal pumping, significantly increasing sediment concentration in the estuarine turbidity maximum zone (Zhu et al., 2022). This, in turn, enhances onshore sediment transport, particularly during spring tide (Song et al., 2013; Teng et al., 2022).

In the early years following the impoundment of the TGR, the Yangtze subaqueous delta also experienced a net accumulation period (Fig. 16b; Dai et al., 2014). Luan et al. (2021) concluded that this net accumulation was due to the construction of training walls in the Yangtze River mouth bar area, which attenuated the local hydrodynamics causing sediment to accumulate in groyne-sheltered areas and their surroundings. Additionally, the anti-seasonal regulation mode of the TGR has dampened peak flows in the Yangtze River (Figs. 5 and S3),

752 thus weakening river momentum and enabling sediment to accumulate in the nearshore area
753 instead of being discharged into the coastal sea (Zhu et al., 2020). However, as the supply of
754 riverine sediment continued to decrease, the Yangtze subaqueous delta became increasingly
755 starved of sediment (Luo et al., 2017). Analysis of sediment transport data from the Yangtze
756 River delta clearly demonstrates the profound changes in delta evolution that have been
757 triggered by the TGR. Prior to the closure of the TGR, the Yangtze River delivered 372 Mt of
758 sediment to the sea annually (Fig. 14b). Simultaneously, approximately 300 Mt/yr of sediment
759 was carried away from the deltaic area by southward longshore currents, primarily during
760 storms (Yang et al., 2023a). This resulted in ~72 Mt of sediment nurturing the delta annually,
761 facilitating delta progradation. After the TGR's closure, however, the sediment discharge from
762 the Yangtze River decreased to 133 Mt/yr. This volume was overshadowed by the estimated
763 ~250 Mt/yr sediment transported away from the delta region (Yang et al., 2023a).
764 Consequently, the subaqueous delta has transitioned to net erosion, with an erosion
765 volumetric rate of 0.17 km^3/yr (Fig. 16b). It is noteworthy that human activities in the deltaic
766 area, such as sand mining and dredging, also influence delta morphology (Du et al., 2016).
767 The yearly dredging amount of the Deepwater Channel Project was averaged to be 61.4 Mt/yr
768 over the past few years, further aggravating the sediment deficits in the Yangtze River delta
769 (Guo et al., 2021).

770 **9.2 Evolution of the Yellow River delta under the impact of the WSRS**

771 Historically, the Yellow River delta was well known for its rapid accretion of deltaic land,
772 due to plentiful sediment supply and frequent channel avulsions driven by the perched
773 (super-elevated) lower river channel Today, the modern Yellow River delta, which covers over

774 5,800 km^2 of new land, is home to more than two million people and is crucial for regional
775 economic development (including the Shengli Oilfield, the second largest oilfield in China).
776 However, due to the sharp decline in sediment delivery to the sea caused by dam construction
777 and soil-conservation practices in the Loess Plateau (Fig. 15), growth of the Yellow River
778 delta slowed down until finally converting into a destruction phase (Wu et al., 2017; Ji et al.,
779 2018).

780 From 1976 to 1998, excess sediment delivered from the Yellow River caused the deltaic
781 land area to increase at high accretion rates of 10-60 km^2/yr (Fig. 16c). During this period, the
782 subaqueous delta experienced accretion at a rate of 0.42 km^3/yr (Bi et al., 2021; Fu et al.,
783 2021). After 1996, however, the Yellow River's sediment supply declined by 60% due to
784 regional drought and human activities such as water abstraction (Fig. 15; Wang et al., 2007).
785 In particular, the impoundment of the XLDR after 1999 caused the active delta lobe to
786 become increasingly starved of sediment trapped behind the dam. Consequently, the subaerial
787 portion of the active delta lobe shrank with an average retreat rate of 4.3 km^2/yr during this
788 period (Wu et al., 2021b). The insufficient sediment supply also caused the subaqueous delta
789 to shift to net erosion, with an erosion rate of -0.18 km^3/yr (Fig. 16d). Furthermore, the
790 subaqueous delta between 5-10 m isobaths experienced significant erosion due to wave action
791 (Wu et al., 2017; Zhou et al., 2020).

792 After implementation of the WSRS in 2002, sediment delivery from the Yellow River to
793 the sea increased to 137 Mt/yr due to channel scouring and sediment flushing from the
794 reservoir (Fig. 15). Nevertheless, the resulting SSC was still comparatively low and
795 hyperpycnal flows, once dominant in sediment dynamics off the river mouth, could not form

(Wang et al., 2010). As a result, the dominant sediment dispersal style was characterized by buoyant river plumes, which facilitated sediment deposition near the river mouth (Wang et al., 2010; Wu et al., 2015). Along with sediment replenishment, the active delta lobe shifted from a destructive phase to a constructive phase, resulting in a 7.1 km^2/yr increase in the land area of the subaerial delta and a net volumetric accumulation of 0.07 km^3/yr in the subaqueous delta (Wu et al., 2017; Bi et al., 2021).

10. Implications of the TGR and XLDR regulation modes for global reservoirs

Similar to other large reservoirs worldwide, the TGR and XLDR disrupted the downstream water-sediment dynamics in their respective river systems. Impoundment and controlled release of reservoir water flattened high flows during the flood season and increased low flows during the dry season, resulting in homogenization of the intra-year discharge downstream of the reservoirs (Figs. 5, 6 and S3). Additionally, the TGR and XLDR interrupted the sediment flux along the main stem of the rivers, trapping 2,054 and 4,204 Mt of sediment within the reservoirs after their impoundment (Fig. 3). The resulting sedimentation in the reservoirs gave rise to unsaturated flows out of the dams (Fig. 7), leading to downstream channel erosion (Fig. 8). Therefore, from a sediment budget perspective, the reservoirs acted as significant sediment traps, but the downstream channels gradually became a new source of sediment (Figs. 14 and 15). However, the new sediment supplied from downstream channel erosion has not been sufficient to offset the deficit caused by dam interception. Consequently, the sediment load reaching the sea has decreased sharply, posing a threat to the sustainability of the deltaic areas.

10.1 Implication for mitigating reservoir sedimentation

818 Sedimentation has always been the greatest threat to the longevity of reservoirs (Kondolf
819 et al., 2014; Schleiss et al., 2016). It progressively reduces reservoir storage capacity and
820 damages hydraulic machinery, thereby shortening the lifespan of the reservoir (Morris and
821 Fan, 1998). At the time of writing, the gross storage capacity of large reservoirs worldwide is
822 about 6,100 km^3, of which approximately 2,000 km^3 (32.8%) has already been lost to
823 sedimentation. The worldwide loss of reservoir storage capacity (0.5-1.0% per annum) has
824 exceeded the capacity gained through the construction of new reservoirs (Sumi and Hirose,
825 2009; Schleiss and De Cesare, 2010). Consequently, the economic and ecological importance
826 of reservoir storage capacity makes the mitigation of reservoir sedimentation a particularly
827 urgent problem to solve.

828 The trapping efficiency (TE), defined as the ratio of reservoir sedimentation to total
829 sediment inflow, is often used to evaluate the severity of reservoir sedimentation (Brune,
830 1953). The TE is usually expressed as an exponential function of the ratio of reservoir
831 capacity to inflow (C/I) for most reservoirs worldwide, including the TGR (Fig. 17). However,
832 the TE of the XLDR has varied greatly according to the different implementation and
833 non-operational episodes of the WSRS (Fig. 17b).

834 Prior to implementation of the WSRS, the TE and C/I ratio relationship of the XLDR
835 closely followed the Brune (1953) curve (Fig. 17b). However, during the 2002-2014 period,
836 when the WSRS was implemented annually, the TE decreased to 76.1%, which was 16.6%
837 lower than the value predicted from the Brune curve. The impact of the WSRS on reservoir
838 sedimentation was further highlighted by a TE of ~100% during the years 2015-2017 when
839 the WSRS was not implemented. This indicates that almost no sediment passed through the

840 Xiaolangdi Dam in these years, similar to the Aswan High Dam (Shalash, 1982). The WSRS
841 was restarted after 2018 and this quickly ended the crisis of heavy sedimentation (Fig. 17b).
842 In 2018 and 2019, there was abundant precipitation in the Yellow River drainage basin
843 (Fan et al., 2022), and thus no urgent need for water storage and drought prevention in the
844 XLDR. Meanwhile, the upstream reservoirs had sufficient stored water to flush the XLDR.
845 Therefore, the WSRS was implemented in 2018 and 2019 under a lower water level in the
846 XLDR than before. Through joint operation of the Sanmenxia Reservoir (water impoundment)
847 and XLDR (water release) before the WSRS, the water level in XLDR was lowered to about
848 210 m, far below the 220 m level in previous years (Fig. 2). In practice, the water stored in the
849 Sanmenxia Reservoir ensured flushing power, while the low water level of the XLDR
850 facilitated sediment flushing. The TE in 2018 was reduced to 5.1%, i.e., 84.5% lower than the
851 value estimated from the Brune curve (Figs. 3 and 17b). In 2019, the XLDR took in 280 Mt of
852 sediment and discharged 545 Mt of sediment, resulting in a TE of -94.6%. Through this
853 process, the XLDR achieved net flushing over a whole year for the first time. The WSRS of
854 the XLDR provides a valuable example for mitigating reservoir sedimentation, noting the
855 severe accumulation of sediment in reservoirs worldwide.

856 **10.2 Implication for flood prevention in the downstream river**

857 In addition to hydroelectric power generation, reservoirs serve as a vital tool for
858 mitigating downstream flood damage through temporal water storage and capping of peak
859 discharge (Harmancioğlu, 1994). However, dam-induced hydrologic changes cause the
860 geomorphology of downstream river channels to evolve continuously. Doubts have therefore
861 been raised as to whether modification of channel morphology raises or decreases the flood

862 risk downstream of dams (Williams and Wolman, 1984; Kondolf, 1997; Petts and Gurnell,
863 2005; Slater et al., 2015). Reservoirs can reduce downstream flood risk by promoting the
864 incision and enlargement of downstream channels, but they may also increase flood risk by
865 causing bed sediment to coarsen and floodplain vegetation to flourish, both of which heighten
866 flow resistance and amplify the flood-stage elevation (Criss and Shock, 2001; Carling et al.,
867 2020; Naito et al., 2019). Due to intensive erosion in the downstream channels of the TGR
868 and the XLDR (Fig. 8), the low water level has dropped significantly in both the mid-lower
869 Yangtze and the lower Yellow rivers (Fig. 12). Despite erosion of the two rivers, the flood
870 level did not decrease, and under certain conditions, even increased after the dams were
871 impounded (Fig. 12). Operation of the TGR led to visible downstream floodplain vegetation
872 expansion (Hu et al., 2022). The backwater water caused by dense vegetation in higher parts
873 of the floodplain during the 2016 Yangtze River flood resulted in a ~1 m increase in water
874 level for medium flood conditions (a discharge of 70,000 m^3/s; Mei et al., 2018). Similarly,
875 operation of the XLDR (i.e., the WSRS) led to significant development of dunes in the lower
876 channel, leading to an increase in the channel resistance and amplifying the moderate and
877 large flood stages of the Yellow River (Ma et al., 2022). Despite 3.44 m of bed degradation
878 since the completion of the XLDR, Ma et al. (2022) found that any flood discharge greater
879 than that of the 5-yr recurrence interval (10,000 m^3/s) would produce a river stage exceeding
880 the pre-dam value. Therefore, reservoirs have complex effects on flood hydrology, and more
881 attention needs to be paid to downstream channel morphology adjustments.

882 **10.3 Implication for sediment-starved deltas**

883 Dams intercepting and trapping huge amounts of fluvial sediment flux appear to have

884 been the dominant cause of reduction in river sediment that has led to delta erosion over the
885 past century (Syvitski et al., 2009; Besset et al., 2019; Van De Giesen, 2020). Both the
886 Yangtze and the Yellow rivers share the same fate as many other rivers worldwide, whereby
887 dam interception has caused significant reduction in fluvial sediment delivery to deltaic areas
888 (Figs. 14 and 15). But the management of the Yangtze and Yellow rivers has provided us with
889 different perspectives on protecting downstream deltas. In the future, sediment deficit is likely
890 to pose a great threat to the Yangtze River delta under the current regulation mode of the TGR
891 (Yang et al., 2020a). But the Yellow River provides us with a new perspective on the role of
892 sediment replenishment of its delta through mega reservoir regulation. The rebound in
893 sediment delivered from the Yellow River to the sea after the operation of WSRS (Fig. 15)
894 illustrates that downstream sediment deficits can be alleviated and deltas sustained if
895 reservoirs are well regulated. However, the sustainability of sediment replenishment needs
896 further attention (Wu et al., 2020a). In the future, two aspects of the WSRS should be
897 considered in terms of replenishing the delta. Firstly, it is feasible to increase water discharge
898 during the water regulation period to scour the downstream channel, as evidenced by the
899 successful incision of the lower Yellow River over the past 20 years. Even so, attention should
900 be paid to the risk of flooding due to dune development (Ma et al., 2022). Secondly, and more
901 specifically, the XLDR should be regulated at a low water level during wet years to create
902 favorable conditions for releasing more dam-trapped sediment, as was done in 2018 and 2019
903 (Fig. 17b).

904 **11. Summary and conclusions**

905 This review has systematically evaluated the impacts of the TGR and the XLDR under

different regulation modes on the downstream functioning of the Yangtze and the Yellow rivers, and highlighted implications for reservoir operation schemes in dammed rivers worldwide. As two giant hydropower works on major Asian rivers, the TGR and XLDR trap 128.4 Mt/yr and 210.2 Mt/yr of sediment, respectively. The trapping efficiency of the TGR remained high (63-86%) throughout the whole impoundment period, whereas the trapping efficiency of the XLDR was only high in years when the WSRS was not implemented. Due to reservoir regulation and sediment interception, water and sediment outflows from both dams have been substantially altered. The twin strategy of storing water in the wet season and releasing it in the dry season means that the water discharge from the TGR correlates well with SSC. By contrast, the outflow under the WSRS can be divided into two phases: one characterized by high water discharge and extremely low SSC; and the second characterized by highly turbid flow. Controlled water releases from the dams have led to new boundary conditions that affect the water and sediment regime along the whole downstream reach of both rivers. Distinct homogenization of river discharge and a sharp reduction in sediment load are evident at downstream gauging stations of the Yangtze and Yellow rivers. At the monthly scale, the flood peaks still coincide with sediment peaks in the Yangtze River under typical anti-seasonal regulation by the TGR, but the suspended sediment is more concentrated in July to September. In the Yellow River, however, sediment peaks lag behind flood peaks with a more even distribution of monthly sediment load, due to modification of the sediment transport capacity under the WSRS. After TGR impoundment, the resulting highly unsaturated flow has caused erosion along the whole mid-lower reaches of the Yangtze River, with the reach-averaged incision decreasing from 3.7 m to 0.1 m in the downstream direction.

928 By contrast, in the lower Yellow River, significant erosion (over 2000 Mt of extra sediment)
929 of the riverbed occurred only after implementation of the WSRS which enhanced the channel
930 capacity for flow and sediment transport. Incision has promoted considerable coarsening of
931 the riverbeds of both rivers, which in turn has limited future incision by armoring part or all
932 the affected reaches. River channel modification was the primary factor behind alterations to
933 the water levels used in operating the TGR and XLDR. The dry season water level became
934 lowered in the Yangtze between Yichang and Luoshan and along the entire downstream reach
935 of the Yellow River, primarily because of riverbed incision. However, the flood season water
936 level was maintained or even raised, because the channel roughness increased due to
937 vegetation growth on floodplains and coarsening of the riverbed, implying higher flood risk.
938 The modification of river channels also altered the sediment budgets of the two rivers. After
939 the TGR and XLDR were impounded, the downstream channels of both rivers switched from
940 sediment sinks to sources due to bed incision, supplying an average of 55 Mt/yr and 136
941 Mt/yr of sediment to the mouths of the Yangtze River and the Yellow River, respectively.
942 Despite this, the reduced seaward sediment fluxes from the Yangtze River have led to a
943 transition from accumulation to erosion of the subaqueous delta. In the Yellow River, the
944 WSRS has replenished the estuarine area by releasing sediment from the XLDR. Globally,
945 reservoir sedimentation, rising flood stage, and deltaic shrinkage have also occurred in other
946 river systems regulated by dams. Hence, the WSRS of the XLDR appears to offer an inspiring
947 example for the mitigation of reservoir sedimentation and the active maintenance of delta
948 areas.

949 **Acknowledgements:**

We extend our sincere gratitude to the Changjiang Water Resources Commission of the Ministry of Water Resources and the Yellow River Conservancy Committee of the Ministry of Water Resources for data support. Additionally, we would like to express our appreciation to Dr. Taian Lu and Mr. Jinhao Guo for their assistance in editing figures. This research was funded by the National Science Foundation of China (No. 42041005, 42176168, 42149301 and 52079094). Support was also received from the Taishan Scholar Project of Shandong Province (No. TS20190913 and TSQN202211054), the Fundamental Research Funds for the Central Universities (No. 202241007), the Youth Innovation Team Program in Colleges and Universities of Shandong Province (No. 2022KJ045) and Dongying City & College Collaboration Project (SXHZ-2022-02-15). L.S. is supported by UKRI (MR/V022008/1) and NERC (NE/S015728/1).

Data Availability

Table 1 lists the data sources used in this study. All cited data synthesized here are available in cited original studies either as tabular data or by digitizing figures. The hydrographic datasets and water level in the Three Gorges Reservoir in Yangtze River and the Xiaolangdi reservoir in the Yellow River used in this study are released by the Changjiang Water Resources Commission of the Ministry of Water Resources (available at http://www.cjw.gov.cn/) and Yellow River Conservancy Committee of the Ministry of Water Resources (available at http://www.yrcc.gov.cn/). Data will also be made available on request.

References:

Anthony, E.J., Marriner, N., Morhange, C., 2014. Human influence and the changing geomorphology of Mediterranean deltas and coasts over the last 6000 years: From progradation to destruction phase? Earth-Science Rev. 139, 336–361. https://doi.org/10.1016/j.earscirev.2014.10.003

Bao, Y., Gao, P., He, X., 2015. The water-level fluctuation zone of Three Gorges Reservoir - A unique geomorphological unit. Earth-Science Rev. 150, 14–24. https://doi.org/10.1016/j.earscirev.2015.07.005

Belletti, B., Garcia de Leaniz, C., Jones, J., Bizzi, S., Börger, L., Segura, G., Castelletti, A., van de Bund, W., Aarestrup, K., Barry, J., Belka, K., Berkhuysen, A., Birnie-Gauvin, K., Bussettini, M., Carolli, M., Consuegra, S., Dopico, E., Feierfeil, T., Fernández, S., Fernandez Garrido, P., Garcia-Vazquez, E., Garrido, S., Giannico, G., Gough, P., Jepsen, N., Jones, P.E., Kemp, P., Kerr, J., King, J., Łapińska, M., Lázaro, G., Lucas, M.C., Marcello, L., Martin, P., McGinnity, P., O'Hanley, J., Olivo del Amo, R., Parasiewicz, P., Pusch, M., Rincon, G., Rodriguez, C., Royte, J., Schneider, C.T., Tummers, J.S., Vallesi, S., Vowles, A., Verspoor, E., Wanningen, H., Wantzen, K.M., Wildman, L., Zalewski, M., 2020. More than one million barriers fragment Europe's rivers. Nature 588, 436–441. https://doi.org/10.1038/s41586-020-3005-2

Besset, M., Anthony, E.J., Bouchette, F., 2019. Multi-decadal variations in delta shorelines and their relationship to river sediment supply: An assessment and review. Earth-Science Rev. 193, 199–219. https://doi.org/10.1016/j.earscirev.2019.04.018

Best, J., 2019. Anthropogenic stresses on the world's big rivers. Nat. Geosci. 12, 7–21. https://doi.org/10.1038/s41561-018-0262-x

Bhattacharyya, K., Singh, V.P., 2019. Reservoir Sedimentation. CRC Press, Boca Raton : Taylor & Francis, a CRC title, part of the Taylor & Francis imprint, a member of the Taylor & Francis Group, the academic division of T&F Informa, plc, 2018. https://doi.org/10.1201/9781351027502

Bi, N., Sun, Z., Wang, H., Wu, X., Fan, Y., Xu, C., Yang, Z., 2019. Response of channel scouring and deposition to the regulation of large reservoirs: A case study of the lower reaches of the Yellow River (Huanghe). J. Hydrol. 568, 972–984. https://doi.org/https://doi.org/10.1016/j.jhydrol.2018.11.039

Bi, N., Wang, H., Wu, X., Saito, Y., Xu, C., Yang, Z., 2021. Phase change in evolution of the modern Huanghe (Yellow River) Delta: Process, pattern, and mechanisms. Mar. Geol. 437. https://doi.org/10.1016/j.margeo.2021.106516

Blum, M.D., Roberts, H.H., 2009. Drowning of the Mississippi Delta due to insufficient sediment supply and global sea-levelrise. Nat. Geosci. 2, 488–491. https://doi.org/10.1038/ngeo553

Brandt, S.A., 2000. Classification of geomorphological effects downstream of dams. Catena 40, 375–401. https://doi.org/10.1016/S0341-8162(00)00093-X

Brown, S., Nicholls, R.J., 2015. Subsidence and human influences in mega deltas: The case of the Ganges-Brahmaputra-Meghna. Sci. Total Environ. 527–528, 362–374. https://doi.org/10.1016/j.scitotenv.2015.04.124

Brune, G.M., 1953. Trap efficiency of reservoirs. Eos, Trans. Am. Geophys. Union 34, 407–448. https://doi.org/10.1029/TR034i003p00407

Carling, P.A., Leyland, J., Kleinhans, M.G., Besozzi, L., Duranton, P., Trieu, H., Teske, R., 2020. Quantifying Fluid Retention Due to Natural Vegetation in a Forest Floodplain Analogue Using the Aggregated Dead Zone (ADZ) Dilution Approach. Water Resour. Res. 56, 1–22. https://doi.org/10.1029/2020WR027070

Chai, Y., Deng, J., Yang, Y., Sun, Z., Li, Y., Zhu, L., 2021. Evolution characteristics and driving factors of the water level at the same discharge in the Jingjiang reach of Yangtze River. Dili Xuebao/Acta Geogr. Sin. 76, 101–113. https://doi.org/10.11821/dlxb202101008

Chai, Y., Yue, Y., Zhang, L., Miao, C., Borthwick, A.G.L., Zhu, B., Li, Y., Dolman, A.J., 2020. Homogenization and polarization of the seasonal water discharge of global rivers in response to climatic and anthropogenic effects. Sci. Total Environ. 709, 136062. https://doi.org/10.1016/j.scitotenv.2019.136062

Chao, B.F., Wu, Y.H., Li, Y.S., 2008. Impact of artificial reservoir water impoundment on global sea level. Science (80-.). 320, 212–214. https://doi.org/10.1126/science.1154580

Chen, J.G., Zhou, W.H., Chen, Q., 2012. Reservoir sedimentation and transformation of morphology in the lower yellow river during 10 year's initial operation of the Xiaolangdi reservoir. J. Hydrodyn. 24, 914–924. https://doi.org/10.1016/S1001-6058(11)60319-3

Chen, X., Zhou, Q., Zhang, E., 2006. In-channel sand extraction from the mid-lower Yangtze channels and its management: Problems and challenges. J. Environ. Plan. Manag. 49, 309–320. https://doi.org/10.1080/09640560500508247

Chen, Y., Syvitski, J.P.M., Gao, S., Overeem, I., Kettner, A.J., 2012. Socio-economic impacts on flooding: A 4000-year history of the yellow river, China. Ambio 41, 682–698. https://doi.org/10.1007/s13280-012-0290-5

Cheng, Y., Xia, J., Zhou, M., Deng, S., Li, D., Li, Z., Wan, Z., 2022. Recent variation in channel erosion efficiency of the Lower Yellow river with different channel patterns. J. Hydrol. 610, 127962. https://doi.org/10.1016/j.jhydrol.2022.127962

Criss, R.E., Shock, E.L., 2001. Flood enhancement through flood control. Geology 29, 875–878. https://doi.org/10.1130/0091-7613(2001)029<0875:FETFC>2.0.CO;2

Dai, Z., Liu, J.T., 2013. Impacts of large dams on downstream fluvial sedimentation: An example of the Three Gorges Dam (TGD) on the Changjiang (Yangtze River). J. Hydrol. 480, 10–18. https://doi.org/10.1016/j.jhydrol.2012.12.003

Dai, Z., Liu, J.T., Fu, G., Xie, H., 2013. A thirteen-year record of bathymetric changes in the North Passage, Changjiang (Yangtze) estuary. Geomorphology 187, 101–107. https://doi.org/10.1016/j.geomorph.2013.01.004

Dai, Z., Liu, J.T., Wei, W., Chen, J., 2014. Detection of the three gorges dam influence on the Changjiang (Yangtze River) submerged delta. Sci. Rep. 4, 1–7. https://doi.org/10.1038/srep06600

Day, J.W., Giosan, L., 2008. Geomorphology: Survive or subside? Nat. Geosci. 1, 156–157. https://doi.org/10.1038/ngeo137

Deng, S., Xia, J., Liu, X., Zhou, M., Mao, Y., Xu, Q., 2022. Contributions of different sources to sediment transport in the Middle Yangtze River under intensive channel degradation. Catena 217, 106511. https://doi.org/10.1016/j.catena.2022.106511

Dethier, E.N., Renshaw, C.E., Magilligan, F.J., 2022. Rapid changes to global river suspended sediment flux by humans. Science (80-.). 376, 1447–1452. https://doi.org/10.1126/science.abn7980

Du J., Yang S., Feng H., 2016 Recent human impacts on the morphological evolution of the Yangtze River delta foreland: A review and new perspectives. Estuarine, Costal and Shelf Science, 181: 160-169. DOI10.1016/j.ecss.2016.08.025

Fan, H., He, D., Wang, H., 2015. Environmental consequences of damming the mainstream lancang-mekong river: A review. Earth-Science Rev. 146, 77–91. https://doi.org/10.1016/j.earscirev.2015.03.007

Fan, X., Wang, L., Li, X., Zhou, J., Chen, D., Yang, H., 2022. Increased discharge across the Yellow River Basin in the 21st century was dominated by precipitation in the headwater region. J. Hydrol. Reg. Stud. 44, 101230. https://doi.org/10.1016/j.ejrh.2022.101230

Fu, Y., Chen, S., Ji, H., Fan, Y., Li, P., 2021. The modern Yellow River Delta in transition: Causes and implications. Mar. Geol. 436, 106476. https://doi.org/10.1016/j.margeo.2021.106476

Gemmer, M., Jiang, T., Su, B., Kundzewicz, Z.W., 2008. Seasonal precipitation changes in the wet season and their influence on flood/drought hazards in the Yangtze River Basin, China. Quat. Int. 186, 12–21. https://doi.org/10.1016/j.quaint.2007.10.001

Giosan, L., Syvitski, J., Constantinescu, S., Day, J., 2014. Protect the world's deltas. Nature 516, 31–33. https://doi.org/10.1038/516031a

Graf, W.L., 2006. Downstream hydrologic and geomorphic effects of large dams on American rivers. Geomorphology 79, 336–360. https://doi.org/10.1016/j.geomorph.2006.06.022

Grill, G., Lehner, B., Thieme, M., Geenen, B., Tickner, D., Antonelli, F., Babu, S., Borrelli, P., Cheng, L., Crochetiere, H., Ehalt Macedo, H., Filgueiras, R., Goichot, M., Higgins, J., Hogan, Z., Lip, B., McClain, M.E., Meng, J., Mulligan, M., Nilsson, C., Olden, J.D., Opperman, J.J., Petry, P., Reidy Liermann, C., S áenz, L., Salinas-Rodr ǵuez, S., Schelle, P., Schmitt, R.J.P., Snider, J., Tan, F., Tockner, K., Valdujo, P.H., van Soesbergen, A., Zarfl, C., 2019. Mapping the world's free-flowing rivers. Nature 569, 215–221. https://doi.org/10.1038/s41586-019-1111-9

Guo, L., Su, N., Zhu, C., He, Q., 2018. How have the river discharges and sediment loads changed in the Changjiang River basin downstream of the Three Gorges Dam? J. Hydrol. 560, 259–274. https://doi.org/10.1016/j.jhydrol.2018.03.035

Guo, X., Fan, D., Zheng, S., Wang, H., Zhao, B., Qin, C., 2021. Revisited sediment budget with latest bathymetric data in the highly altered Yangtze (Changjiang) Estuary. Geomorphology 391, 107873. https://doi.org/10.1016/j.geomorph.2021.107873

Harmancioğlu, N.B., 1994. Flood control by reservoirs, in: Coping with Floods. Springer Netherlands, Dordrecht, pp. 637–652. https://doi.org/10.1007/978-94-011-1098-3_38

Hori, K., Saito, Y., Zhao, Q., Cheng, X., Wang, P., Sato, Y., Li, C., 2001. Sedimentary facies and Holocene progradation rates of the Changjiang (Yangtze) delta, China. Geomorphology 41, 233–248. https://doi.org/10.1016/S0169-555X(01)00119-2

Hu, Y., Li, D., Deng, J., Yue, Y., Zhou, J., Chai, Y., Li, Y., 2022. Mechanisms Controlling Water-Level Variations in the Middle Yangtze River Following the Operation of the Three Gorges Dam. Water Resour. Res. 58, 1–19. https://doi.org/10.1029/2022WR032338

Ji, H., Chen, S., Pan, S., Xu, C., Jiang, C., Fan, Y., 2018. Morphological variability of the active Yellow River mouth under the new regime of riverine delivery. J. Hydrol. 564, 329–341. https://doi.org/https://doi.org/10.1016/j.jhydrol.2018.07.014

Jiang, C., De Swart, H.E., Li, J., Liu, G., 2013. Mechanisms of along-channel sediment

transport in the North Passage of the Yangtze Estuary and their response to large-scale interventions Topical Collection on the 11th International Conference on Cohesive Sediment Transport. Ocean Dyn. 63, 283–305. https://doi.org/10.1007/s10236-013-0594-4

Jiang, W., Liu, G., Wang, G., Zhang, R., Liu, J., 2022. Medium-Term Multiobjective Operation Mode of Cascade Reservoirs Using Multisource Information. J. Hydrol. Eng. 27, 1–11. https://doi.org/10.1061/(asce)he.1943-5584.0002189

Kesel, R.H., Yodis, E.G., McCraw, D.J., 1992. An approximation of the sediment budget of the lower mississippi river prior to major human modification. Earth Surf. Process. Landforms 17, 711–722. https://doi.org/10.1002/esp.3290170707

Kim, W., Mohrig, D., Twilley, R., Paola, C., Parker, G., 2009. Is it feasible to build new land in the mississippi river delta? Eos (Washington. DC). 90, 373–374. https://doi.org/10.1029/2009EO420001

Kingsford, R.T., 2000. Ecological impacts of dams, water diversions and river management on floodplain wetlands in Australia. Austral Ecol. 25, 109–127. https://doi.org/10.1046/j.1442-9993.2000.01036.x

Kondolf, G.M., 1997. Hungry water: Effects of dams and gravel mining on river channels. Environ. Manage. 21, 533–551. https://doi.org/10.1007/s002679900048

Kondolf, G.M., Gao, Y., Annandale, G.W., Morris, G.L., Jiang, E., Zhang, J., Cao, Y., Carling, P., Fu, K., Guo, Q., Hotchkiss, R., Peteuil, C., Sumi, T., Wang, H., Wang, Z., Wei, Z., Wu, B., Wu, C., Yang, C.T., 2014. Sustainable sediment management in reservoirs and regulated rivers: Experiences from five continents. Earth's Futur. 2, 256–280. https://doi.org/10.1002/2013ef000184

Kong, D., Miao, C., Li, J., Zheng, H., 2022. Full-stream erosion in the lower Yellow River: Feasibility, sustainability and opportunity. Sci. Total Environ. 807, 150810. https://doi.org/10.1016/j.scitotenv.2021.150810

Lai, X., Yin, D., Finlayson, B.L., Wei, T., Li, M., Yuan, W., Yang, S., Dai, Z., Gao, S., Chen, Z., 2017. Will river erosion below the Three Gorges Dam stop in the middle Yangtze? J. Hydrol. 554, 24–31. https://doi.org/10.1016/j.jhydrol.2017.08.057

Leonardi, N., Mei, X., Carnacina, I., Dai, Z., 2021. Marine sediment sustains the accretion of a mixed fluvial-tidal delta. Mar. Geol. 438, 106520. https://doi.org/10.1016/j.margeo.2021.106520

Li, Q., Yu, M., Lu, G., Cai, T., Bai, X., Xia, Z., 2011. Impacts of the gezhouba and three gorges reservoirs on the sediment regime in the yangtze river, china. J. Hydrol. 403,

224–233. https://doi.org/10.1016/j.jhydrol.2011.03.043

Li, S., Xu, Y.J., Ni, M., 2021. Changes in sediment, nutrients and major ions in the world largest reservoir: Effects of damming and reservoir operation. J. Clean. Prod. 318, 128601. https://doi.org/10.1016/j.jclepro.2021.128601

Li, Y., Zhang, Q., Tan, Z., Yao, J., 2020. On the hydrodynamic behavior of floodplain vegetation in a flood-pulse-influenced river-lake system (Poyang Lake, China). J. Hydrol. 585, 124852. https://doi.org/10.1016/j.jhydrol.2020.124852

Liang, C., Xin, S., Dongsheng, W., Xiuying, Y., Guodong, J., 2016. The ecological benefit–loss evaluation in a riverine wetland for hydropower projects – A case study of Xiaolangdi reservoir in the Yellow River, China. Ecol. Eng. 96, 34–44. https://doi.org/10.1016/j.ecoleng.2015.12.037

Liu, S., Li, D., Liu, D., Zhang, X., Wang, Z., 2022. Characteristics of sedimentation and sediment trapping efficiency in the Three Gorges Reservoir, China. Catena 208, 105715. https://doi.org/10.1016/j.catena.2021.105715

López-Tarazón, J.A., Batalla, R.J., Vericat, D., Francke, T., 2012. The sediment budget of a highly dynamic mesoscale catchment: The River Isábena. Geomorphology 138, 15–28. https://doi.org/10.1016/j.geomorph.2011.08.020

Luan, H.L., Ding, P.X., Wang, Z.B., Ge, J.Z., Yang, S.L., 2016. Decadal morphological evolution of the Yangtze Estuary in response to river input changes and estuarine engineering projects. Geomorphology 265, 12–23. https://doi.org/10.1016/j.geomorph.2016.04.022

Luan, H.L., Ding, P.X., Yang, S.L., Wang, Z.B., 2021. Accretion-erosion conversion in the subaqueous Yangtze Delta in response to fluvial sediment decline. Geomorphology 382, 107680. https://doi.org/10.1016/j.geomorph.2021.107680

Luo, X.X., Yang, S.L., Wang, R.S., Zhang, C.Y., Li, P., 2017. New evidence of Yangtze delta recession after closing of the Three Gorges Dam. Sci. Rep. 7, 1–10. https://doi.org/10.1038/srep41735

Ma, H., Nittrouer, J.A., Fu, X., Parker, G., Zhang, Y., Wang, Y., Wang, Y., Lamb, M.P., Cisneros, J., Best, J., Parsons, D.R., Wu, B., 2022. Amplification of downstream flood stage due to damming of fine-grained rivers. Nat. Commun. 13, 1–11. https://doi.org/10.1038/s41467-022-30730-9

Macklin, M.G., Lewin, J., 2015. The rivers of civilization. Quat. Sci. Rev. 114, 228–244. https://doi.org/10.1016/j.quascirev.2015.02.004

Mei, X., Dai, Z., Darby, S.E., Gao, S., Wang, J., Jiang, W., 2018. Modulation of Extreme

Flood Levels by Impoundment Significantly Offset by Floodplain Loss Downstream of the Three Gorges Dam. Geophys. Res. Lett. 45, 3147–3155. https://doi.org/10.1002/2017GL076935

Miao, C., Kong, D., Wu, J., Duan, Q., 2016. Functional degradation of the water-sediment regulation scheme in the lower Yellow River: Spatial and temporal analyses. Sci. Total Environ. 551–552, 16–22. https://doi.org/10.1016/j.scitotenv.2016.02.006

Miao, C., Ni, J., Borthwick, A.G.L., 2010. Recent changes of water discharge and sediment load in the Yellow River basin, China. Prog. Phys. Geogr. 34, 541–561. https://doi.org/10.1177/0309133310369434

Milliman, J.D., Farnsworth, K.L., Jones, P.D., Xu, K.H., Smith, L.C., 2008. Climatic and anthropogenic factors affecting river discharge to the global ocean, 1951-2000. Glob. Planet. Change 62, 187–194. https://doi.org/10.1016/j.gloplacha.2008.03.001

Milliman, J.D., Meade, R.H., 1983. World-Wide Delivery of River Sediment to the Oceans. J. Geol. 91, 1–21. https://doi.org/10.1086/628741

Milliman, J.D., Syvitski, J.P.M., 1992. Geomorphic/tectonic control of sediment discharge to the ocean: the importance of small mountainous rivers. J. Geol. 100, 525–544. https://doi.org/10.1086/629606

Milliman, J.D., Yun-Shan, Q., Mei-E, R., Saito, Y., 2009. Man's Influence on the Erosion and Transport of Sediment by Asian Rivers: The Yellow River (Huanghe) Example. J. Geol. 95, 751–762. https://doi.org/10.1086/629175

Morris, G.L., Fan, J., 1998. Reservoir Sedimentation Handbook. Desingn and management of dams, reservoirs and watersheds for sustainable use. p. 805.

Mulligan, M., van Soesbergen, A., Sáenz, L., 2020. GOODD, a global dataset of more than 38,000 georeferenced dams. Sci. Data 7, 1–8. https://doi.org/10.1038/s41597-020-0362-5

Munoz, S.E., Giosan, L., Therrell, M.D., Remo, J.W.F., Shen, Z., Sullivan, R.M., Wiman, C., O'Donnell, M., Donnelly, J.P., 2018. Climatic control of Mississippi River flood hazard amplified by river engineering. Nature 556, 95–98. https://doi.org/10.1038/nature26145

Naito, K., Ma, H., Nittrouer, J.A., Zhang, Y., Wu, B., Wang, Y., Fu, X., Parker, G., 2019. Extended Engelund–Hansen type sediment transport relation for mixtures based on the sand-silt-bed Lower Yellow River, China. J. Hydraul. Res. 57, 770–785. https://doi.org/10.1080/00221686.2018.1555554

Nicolás Ruiz, N., Suárez Alonso, M.L., Vidal-Abarca, M.R., 2021. Contributions of dry rivers to human well-being: A global review for future research. Ecosyst. Serv. 50.

https://doi.org/10.1016/j.ecoser.2021.101307
Nishimura, S., Lee, S.B., Ito, K., Senge, M., 2005. The mode of operation of a regulating reservoir for effective use of river flow. Paddy Water Environ. 3, 149–154. https://doi.org/10.1007/s10333-005-0011-9
Patro, E.R., De Michele, C., Granata, G., Biagini, C., 2022. Assessment of current reservoir sedimentation rate and storage capacity loss: An Italian overview. J. Environ. Manage. 320, 115826. https://doi.org/10.1016/j.jenvman.2022.115826
Petts, G.E., Gurnell, A.M., 2005. Dams and geomorphology: Research progress and future directions. Geomorphology 71, 27–47. https://doi.org/10.1016/j.geomorph.2004.02.015
Pinter, N., Jemberie, A.A., Remo, J.W.F., Heine, R.A., Ickes, B.S., 2008. Flood trends and river engineering on the Mississippi River system. Geophys. Res. Lett. 35, 1–5. https://doi.org/10.1029/2008GL035987
Piqué, G., Batalla, R.J., López, R., Sabater, S., 2017. The fluvial sediment budget of a dammed river (upper Muga, southern Pyrenees). Geomorphology 293, 211–226. https://doi.org/10.1016/j.geomorph.2017.05.018
Poff, N.L.R., Olden, J.D., Merritt, D.M., Pepin, D.M., 2007. Homogenization of regional river dynamics by dams and global biodiversity implications. Proc. Natl. Acad. Sci. U. S. A. 104, 5732–5737. https://doi.org/10.1073/pnas.0609812104
Ren, S., Zhang, B., Wang, W.J., Yuan, Y., Guo, C., 2021. Sedimentation and its response to management strategies of the Three Gorges Reservoir, Yangtze River, China. Catena 199, 105096. https://doi.org/10.1016/j.catena.2020.105096
Richards, K., 1982. Rivers: Form and Process in Alluvial Channels. Methuen, London.
Schleiss, A.J., De Cesare, G., 2010. Physical model experiments on reservoir sedimentation. IAHR Hydrolink 4, 54–57.
Schleiss, A.J., Franca, M.J., Juez, C., De Cesare, G., 2016. Reservoir sedimentation. J. Hydraul. Res. 54, 595–614. https://doi.org/10.1080/00221686.2016.1225320
Shalash, S., 1982. Effects of sedimentation on the storage capacity of the High Aswan Dam reservoir. Hydrobiologia 91–92, 623–639. https://doi.org/10.1007/BF00000061
Slater, L.J., Singer, M.B., Kirchner, J.W., 2015. Hydrologic versus geomorphic drivers of trends in flood hazard. Geophys. Res. Lett. 42, 370–376. https://doi.org/10.1002/2014GL062482
Slaymaker, O., 2003. The sediment budget as conceptual framework and management tool. Interact. between Sediments Water 71–82. https://doi.org/10.1007/978-94-017-3366-3_12

Słowik, M., Dezső, J., Marciniak, A., Tóth, G., Kovács, J., 2018. Evolution of river planforms downstream of dams: Effect of dam construction or earlier human-induced changes? Earth Surf. Process. Landforms 43, 2045–2063. https://doi.org/10.1002/esp.4371

Song D., Wang X., Cao Z., Guan W., 2013. Suspended sediment transport in the Deepwater Navigation Channel, Yangtze River Estuary, China, in the dry season 2009:1. Observations over spring and neap tidal cycles. J Geophys. Res. - Oceans. 2013, 118(10): 5555-5567. DOI10.1002/jgrc.20410

Stanley, D.J., Warne, A.G., 1993. Nile delta: Recent geological evolution and human impact. Science (80-.). 260, 628–634. https://doi.org/10.1126/science.260.5108.628

Sumi, T., Hirose, T., 2009. Accumulation of sediment in reservoirs. Water storage, Transp. Distrib. 224–252.

Syvitski, J., Ángel, J.R., Saito, Y., Overeem, I., Vörösmarty, C.J., Wang, H., Olago, D., 2022a. Earth's sediment cycle during the Anthropocene. Nat. Rev. Earth Environ. 3, 179–196. https://doi.org/10.1038/s43017-021-00253-w

Syvitski, J., Anthony, E., Saito, Y., Zăinescu, F., Day, J., Bhattacharya, J.P., Giosan, L., 2022b. Large deltas, small deltas: Toward a more rigorous understanding of coastal marine deltas. Glob. Planet. Change 218. https://doi.org/10.1016/j.gloplacha.2022.103958

Syvitski, J.P.M., Kettner, A.J., Overeem, I., Hutton, E.W.H., Hannon, M.T., Brakenridge, G.R., Day, J., Vörösmarty, C., Saito, Y., Giosan, L., Nicholls, R.J., 2009. Sinking deltas due to human activities. Nat. Geosci. 2, 681. https://doi.org/10.1038/ngeo629https://www.nature.com/articles/ngeo629#supplementary-information

Tang, C., Yan, Q., Li, W., Yang, X., Zhang, S., 2022. Impact of dam construction on the spawning grounds of the four major Chinese carps in the Three Gorges Reservoir. J. Hydrol. 609, 127694. https://doi.org/10.1016/j.jhydrol.2022.127694

Tang, X., Tong, S., Huang, G., Xu, G., Li, X., Lei, K., Yao, S., 2021. Characteristics of sedimentation and channel adjustment linked to the Three Gorges Reservoir. Int. J. Sediment Res. 36, 177–189. https://doi.org/10.1016/j.ijsrc.2020.10.003

Teng L., Cheng H., Zhang E., Wang Y., 2022. Lateral Variation of Tidal Mixing Asymmetry and Its Impact on the Longitudinal Sediment Transport in Turbidity Maximum Zone of Salt Wedge Estuary. Journal of Marine Science and Engineering, 10(7): 907. DOI10.3390/jmse10070907

Tian, Q., Yang, S., 2017. Regional climatic response to global warming: Trends in

temperature and precipitation in the Yellow, Yangtze and Pearl River basins since the 1950s. Quat. Int. 440, 1–11. https://doi.org/10.1016/j.quaint.2016.02.066

Van De Giesen, N., 2020. The changing shapes of river deltas Expert insight into current research. Nature 577, 473.

Vörösmarty, C.J., Meybeck, M., Fekete, B., Sharma, K., Green, P., Syvitski, J.P.M., 2003. Anthropogenic sediment retention: Major global impact from registered river impoundments. Glob. Planet. Change 39, 169–190. https://doi.org/10.1016/S0921-8181(03)00023-7

Wang, G., Wu, B., Wang, Z.Y., 2005. Sedimentation problems and management strategies of Sanmenxia Reservoir, Yellow River, China. Water Resour. Res. 41, 1–17. https://doi.org/10.1029/2004WR003919

Wang, H., Bi, N., Wang, Y., Saito, Y., Yang, Z., 2010. Tide-modulated hyperpycnal flows off the Huanghe (Yellow River) mouth, China. Earth Surf. Process. Landforms 35, 1315–1329. https://doi.org/10.1002/esp.2032

Wang, H., Sun, F., Liu, W., 2020. Characteristics of streamflow in the main stream of Changjiang River and the impact of the Three Gorges Dam. Catena 189, 104498. https://doi.org/10.1016/j.catena.2020.104498

Wang, H., Wu, X., Bi, N., Li, S., Yuan, P., Wang, A., Syvitski, J.P.M., Saito, Y., Yang, Z., Liu, S., Nittrouer, J., 2017. Impacts of the dam-orientated water-sediment regulation scheme on the lower reaches and delta of the Yellow River (Huanghe): A review. Glob. Planet. Change 157, 93–113. https://doi.org/https://doi.org/10.1016/j.gloplacha.2017.08.005

Wang, H., Yang, Z., Saito, Y., Liu, J.P., Sun, X., Wang, Y., 2007. Stepwise decreases of the Huanghe (Yellow River) sediment load (1950–2005): Impacts of climate change and human activities. Glob. Planet. Change 57, 331–354. https://doi.org/https://doi.org/10.1016/j.gloplacha.2007.01.003

Wang, H.W., Kondolf, G.M., 2014. Upstream sediment-control dams: Five decades of experience in the rapidly eroding dahan river basin, Taiwan. J. Am. Water Resour. Assoc. 50, 735–747. https://doi.org/10.1111/jawr.12141

Wang, S., Fu, B., Piao, S., Lü, Y., Ciais, P., Feng, X., Wang, Y., 2016. Reduced sediment transport in the Yellow River due to anthropogenic changes。 Nat. Geosci. 9, 38–41. https://doi.org/10.1038/ngeo2602

Wang, Y., Borthwick, A.G.L., Ni, J., 2022. Human affinity for rivers. River 1, 4–14. https://doi.org/10.1002/rvr2.12

Warrick, J.A., Bountry, J.A., East, A.E., Magirl, C.S., Randle, T.J., Gelfenbaum, G., Ritchie, A.C., Pess, G.R., Leung, V., Duda, J.J., 2015. Large-scale dam removal on the Elwha River, Washington, USA: Source-to-sink sediment budget and synthesis. Geomorphology 246, 729–750. https://doi.org/10.1016/j.geomorph.2015.01.010

Wei, W., Dai, Z., Mei, X., Gao, S., Liu, J.P., 2019. Multi-decadal morpho-sedimentary dynamics of the largest Changjiang estuarine marginal shoal: Causes and implications. L. Degrad. Dev. 30, 2048–2063. https://doi.org/10.1002/ldr.3410

Williams, G.P., Wolman, M.G., 1984. Downstream effects of dams on alluvial rivers. US Geol. Surv. Prof. Pap. 1286.

Wright, L.D., 1977. Sediment transport and deposition at river mouths: A synthesis. Bull. Geol. Soc. Am. 88, 857–868. https://doi.org/10.1130/0016-7606(1977)88<857:STADAR>2.0.CO;2

Wu, X., Bi, N., Syvitski, J., Saito, Y., Xu, J., Nittrouer, J.A., Bianchi, T.S., Yang, Z., Wang, H., 2020a. Can Reservoir Regulation Along the Yellow River Be a Sustainable Way to Save a Sinking Delta? Earth's Futur. 8, 1–9. https://doi.org/10.1029/2020EF001587

Wu, X., Bi, N., Xu, J., Nittrouer, J.A., Yang, Z., Saito, Y., Wang, H., 2017. Stepwise morphological evolution of the active Yellow River (Huanghe) delta lobe (1976–2013): Dominant roles of riverine discharge and sediment grain size. Geomorphology 292, 115–127. https://doi.org/10.1016/j.geomorph.2017.04.042

Wu, X., Bi, N., Yuan, P., Li, S., Wang, H., 2015. Sediment dispersal and accumulation off the present Huanghe (Yellow River) delta as impacted by the Water-Sediment Regulation Scheme. Cont. Shelf Res. 111, 126–138. https://doi.org/https://doi.org/10.1016/j.csr.2015.11.003

Wu, X., Fan, Y., Wang, H., Bi, N., Yang, Z., Xu, C., 2021a. Geomorphological responses of the lower river channel and delta to interruption of reservoir regulation in the Yellow River, 2015-2017. Chinese Sci. Bull. 66, 3059–3070. https://doi.org/10.1360/TB-2020-0975. (in Chinese with English Abstract)

Wu, X., Wang, H., Bi, N., Saito, Y., Xu, J., Zhang, Y., Lu, T., Cong, S., Yang, Z., 2020b. Climate and human battle for dominance over the Yellow River's sediment discharge: From the Mid-Holocene to the Anthropocene. Mar. Geol. 425. https://doi.org/10.1016/j.margeo.2020.106188

Wu, X., Wang, H., Bi, N., Xu, J., Nittrouer, J.A., Yang, Z., Lu, T., Li, P., 2021b. Impact of Artificial Floods on the Quantity and Grain Size of River-Borne Sediment: A Case Study of a Dam Regulation Scheme in the Yellow River Catchment. Water Resour. Res.

57, 1–18. https://doi.org/10.1029/2021wr029581

Xu, A., Mo, L., Wang, Q., 2022. Research on Operation Mode of the Yalong River Cascade Reservoirs Based on Improved Stochastic Fractal Search Algorithm. Energies 15. https://doi.org/10.3390/en15207779

Xu, X., Tan, Y., Chen, S., Yang, G., 2014. Changing patterns and determinants of natural capital in the Yangtze River Delta of China 2000-2010. Sci. Total Environ. 466–467, 326–337. https://doi.org/10.1016/j.scitotenv.2013.07.043

Yan H., Zhang X., Xu Q.. 2021. Variation of runoff and sediment inflows to the Three Gorges Reservoir: Impact of upstream cascade reservoirs. J. Hydrol. 603: 126875. DOI10.1016/j.jhydrol.2021.126875

Yang, H.F., Yang, S.L., Li, B.C., Wang, Y.P., Wang, J.Z., Zhang, Z.L., Xu, K.H., Huang, Y.G., Shi, B.W., Zhang, W.X., 2021. Different fates of the Yangtze and Mississippi deltaic wetlands under similar riverine sediment decline and sea-level rise. Geomorphology 381. https://doi.org/10.1016/j.geomorph.2021.107646

Yang, H. F., Yang, S. L., Xu, K. H., Milliman, J. D., Wang, H., Yang, Z., et al. (2018). Human impacts on sediment in the yangtze river: a review and new perspectives. Global and Planetary Change, 162, 8-17. 10.1016/j.gloplacha.2018.01.001

Yang, S., Bouma, T.J., Xu, K., Shi, B., Yang, H., Zhang, W., Luo, X., Li, P., Huang, Y., Tian, M., Guo, L., Dai, Z., 2023a. Storms dominate the erosion of the Yangtze Delta and southward sediment transport. Sci. Bull. 68, 553–556. https://doi.org/10.1016/j.scib.2023.03.005

Yang, S.L., Luo, X., Temmerman, S., Kirwan, M., Bouma, T., Xu, K., Zhang, S., Fan, J., Shi, B., Yang, H., Wang, Y.P., Shi, X., Gao, S., 2020a. Role of delta-front erosion in sustaining salt marshes under sea-level rise and fluvial sediment decline. Limnol. Oceanogr. 65, 1990–2009. https://doi.org/10.1002/lno.11432

Yang, S.L., Shi, B., Fan, J., Luo, X., Tian, Q., Yang, H., Chen, S., Zhang, Y., Zhang, S., Shi, X., Wang, H., 2020b. Streamflow decline in the yellow river along with socioeconomic development: Past and future. Water (Switzerland) 12, 1–27. https://doi.org/10.3390/w12030823

Yang, S.L., Milliman, J.D., Li, P., Xu, K., 2011. 50,000 dams later: Erosion of the Yangtze River and its delta. Glob. Planet. Change 75, 14–20. https://doi.org/10.1016/j.gloplacha.2010.09.006

Yang, S.L., Milliman, J.D., Xu, K.H., Deng, B., Zhang, X.Y., Luo, X.X., 2014. Downstream sedimentary and geomorphic impacts of the Three Gorges Dam on the Yangtze River.

Earth-Science Rev. 138, 469–486. https://doi.org/10.1016/j.earscirev.2014.07.006

Yang, X., Xiong, H., Li, D., Li, Y., Hu, Y., 2023b. Disproportional erosion of the middle-lower Yangtze River following the operation of the Three Gorges Dam. Sci. Total Environ. 859, 160264. https://doi.org/10.1016/j.scitotenv.2022.160264

Yang, Y., Zhang, M., Zhu, L., Liu, W., Han, J., Yang, Y., 2017. Influence of Large Reservoir Operation on Water-Levels and Flows in Reaches below Dam: Case Study of the Three Gorges Reservoir. Sci. Rep. 7, 1–14. https://doi.org/10.1038/s41598-017-15677-y

Yang, Y., Zheng, J., Zhu, L., Zhang, H., Wang, J., 2022. Influence of the Three Gorges Dam on the transport and sorting of coarse and fine sediments downstream of the dam. J. Hydrol. 615, 128654. https://doi.org/10.1016/j.jhydrol.2022.128654

Yue Y., Ni J., Ciai P, Piao S., Wang T., Huang M., Borthwick A., Li T., Wang Y., Chappell A., Van Oost K., 2016. Lateral transport of soil carbon and land-atmosphere CO_2 flux induced by water erosion in China. Proceedings of the National Academy of Sciences of the United Sstates of America, 2016, 113(24): 6617-6622. DOI10.1073/pnas.1523358113

Zhang, N., Wu, Z., Tang, J., 2009. The Operation Mode of the Regulating Reservoirs in Intake Areas of the Middle Route of the South-to-North Water Transfer Project. South-to-North Water Transfers Water Sci. Technol. 7(6), 194-197. (in Chinese with English Abstract)

Zhang, R., 1998. Dynamics of river sediment. China Water Power Press, Beijing.

Zhang, W., Yang, Y., Zhang, M., Li, Y., Zhu, L., You, X., Wang, D., Xu, J., 2017. Mechanisms of suspended sediment restoration and bed level compensation in downstream reaches of the Three Gorges Projects (TGP). J. Geogr. Sci. 27, 463–480. https://doi.org/10.1007/s11442-017-1387-3

Zhang, S., Tu, Q., 2005. Analysis of Water and Sediment Regulation Based on Sediment Transport Capacity and Rule of Hydraulic Channel Shape. Hydrology. 25(06), 33-36. (in Chinese with English Abstract)

Zhang, Y., Jiang, Z., Ji, C., Sun, P., 2015. Contrastive analysis of three parallel modes in multi-dimensional dynamic programming and its application in cascade reservoirs operation. J. Hydrol. 529, 22–34. https://doi.org/10.1016/j.jhydrol.2015.07.017

Zhou, L., Liu, J., Saito, Y., Diao, S., Gao, M., Qiu, J., Xu, C., He, L., Ye, S., 2020. Sediment budget of the Yellow River delta during 1959–2012, estimated from morphological changes and accumulation rates. Mar. Geol. 430, 106363. http://doi.org/10.1016/j.margeo.2020.106363

Zhu, B., Li, Y., Yue, Y., Yang, Y., Liang, E., Zhang, C., Borthwick, A.G.L., 2020. Alternate erosion and deposition in the Yangtze Estuary and the future change. J. Geogr. Sci. 30, 145–163. https://doi.org/10.1007/s11442-020-1720-0

Zhu C., Maren D., Guo L., Lin J., He Q., Wang Z., 2022. Feedback Effects of Sediment Suspensions on Transport Mechanisms in an Estuarine Turbidity Maximum. J Geophys. Res. - Oceans. 2022, 127(6): e2021JC018029. DOI10.1029/2021JC018029

Table and Figure Captions

Table 1. Datasets used in the present study

Fig. 1. (a) Topography and drainage network of the Yangtze and the Yellow river basins, with the locations of major reservoirs and gauging stations considered in this study. The schematic diagrams indicate the (b) Three Gorges Reservoir (TGR), (c) Three Gorges Dam (TGD), (d) Xiaolangdi Reservoir (XLDR), and (e) Xiaolangdi Dam.

Fig. 2. Daily water level time series for (a) TGR and (b) XLDR in four different years. Colored arrows in panel b indicate the abrupt drop in water level during the WSRS in corresponding years. Note that the WSRS was not implemented in 2016 due to a regional drought.

Fig. 3. Time series of annual sediment inflow, outflow, sedimentation, and trapping efficiency of (a) TGR and (b) XLDR since impoundment. Note that the sediment inflow into the TGR referred to herein encompasses cumulative sediment flux from both monitored gauged stations and ungauged areas. Detailed information and calculations are available in the paper by Liu et al. (2022).

Fig. 4. Daily inflow and outflow hydrographs of (a) TGR and (c) XLDR in 2012. Panels (b) and (d) indicate the outflow discharge and SSC of the TGR during the flood season and the XLDR during the WSRS, respectively.

Fig. 5. Mean daily water discharge time series at (a) Yichang, (b) Hankou and (c) Datong gauging stations in the Yangtze River basin before and after TGR operation, and at (d) Huayuankou, (e) Gaocun and (f) Lijin in the Yellow River basin in 1998 and 2008, before and after XLDR operation. Locations of these stations are shown in Fig. 1a.

Fig. 6. Monthly runoff and sediment load at (a) Yichang and (b) Datong, downstream of the TGR from 1980 to 2002 and 2003 to 2018. Monthly runoff and sediment load at (c) Huayuankou and (d) Lijin, downstream of the XLDR from 1980 to1998 and 2002 to 2018.

Fig. 7. Changes in water energy and sediment transport capacity over a year. Plots (a) and (b) show the monthly averaged U^3/h (see equation 4) time series at Hankou station, Yangtze River, and at Huayuankou station, Yellow River, before (brown line) and after (blue line) upstream dam impoundment. Plots (c) and (d) show the monthly relative sediment transport capacity (Q_{*r} = Q_* / (mean Q_* of pre-dam level)) time series at Hankou and Huayuankou before and

after upstream dam impoundment.

Fig. 8. Channel deposition (+ve, blue shading) or erosion (-ve, ochre shading) and SSC in: (a) the mid-lower Yangtze River (Yichang-Datong), and (b) the lower Yellow River (Huayuankou-Lijin) during the period from 1980 to 2018.

Fig. 9. Variations in (a) bankfull area, (b) bankfull discharge, and (c) U^3/h and relative sediment transport capacity at Huayuankou Station, Yellow River during 1986-2016.

Fig. 10. Changes in median grain size of riverbed sediment in (a) the mid-lower Yangtze River and (b) the lower Yellow River before and after reservoir regulation was implemented.

Fig. 11. Average annual erosion intensity (10^4 t/km/yr) from 2002 to 2018 in (a) the mid-lower Yangtze River and (b) the lower Yellow River.

Fig. 12. Responses of water level to water discharge in the years before and after impoundment of the TGR and the XLDR. (a) Yichang, (b) Hankou, and (c) Datong stations along the Yangtze River; (d) Huayuankou, and (e) Lijin stations along the lower Yellow River.

Fig. 13. Variation in (a) Manning roughness coefficient ($s/m^{1/3}$) in the mid-lower Yangtze River before and after TGR impoundment; (b) riverbed resistance (a dimensionless coefficient, following Ma et al., 2022) of the lower Yellow River before and after XLDR impoundment; and (c) amplification ratio of Manning roughness coefficient with rising discharge magnitude in the mid-lower Yangtze River.

Fig. 14. Flowcharts of the annual sediment budget along the Yangtze River downstream of Zhutuo: (a) pre-TGR period, 1956-1980; (b) pre-TGR period, 1981-2002; and (c) post-TGR period, 2003-2018. Prefixes "+" or "-" represent erosion or deposition along the river channel or in Dongting Lake.

Fig. 15. Flowcharts of the annual sediment budget along the Yellow River downstream of Sanmenxia Reservoir: (a) pre-XLDR period; (b) after XLDR impoundment but before the WSRS was implemented; and (c) post-WSRS implementation. Prefixes "+" or "-" represent erosion or deposition along the river channel.

Fig. 16. Time-averaged variations in: (a) land area of Eastern Chongming, the Yangtze River subaerial delta; (b) sediment accumulation rate in the Yangtze River subaqueous delta; (c) land area of the Yellow River subaerial delta; and (d) sediment accumulation rate in the Yellow River subaqueous delta. The boundary between subaerial and subaqueous delta is

1479 referenced to the lowest tide datum. Data obtained from Yang et al. (2020a), Bi et al. (2021)
1480 and Luan et al. (2021).
1481 **Fig. 17.** (a) Brune (1953) curve and trapping efficiency of large reservoirs. Each circle
1482 indicates the observed trapping data for one individual reservoir. The C/I ratio indicates the
1483 ratio of reservoir capacity to inflow. (b) Observed trapping data for the TGR and XLDR. Note
1484 that the WSRS was implemented from 2002-2014 but was not operated in 2015-2017. During
1485 the WSRS period in 2018 and 2019, the water level of the XLDR was further lowered to
1486 better release sediment.

Table 1. Datasets used in the present study

Datasets	Description	Time range	Data source
Hydrographic data	• Daily water discharge at Yichang, Hankou and Datong stations along the Yangtze River and at Huayuankou, Gaocun and Lijin stations along the Yellow River	1980-2018	CJWRC; YRCC; Wang et al., 2020
	• Daily inflow and outflow of the TGR and XLDR	2012	CJWRC; YRCC
	• Monthly water discharge and sediment load at Yichang, Hankou and Datong stations along the Yangtze River mainstream and at Huayuankou, Gaocun and Lijin stations along the Yellow River mainstream	1980-2018	CJWRC; YRCC
	• Annual sediment load at Xinjiangkou, Shadaoguan, Mituosi, Ouchi (Kang), Ouchi (Guan), Chenglingji, Huangzhuang, and Hukou stations along tributaries of the Yangtze River and Heishiguan and Wuzhi stations along tributaries of the Yellow River	2000-2018	CJWRC; YRCC
	• Daily water level at Yichang, Hankou and Datong stations along the Yangtze River and at Huayuankou and Lijin stations along the Yellow River	2002, 2012 and 2016 for Yangtze River;1981 and 2018 for Yellow River	CJWRC; YRCC
Reservoir sedimentation	• Monthly and annual sedimentation in the TGR and XLDR	2003-2018	Yang et al., 2014; Liu et al., 2022; Present study
Water level in reservoir	• Daily water level in the TGR and XLDR	2006-2018	CJWRC; YRCC
Grain size of riverbed sediment	• Median grain size of riverbed sediment in the mid-lower Yangtze River and the lower Yellow River	2002 and 2021 for Yangtze River; 1999 and 2019 for Yellow River	Yang et al., 2022; YRCC

Channel deposition	• Channel deposition or erosion in the mid-lower Yangtze River and the lower Yellow River	1980-2018	Yang et al., 2014 Present study
Sediment budget	• Sediment budget along the Yangtze River downstream of the Zhutuo Station and along the Yellow River downstream of the Sanmenxia Reservoir	1956-2018 for Yangtze River and 1980-2018 for Yellow River	Wang et al., 2007; Yang et al., 2014; Present study
Delta evolution	• Time-averaged variation of land areas of the subaerial delta and accumulation rates in the subaqueous delta	1958-2015 for Yangtze River Delta; 1976-2013 for Yellow River Delta	Bi et al., 2021; Luan et al., 2021; Yang et al., 2020a

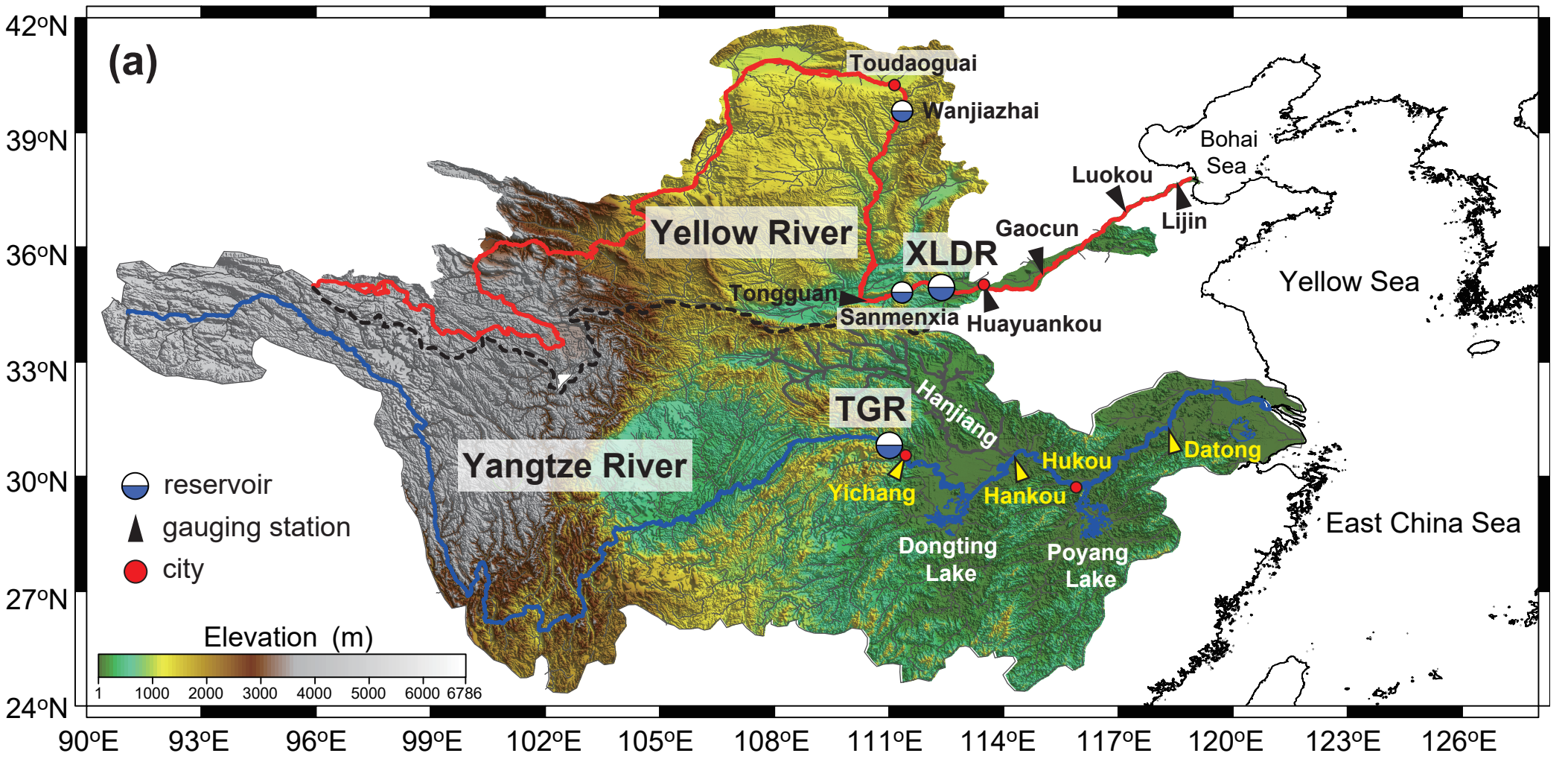
(a)
42°N
39°N
36°N
33°N
30°N
27°N
24°N
90°E
93°E
96°E
99°E
102°E
105°E
108°E
111°E
114°E
117°E
120°E
123°E
126°E
Toudaoguai
Wanjiazhai
Yellow River
XLDR
Tongguan
Sanmenxia
Huayuankou
Gaocun
Luokou
Lijin
Bohai Sea
Yellow Sea
East China Sea
TGR
Hanjiang
Yangtze River
Yichang
Hukou
Hankou
Datong
Dongting Lake
Poyang Lake
reservoir
gauging station
city
Elevation (m)
1
1000
2000
3000
4000
5000
6000
6786

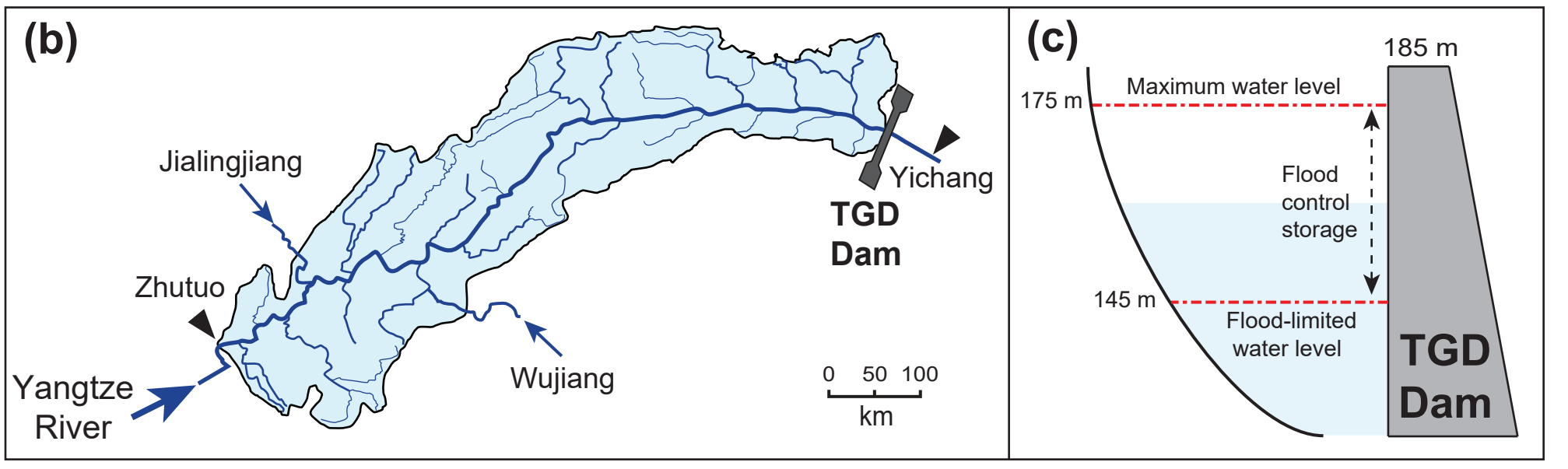
(b)
Jialingjiang
Zhutuo
Yangtze River
Wujiang
Yichang
TGD Dam
0 50 100
km
(c)
185 m
Maximum water level
175 m
Flood control storage
145 m
Flood-limited water level
TGD Dam

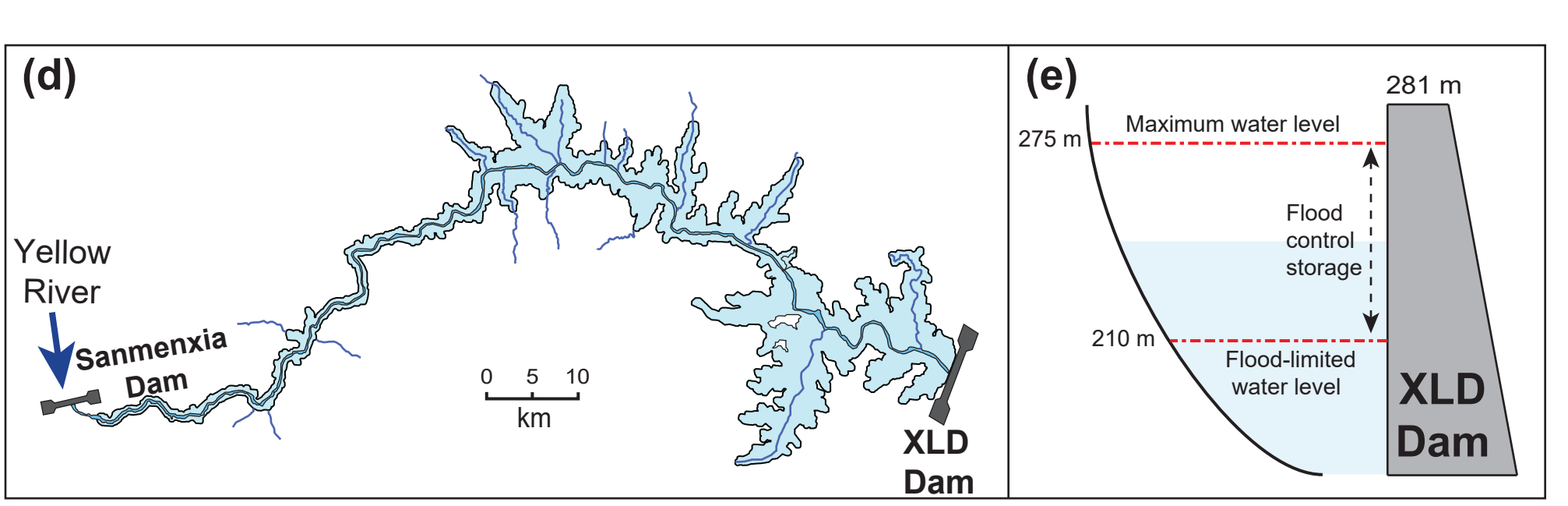
(d)
Yellow River
Sanmenxia Dam
0 5 10
km
XLD Dam
(e)
281 m
Maximum water level
275 m
Flood control storage
210 m
Flood-limited water level
XLD Dam

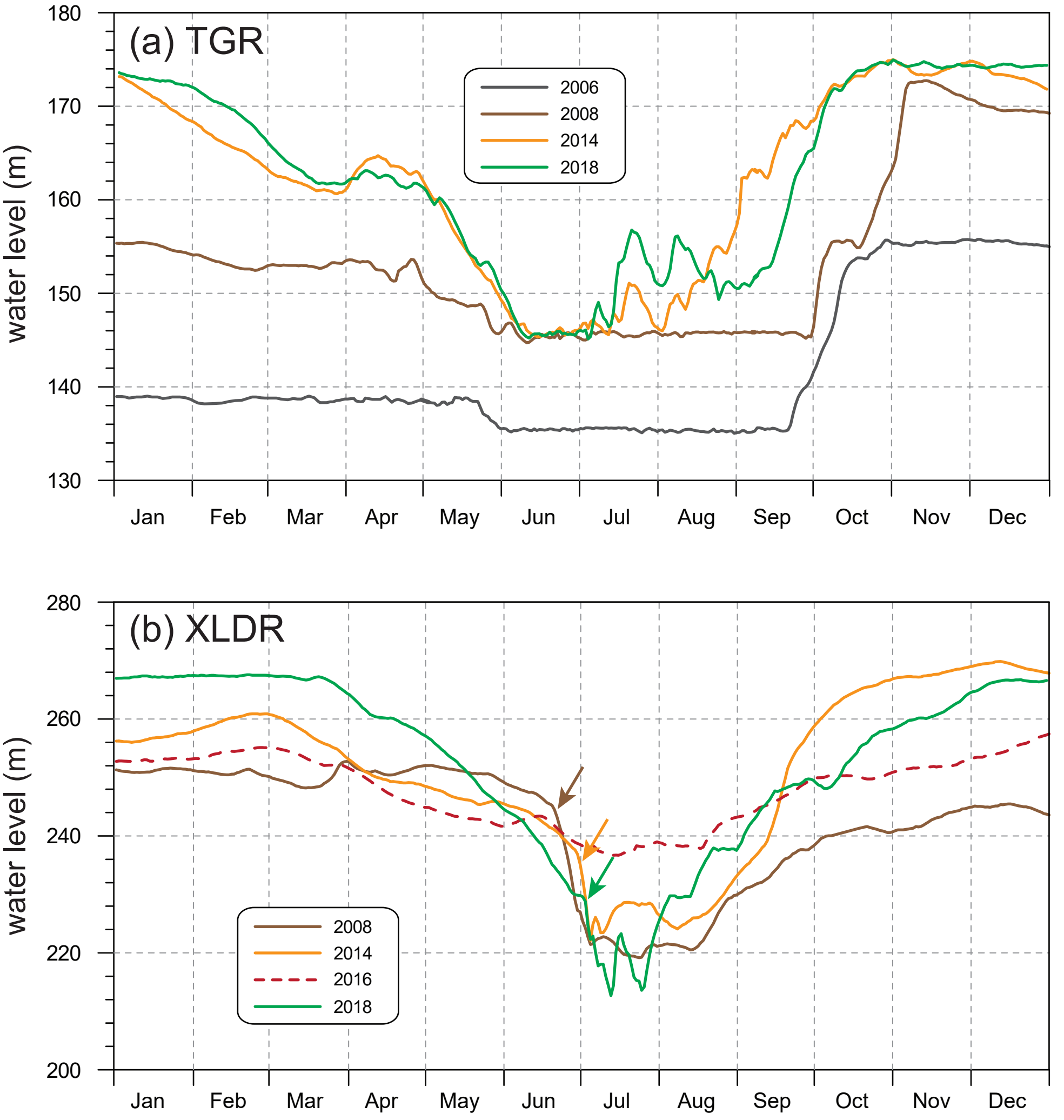
(a) TGR
water level (m)
180
170
160
150
140
130
Jan
Feb
Mar
Apr
May
Jun
Jul
Aug
Sep
Oct
Nov
Dec
2006
2008
2014
2018
(b) XLDR
water level (m)
280
260
240
220
200
2008
2014
2016
2018

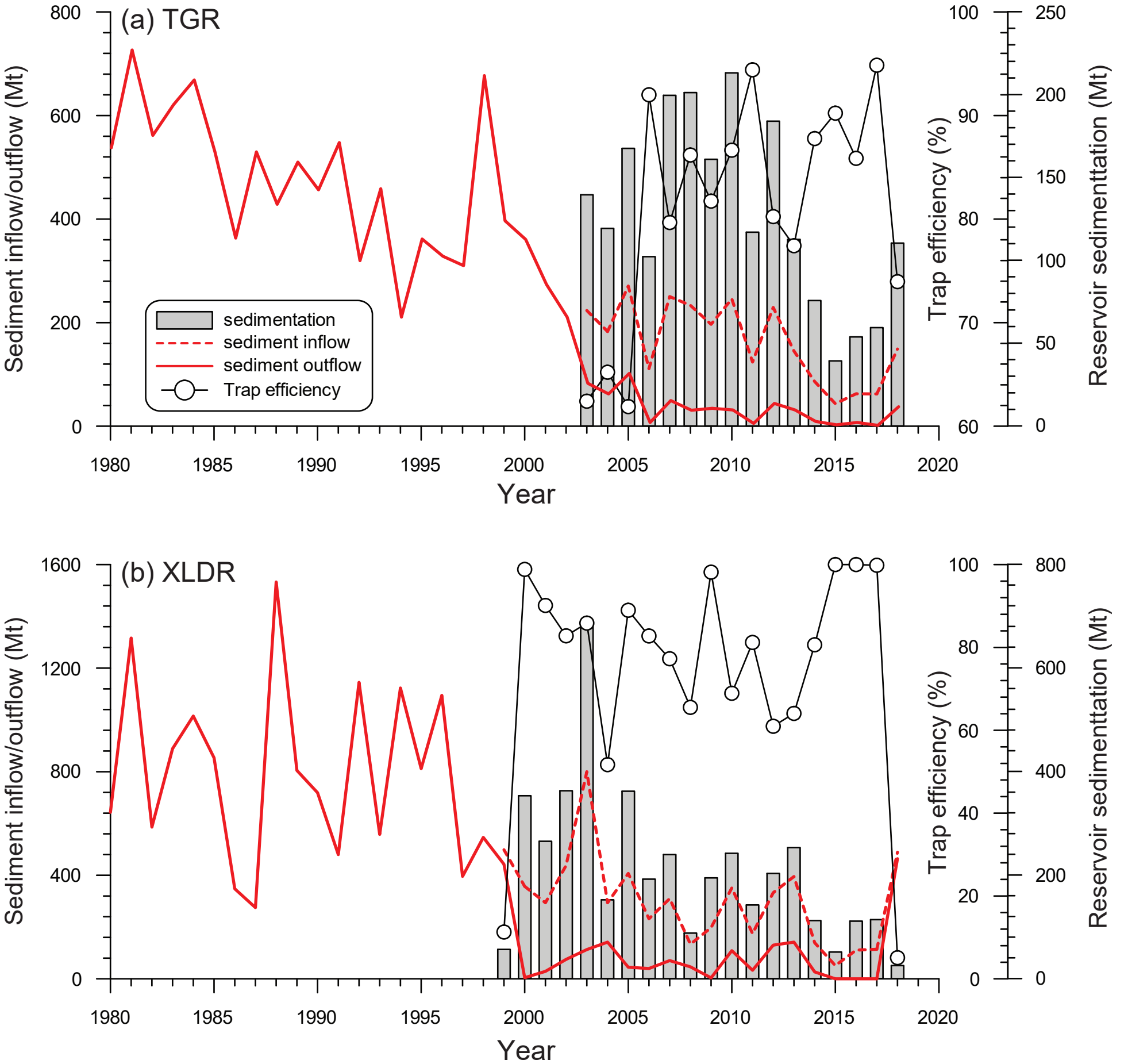
(a) TGR
Sediment inflow/outflow (Mt)
Trap efficiency (%)
Reservoir sedimenttation (Mt)
sedimentation
sediment inflow
sediment outflow
Trap efficiency
Year
(b) XLDR
Sediment inflow/outflow (Mt)
Trap efficiency (%)
Reservoir sedimenttation (Mt)
Year

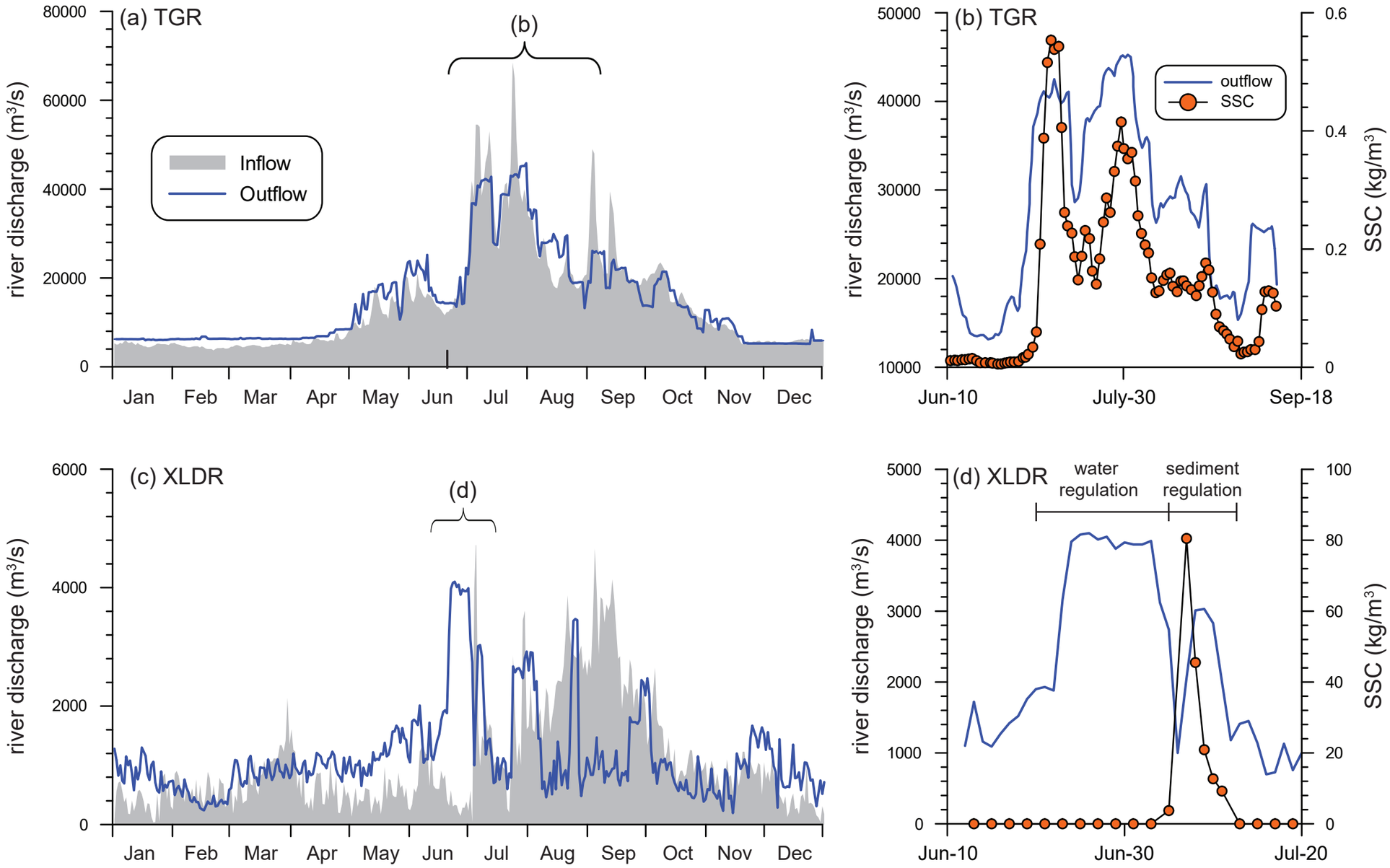
(a) TGR
(b)
Inflow
Outflow
river discharge (m³/s)
80000
60000
40000
20000
0
Jan
Feb
Mar
Apr
May
Jun
Jul
Aug
Sep
Oct
Nov
Dec
(b) TGR
outflow
SSC
river discharge (m³/s)
SSC (kg/m³)
50000
40000
30000
20000
10000
0.6
0.4
0.2
0
Jun-10
July-30
Sep-18
(c) XLDR
(d)
river discharge (m³/s)
6000
4000
2000
0
(d) XLDR
water regulation
sediment regulation
SSC (kg/m³)
5000
4000
3000
2000
1000
0
100
80
60
40
20
0
Jun-10
Jun-30
Jul-20

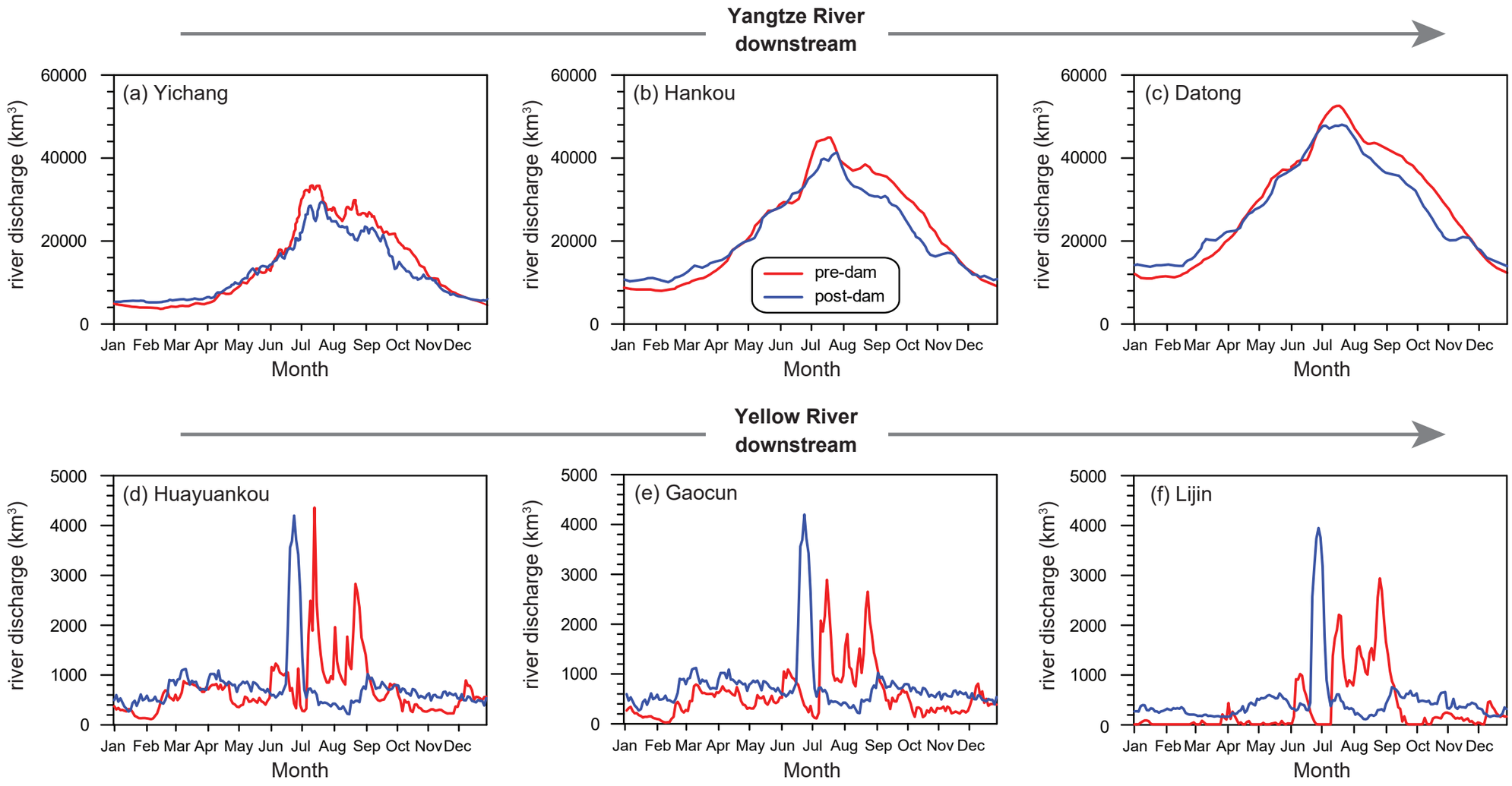
Yangtze River
downstream
(a) Yichang
(b) Hankou
(c) Datong
pre-dam
post-dam
river discharge (km3)
60000
40000
20000
0
Jan Feb Mar Apr May Jun Jul Aug Sep Oct Nov Dec
Month
Yellow River
downstream
(d) Huayuankou
(e) Gaocun
(f) Lijin
5000
4000
3000
2000
1000
0

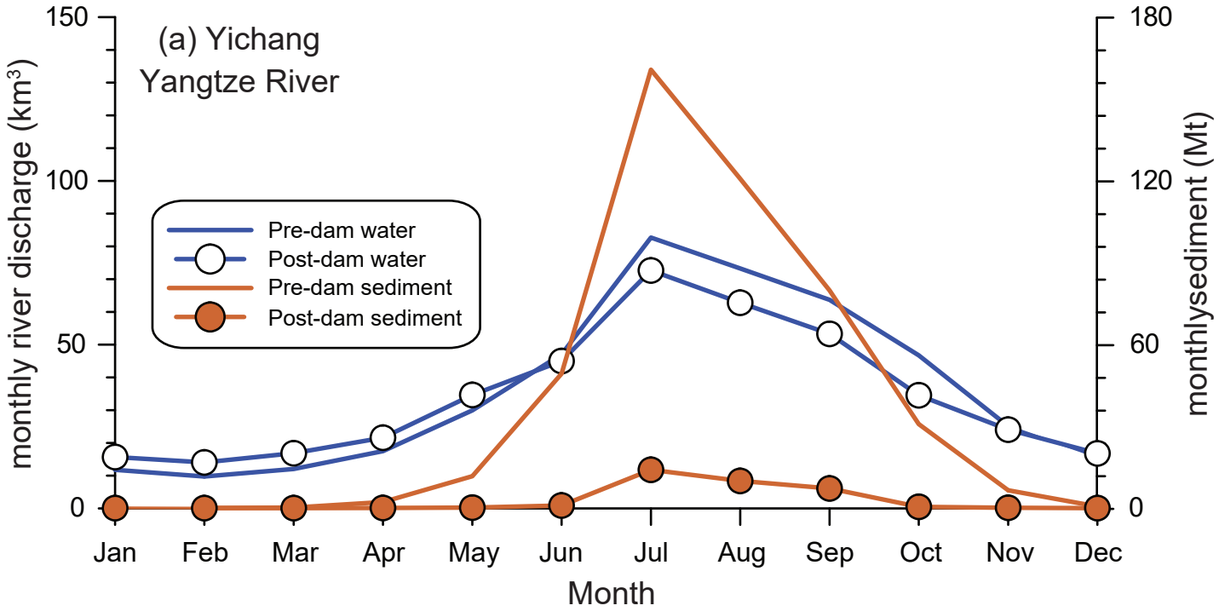
(a) Yichang
Yangtze River
Pre-dam water
Post-dam water
Pre-dam sediment
Post-dam sediment
monthly river discharge (km3)
monthlysediment (Mt)
0
50
100
150
0
60
120
180
Jan
Feb
Mar
Apr
May
Jun
Jul
Aug
Sep
Oct
Nov
Dec
Month

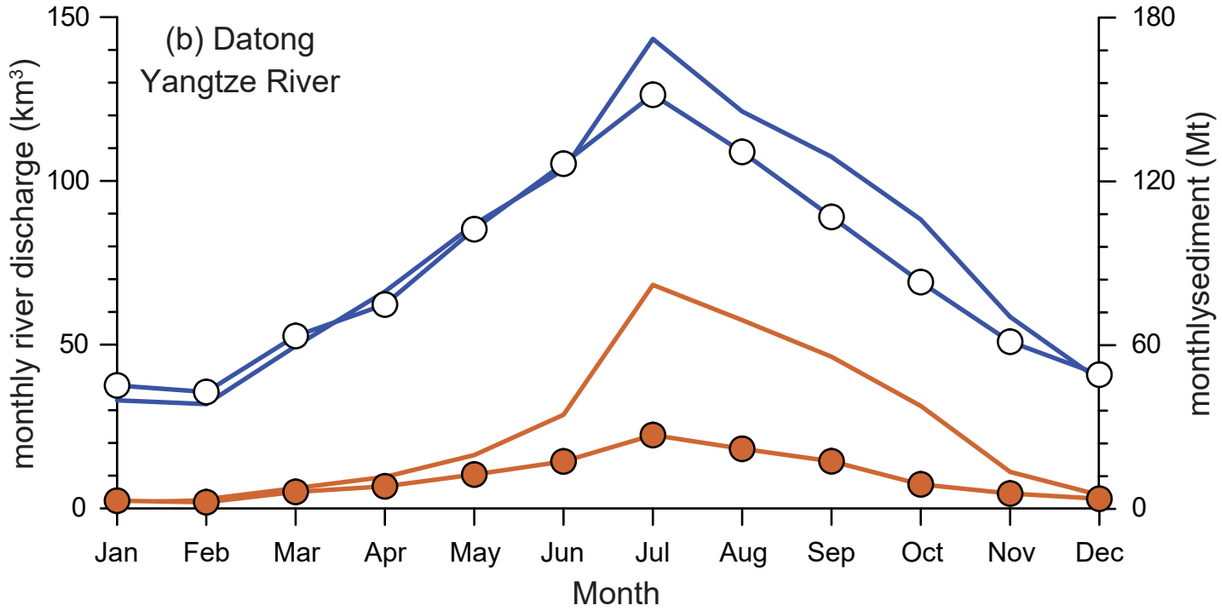
(b) Datong
Yangtze River
monthly river discharge (km3)
monthlysediment (Mt)
0
50
100
150
0
60
120
180
Jan
Feb
Mar
Apr
May
Jun
Jul
Aug
Sep
Oct
Nov
Dec
Month

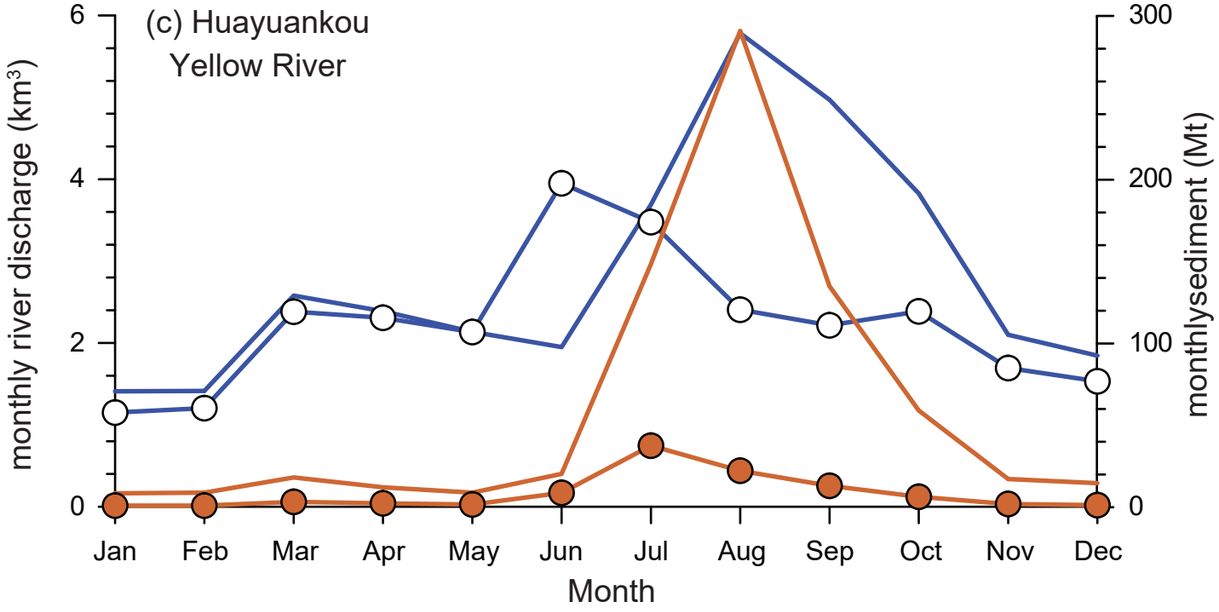
(c) Huayuankou
Yellow River
monthly river discharge (km3)
monthlysediment (Mt)
0
2
4
6
0
100
200
300
Jan
Feb
Mar
Apr
May
Jun
Jul
Aug
Sep
Oct
Nov
Dec
Month

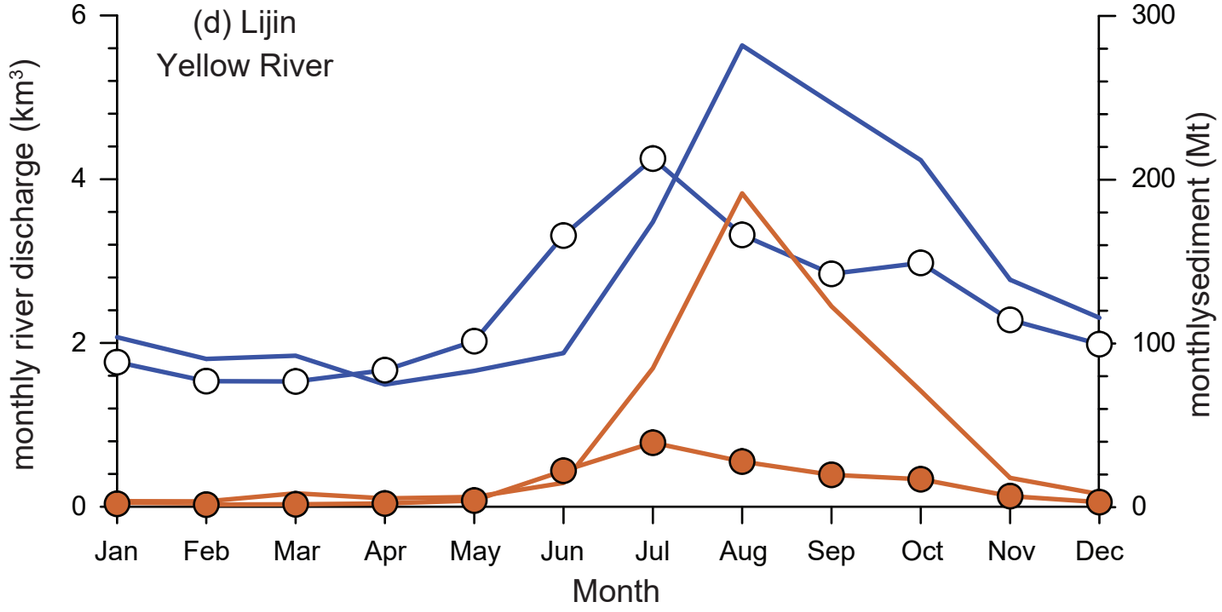
(d) Lijin
Yellow River
monthly river discharge (km3)
monthlysediment (Mt)
0
2
4
6
0
100
200
300
Jan
Feb
Mar
Apr
May
Jun
Jul
Aug
Sep
Oct
Nov
Dec
Month

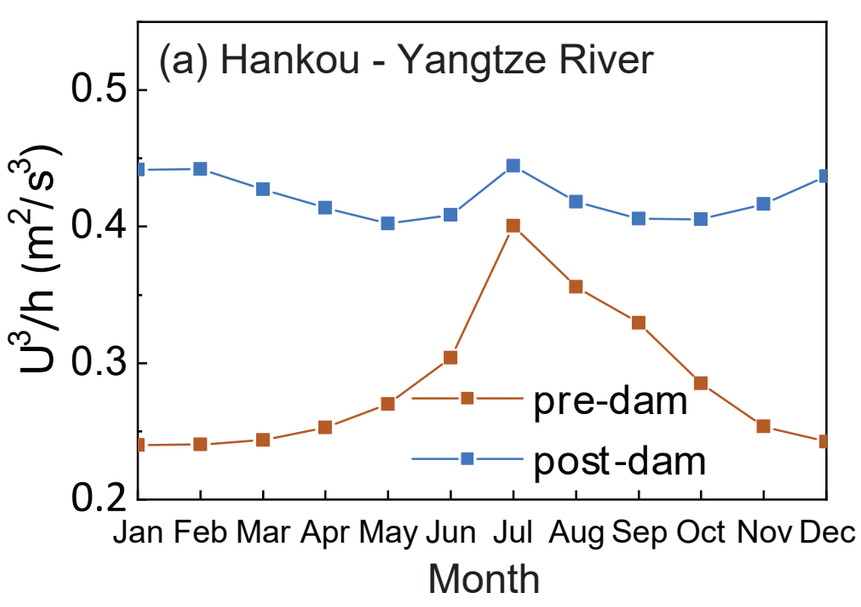
(a) Hankou - Yangtze River
0.5
0.4
0.3
0.2
U³/h (m²/s³)
pre-dam
post-dam
Jan Feb Mar Apr May Jun Jul Aug Sep Oct Nov Dec
Month

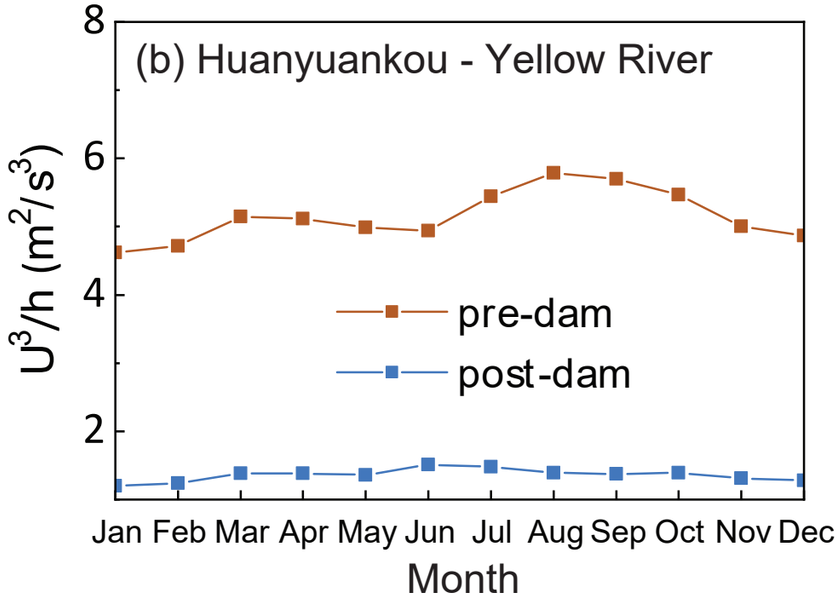
(b) Huanyuankou - Yellow River
8
6
4
2
U³/h (m²/s³)
pre-dam
post-dam
Jan Feb Mar Apr May Jun Jul Aug Sep Oct Nov Dec
Month

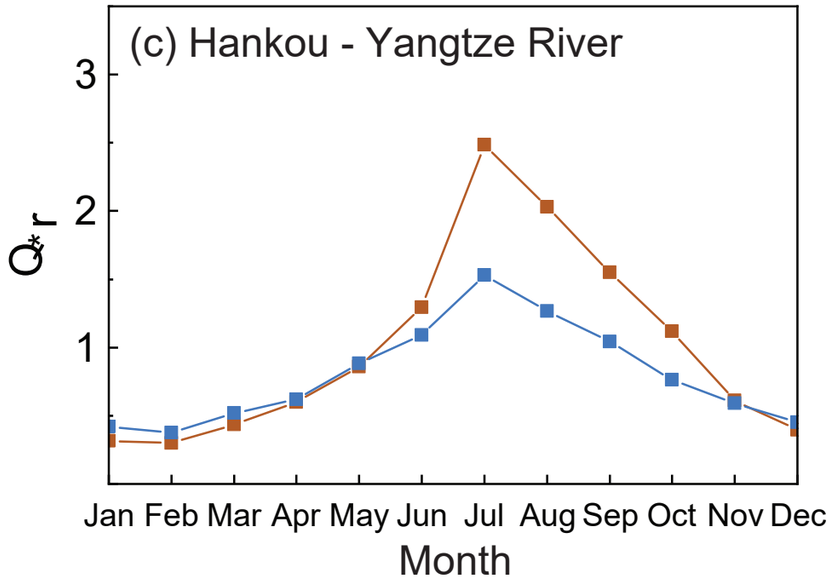
(c) Hankou - Yangtze River
3
2
1
Q*r
Jan Feb Mar Apr May Jun Jul Aug Sep Oct Nov Dec
Month

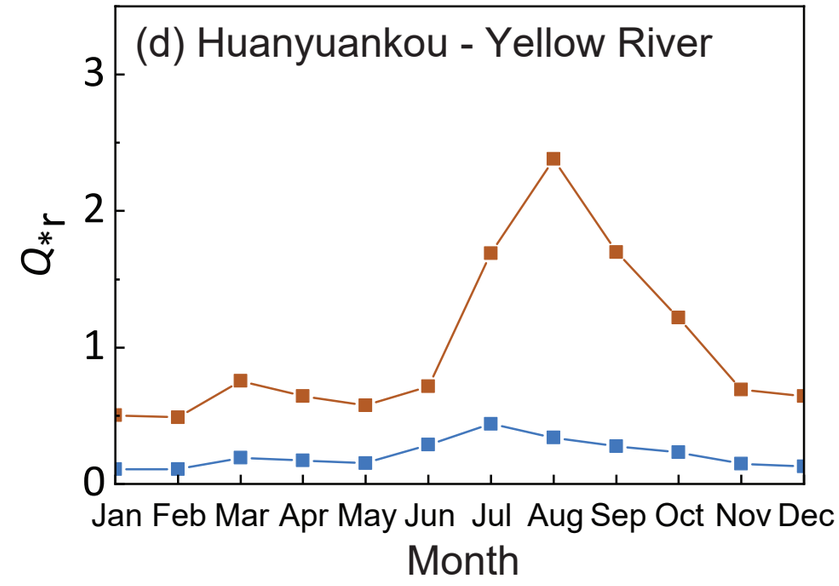
(d) Huanyuankou - Yellow River
3
2
1
0
Q*r
Jan Feb Mar Apr May Jun Jul Aug Sep Oct Nov Dec
Month

(a) Mid-lower Yangtze River

channel deposition (+) or erosion (-) (Mt/yr)

SSC at Yichang (kg/m^3)

Channel deposition (+) / erosion (-)

SSC into the mid-lower channel

(b) Lower Yellow River

channel deposition (+) or erosion (-) (Mt/yr)

SSC at Huayuankou (kg/m^3)

Channel deposition (+) / erosion (-)

SSC into the lower channel

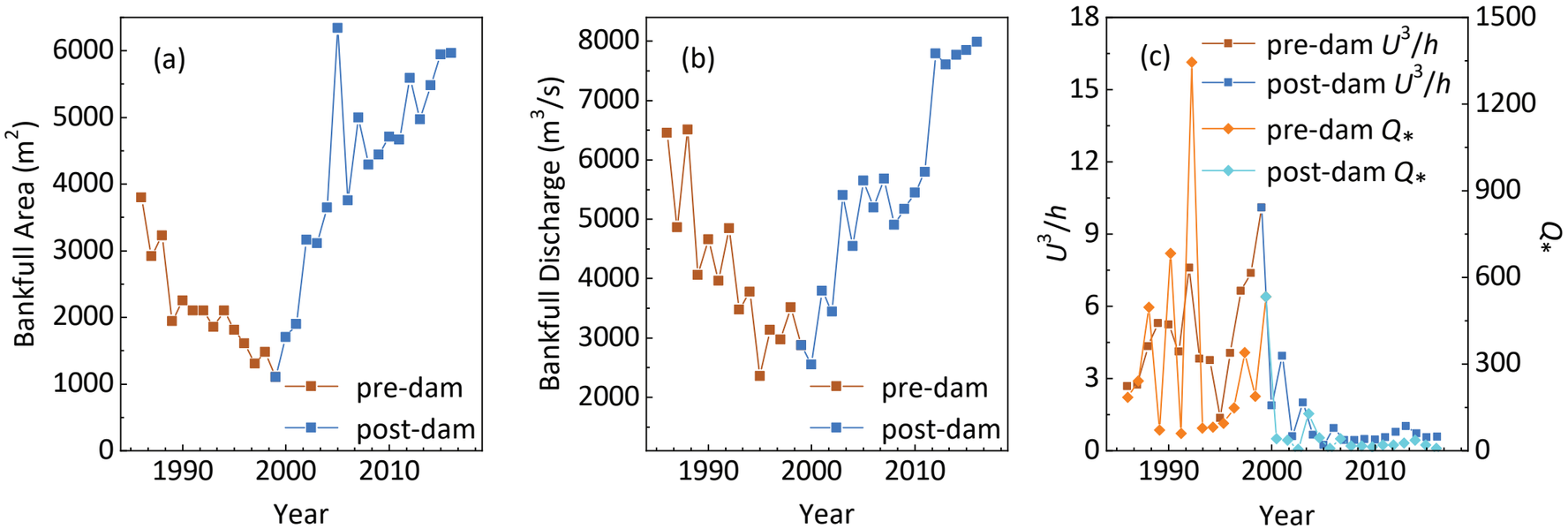
(a)
Bankfull Area (m^2)
6000
5000
4000
3000
2000
1000
0
1990
2000
2010
Year
pre-dam
post-dam
(b)
Bankfull Discharge (m^3/s)
8000
7000
6000
5000
4000
3000
2000
1990
2000
2010
Year
pre-dam
post-dam
(c)
U^3/h
18
15
12
9
6
3
0
Q_*
1500
1200
900
600
300
0
1990
2000
2010
Year
pre-dam U^3/h
post-dam U^3/h
pre-dam Q_*
post-dam Q_*

(a)

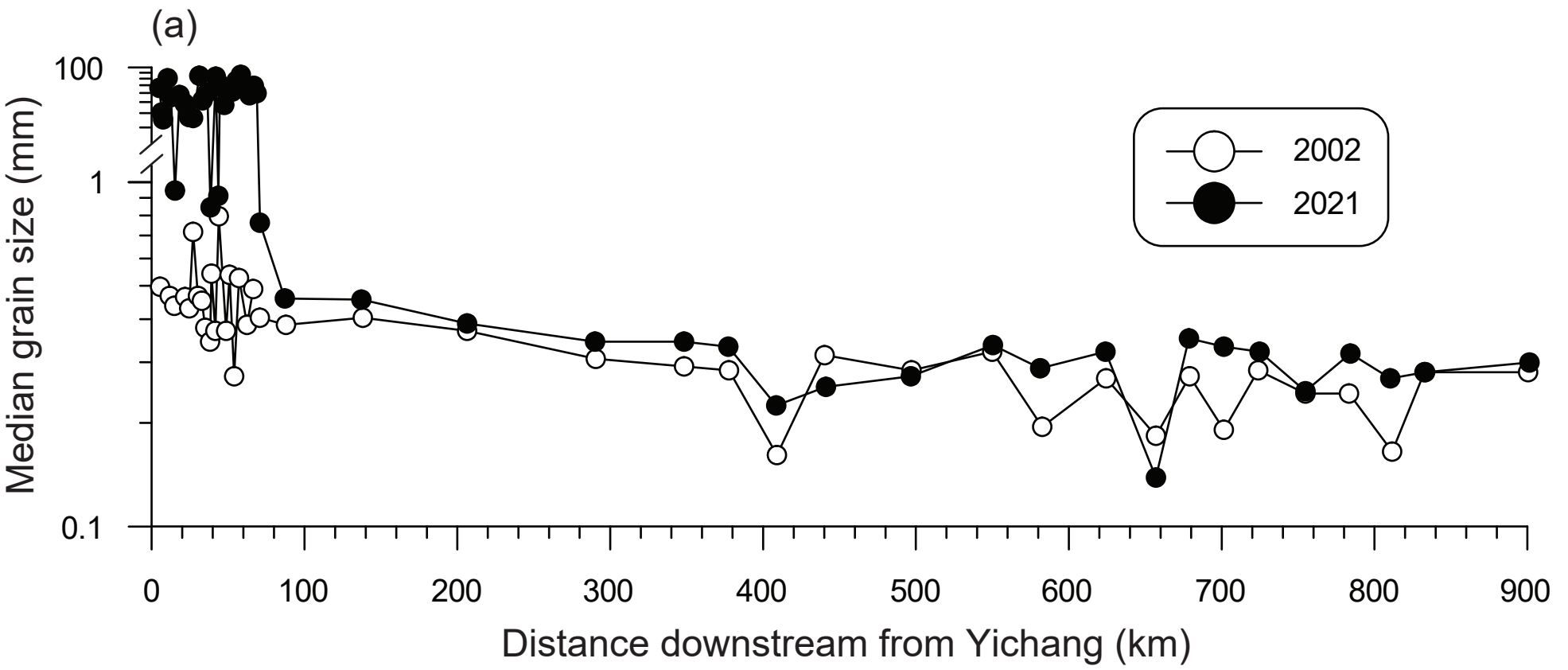
Median grain size (mm)
100
1
0.1
0
100
200
300
400
500
600
700
800
900
Distance downstream from Yichang (km)
2002
2021

(b)

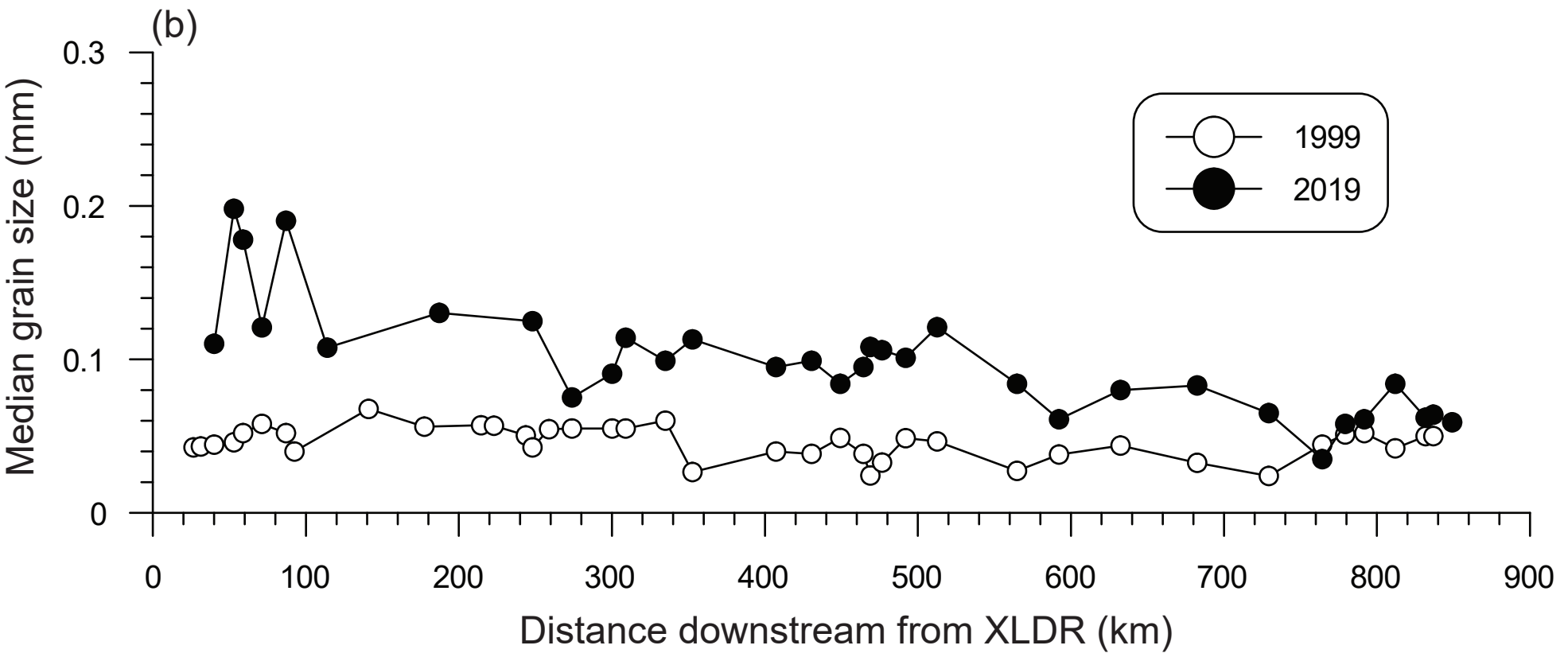
Median grain size (mm)
0.3
0.2
0.1
0
0
100
200
300
400
500
600
700
800
900
Distance downstream from XLDR (km)
1999
2019

(a) Yangtze River

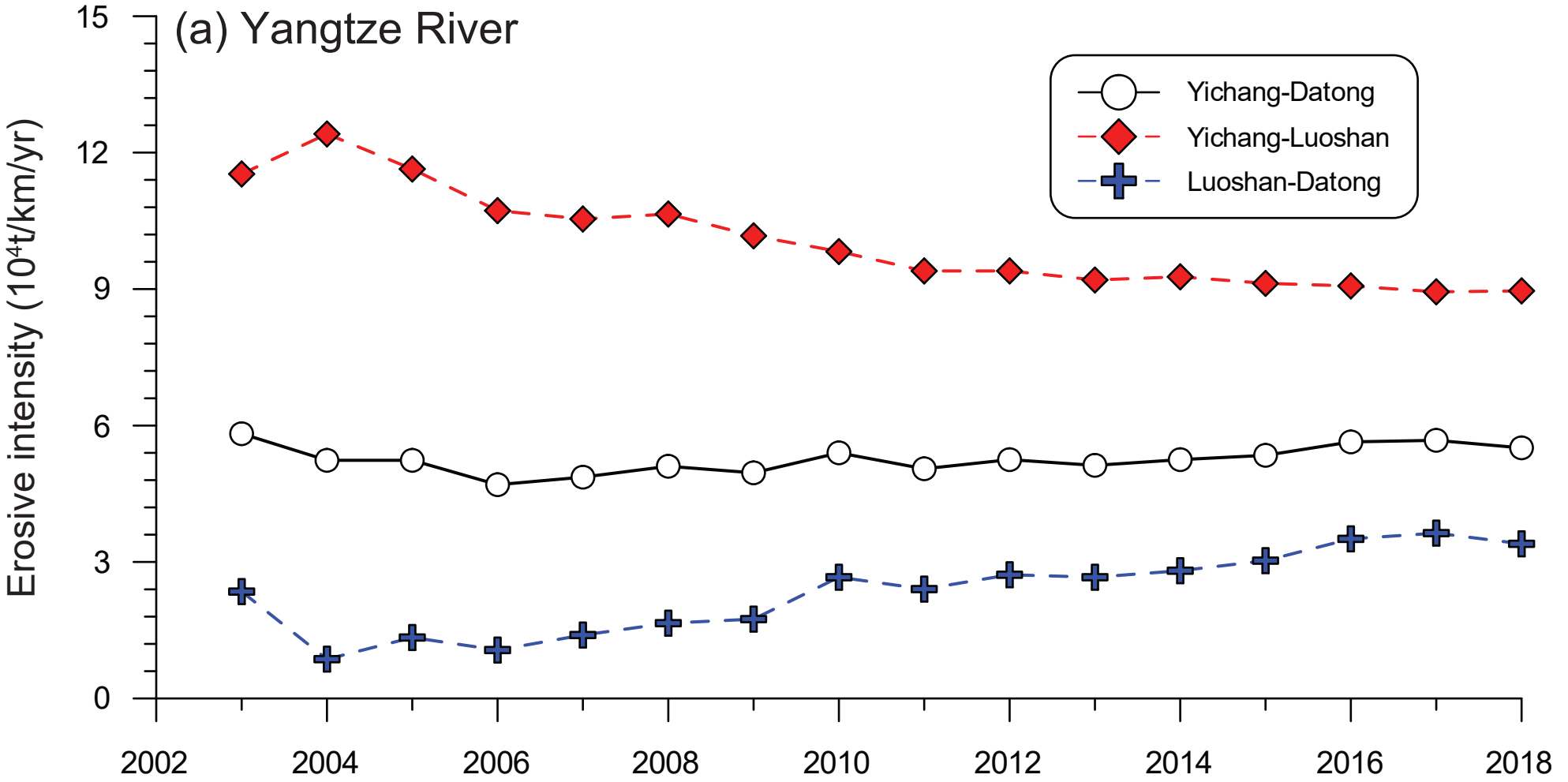

(b) Yellow River

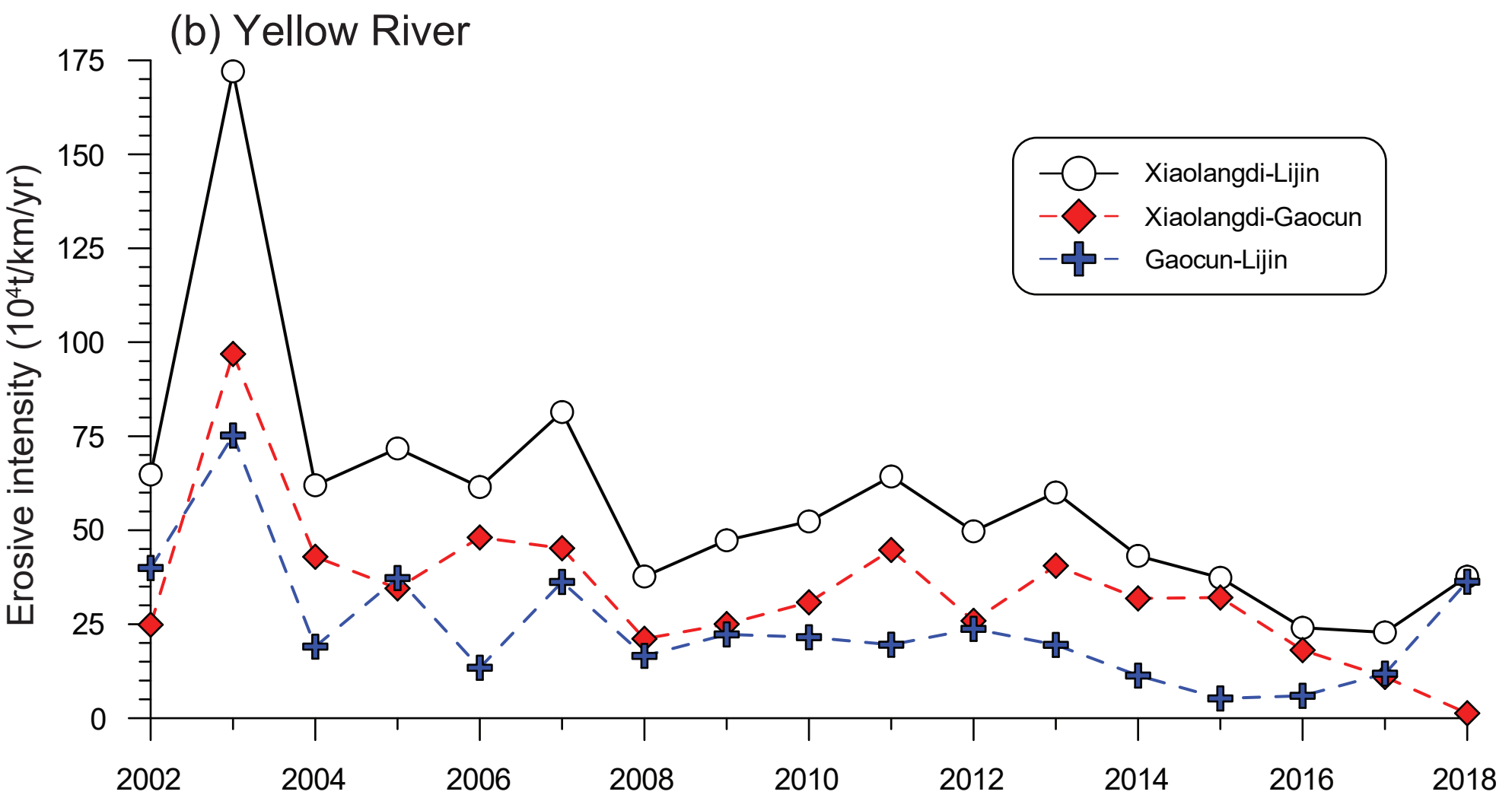

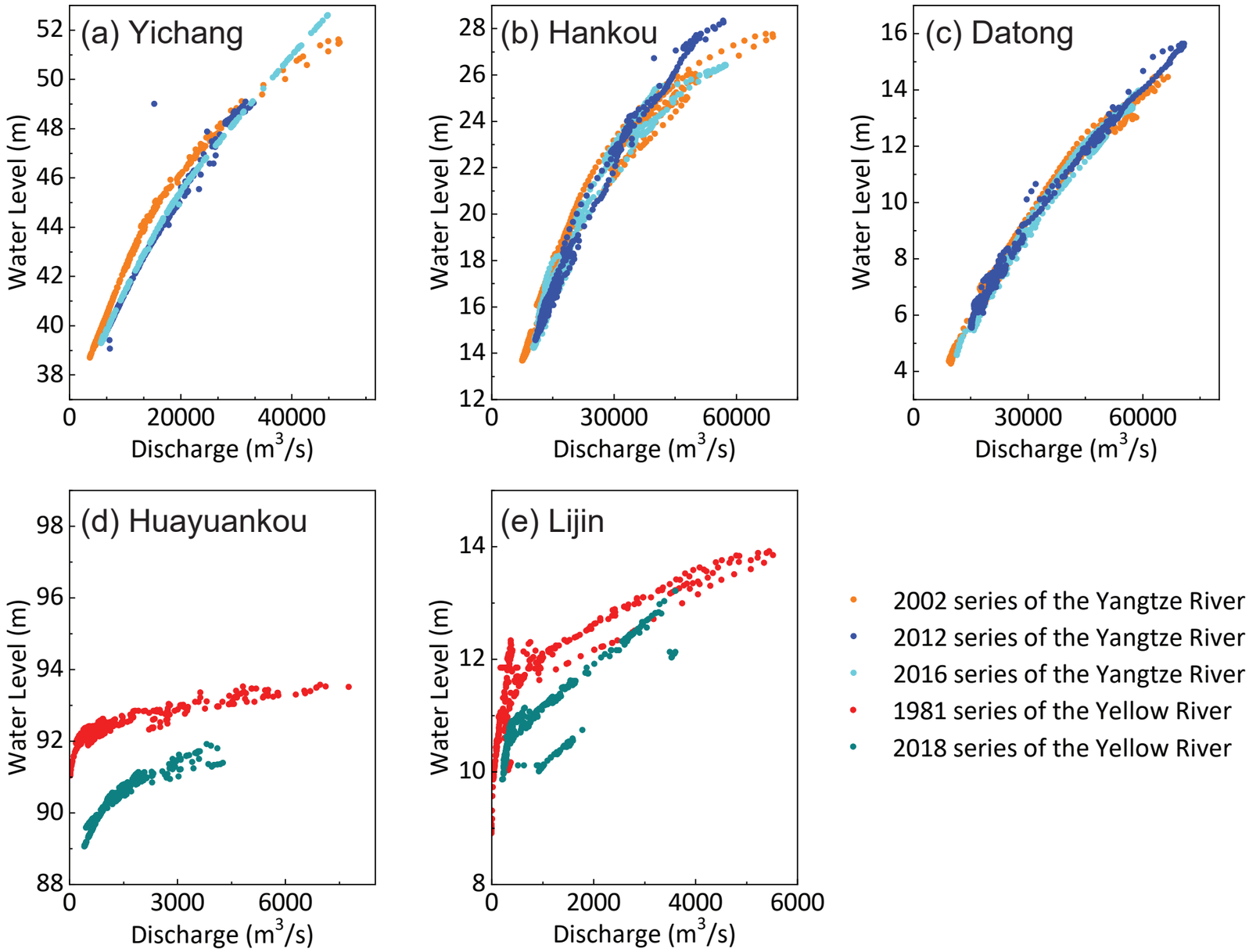
(a) Yichang
(b) Hankou
(c) Datong
(d) Huayuankou
(e) Lijin
Water Level (m)
Discharge (m3/s)
2002 series of the Yangtze River
2012 series of the Yangtze River
2016 series of the Yangtze River
1981 series of the Yellow River
2018 series of the Yellow River

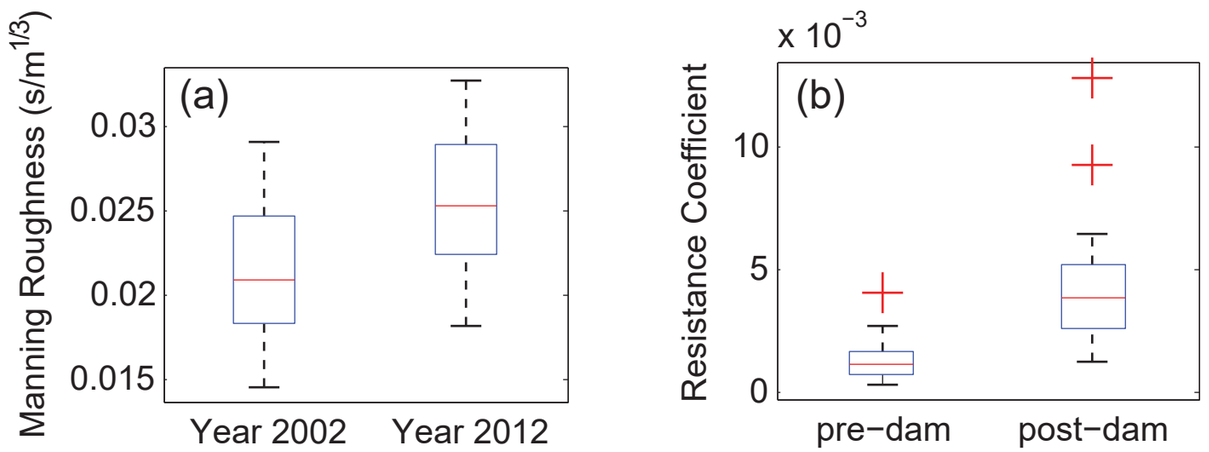
(a)
Manning Roughness (s/m^1/3)
0.03
0.025
0.02
0.015
Year 2002
Year 2012
(b)
x 10^-3
Resistance Coefficient
10
5
0
pre−dam
post−dam
(c)
Amplification Ratio of Manning Roughness
1.35
1.3
1.25
1.2
1.15
1.1
0.5
1
1.5
2
2.5
3
3.5
4
x 10^4
Discharge Magnitude (m^3/s)

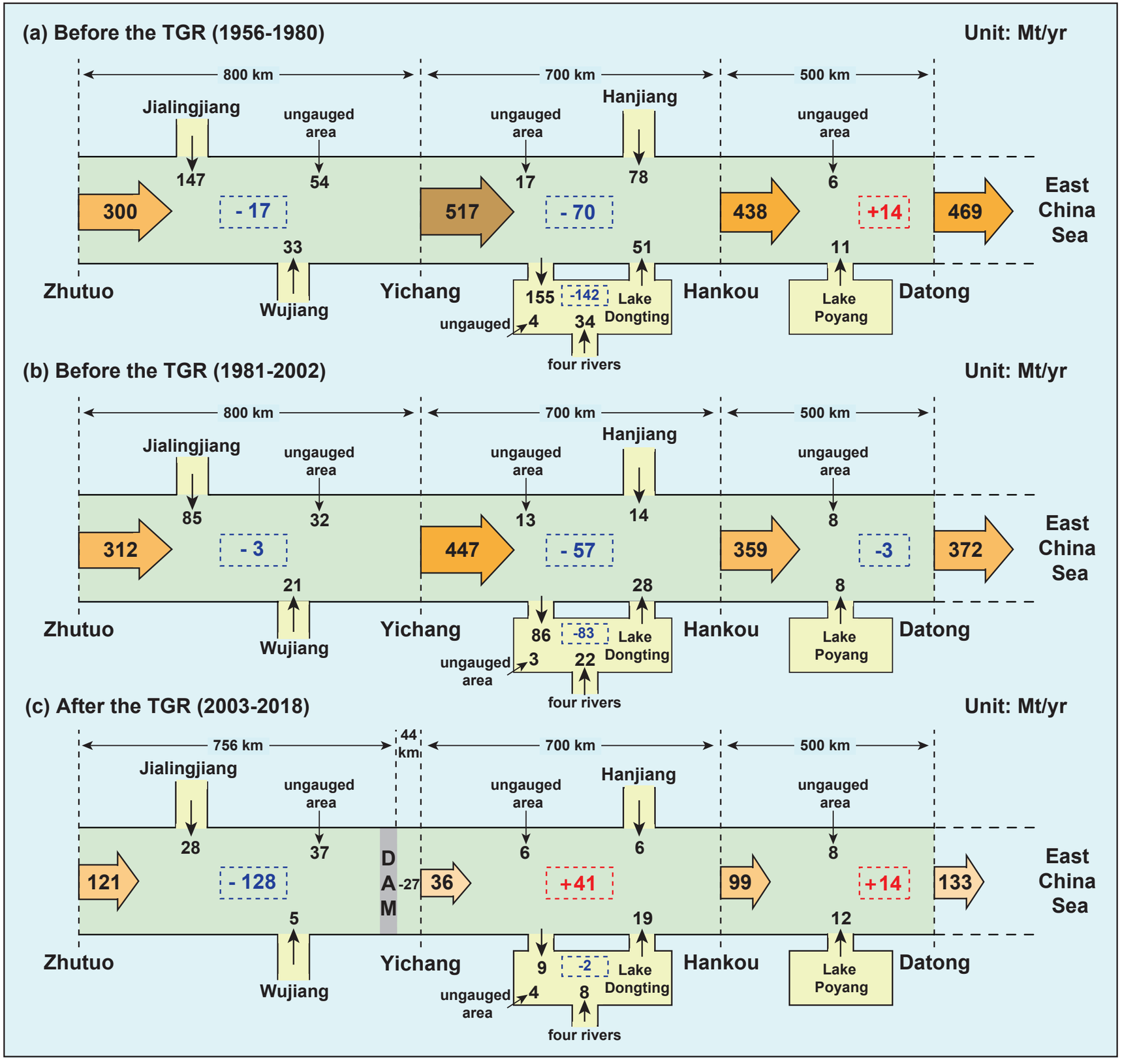
(a) Before the TGR (1956-1980)
Unit: Mt/yr
800 km
700 km
500 km
Jialingjiang
Hanjiang
ungauged area
ungauged area
ungauged area
147
54
17
78
6
300
- 17
517
- 70
438
+14
469
East China Sea
33
51
11
Zhutuo
Wujiang
Yichang
155
-142
Lake Dongting
Hankou
Lake Poyang
Datong
ungauged
4
34
four rivers
(b) Before the TGR (1981-2002)
Unit: Mt/yr
800 km
700 km
500 km
Jialingjiang
Hanjiang
ungauged area
ungauged area
ungauged area
85
32
13
14
8
312
- 3
447
- 57
359
-3
372
East China Sea
21
28
8
Zhutuo
Wujiang
Yichang
86
-83
Lake Dongting
Hankou
Lake Poyang
Datong
ungauged area
3
22
four rivers
(c) After the TGR (2003-2018)
Unit: Mt/yr
756 km
44 km
700 km
500 km
Jialingjiang
Hanjiang
ungauged area
ungauged area
ungauged area
28
37
6
6
8
121
- 128
DAM
-27
36
+41
99
+14
133
East China Sea
5
19
12
Zhutuo
Wujiang
Yichang
9
-2
Lake Dongting
Hankou
Lake Poyang
Datong
ungauged area
4
8
four rivers

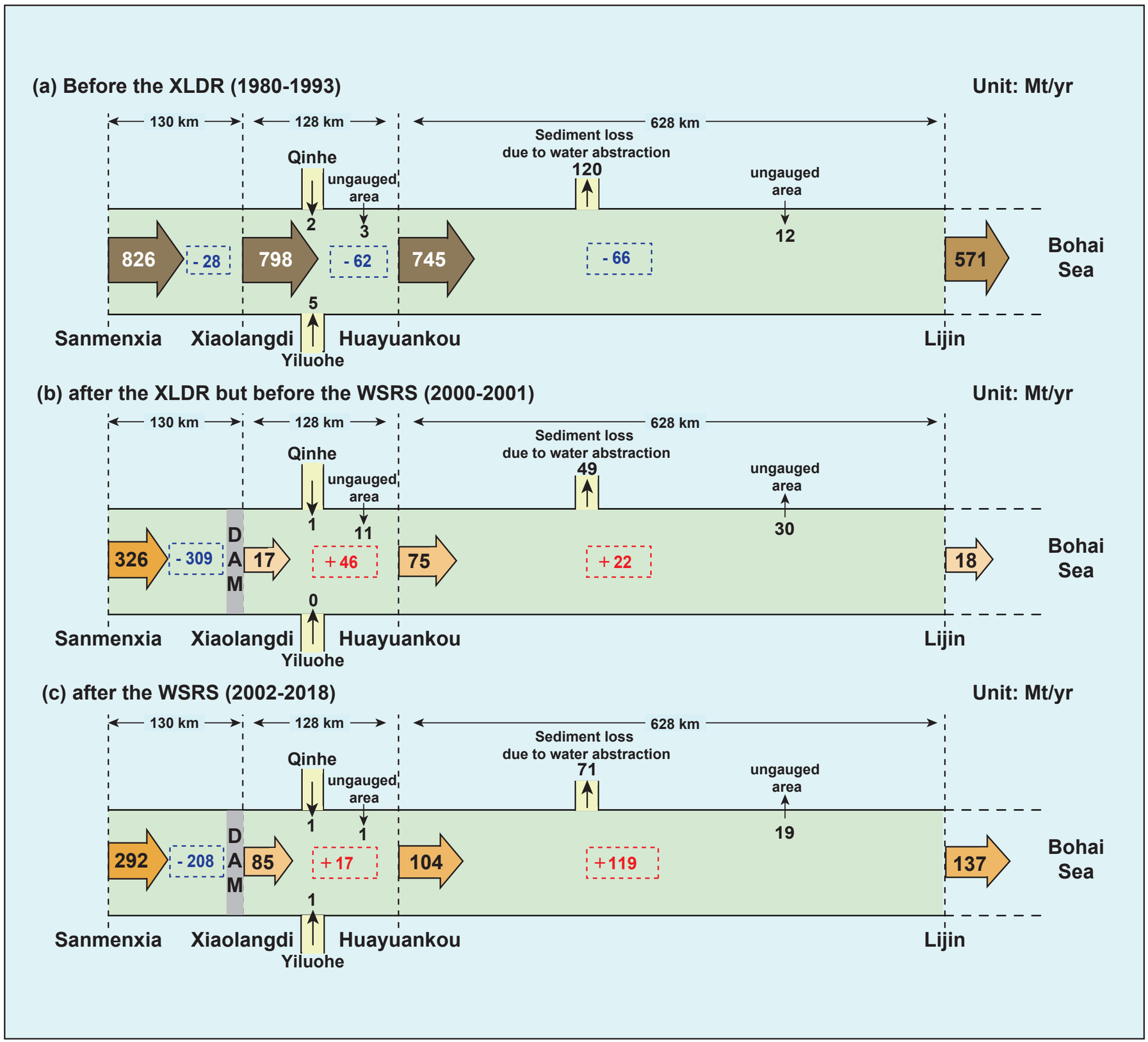
(a) Before the XLDR (1980-1993)
Unit: Mt/yr
130 km
128 km
628 km
Sediment loss
due to water abstraction
Qinhe
ungauged
area
120
ungauged
area
2
3
12
826
- 28
798
- 62
745
- 66
571
Bohai
Sea
5
Sanmenxia
Xiaolangdi
Huayuankou
Lijin
Yiluohe
(b) after the XLDR but before the WSRS (2000-2001)
Unit: Mt/yr
130 km
128 km
628 km
Sediment loss
due to water abstraction
Qinhe
ungauged
area
49
ungauged
area
1
11
30
326
- 309
DAM
17
+ 46
75
+ 22
18
Bohai
Sea
0
Sanmenxia
Xiaolangdi
Huayuankou
Lijin
Yiluohe
(c) after the WSRS (2002-2018)
Unit: Mt/yr
130 km
128 km
628 km
Sediment loss
due to water abstraction
Qinhe
ungauged
area
71
ungauged
area
1
1
19
292
- 208
DAM
85
+ 17
104
+ 119
137
Bohai
Sea
1
Sanmenxia
Xiaolangdi
Huayuankou
Lijin
Yiluohe

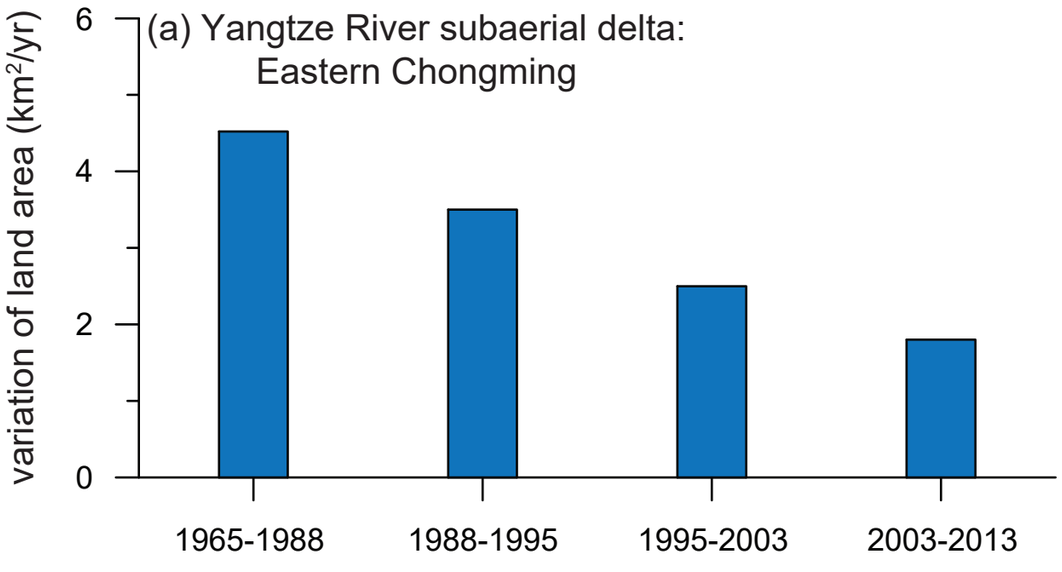
(a) Yangtze River subaerial delta:
Eastern Chongming
variation of land area (km²/yr)
6
4
2
0
1965-1988
1988-1995
1995-2003
2003-2013

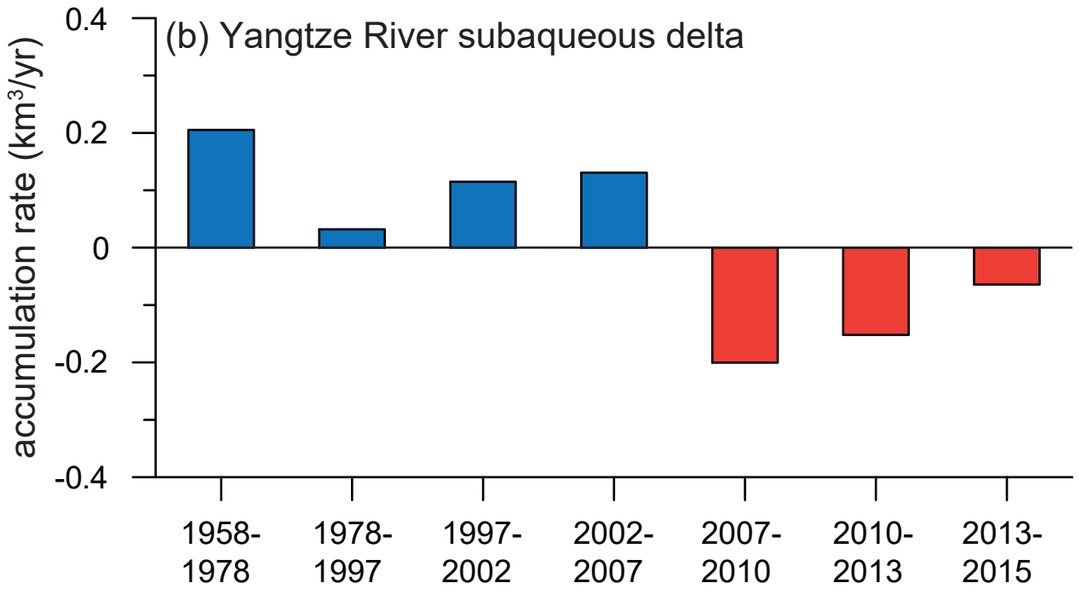
(b) Yangtze River subaqueous delta
accumulation rate (km³/yr)
0.4
0.2
0
-0.2
-0.4
1958-1978
1978-1997
1997-2002
2002-2007
2007-2010
2010-2013
2013-2015

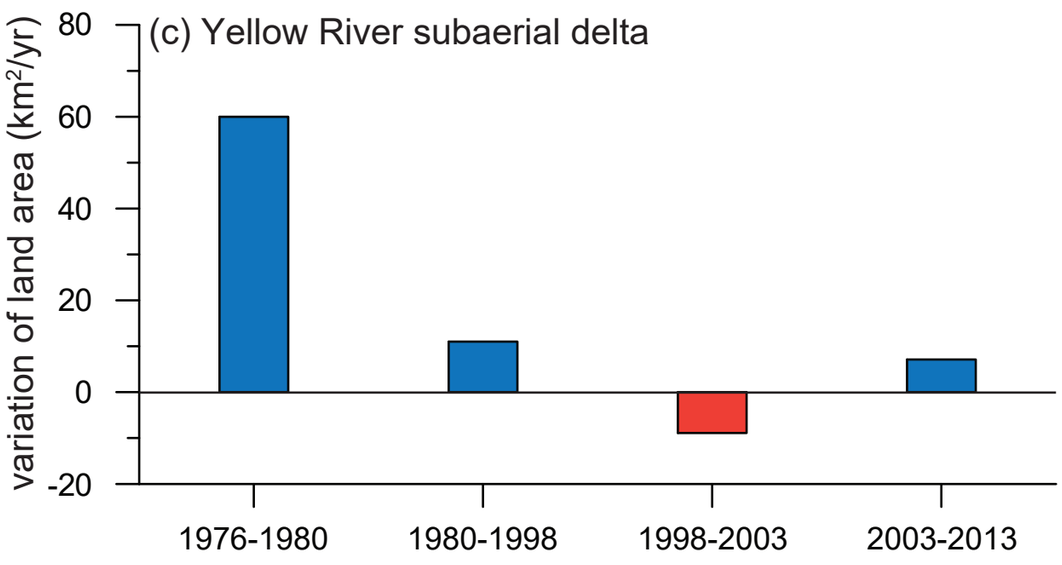
(c) Yellow River subaerial delta
variation of land area (km²/yr)
80
60
40
20
0
-20
1976-1980
1980-1998
1998-2003
2003-2013

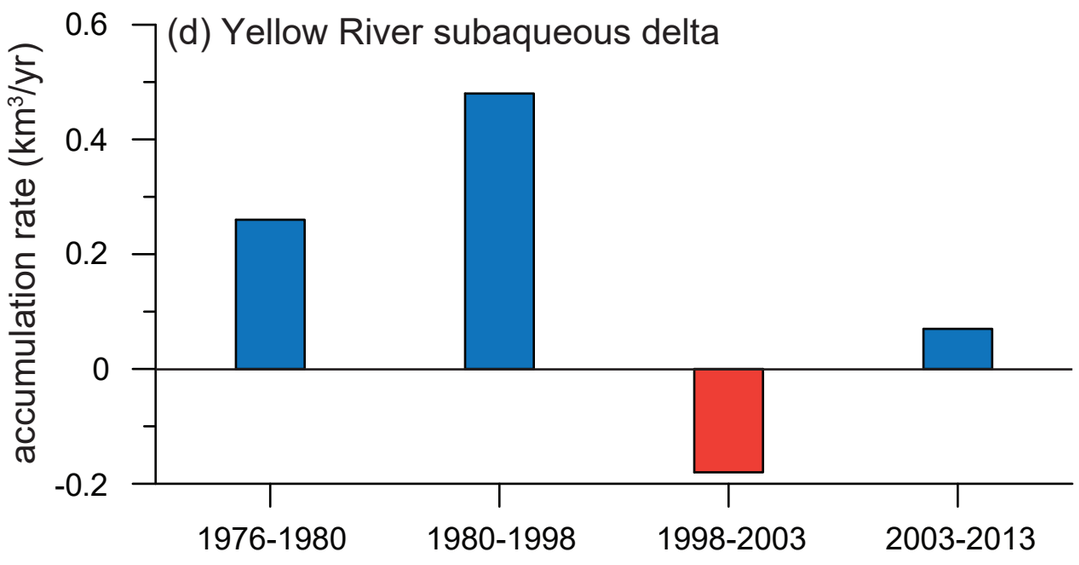
(d) Yellow River subaqueous delta
accumulation rate (km³/yr)
0.6
0.4
0.2
0
-0.2
1976-1980
1980-1998
1998-2003
2003-2013

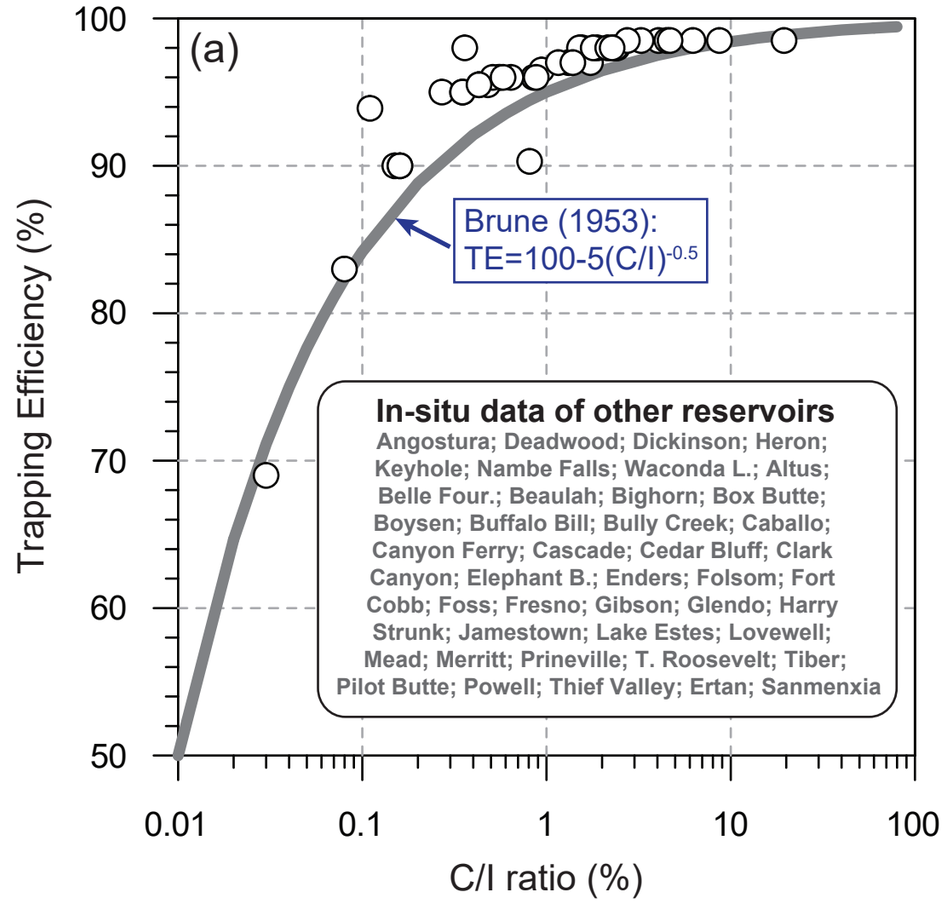
(a)
Trapping Efficiency (%)
C/I ratio (%)
Brune (1953):
TE=100-5(C/I)-0.5
In-situ data of other reservoirs
Angostura; Deadwood; Dickinson; Heron; Keyhole; Nambe Falls; Waconda L.; Altus; Belle Four.; Beaulah; Bighorn; Box Butte; Boysen; Buffalo Bill; Bully Creek; Caballo; Canyon Ferry; Cascade; Cedar Bluff; Clark Canyon; Elephant B.; Enders; Folsom; Fort Cobb; Foss; Fresno; Gibson; Glendo; Harry Strunk; Jamestown; Lake Estes; Lovewell; Mead; Merritt; Prineville; T. Roosevelt; Tiber; Pilot Butte; Powell; Thief Valley; Ertan; Sanmenxia

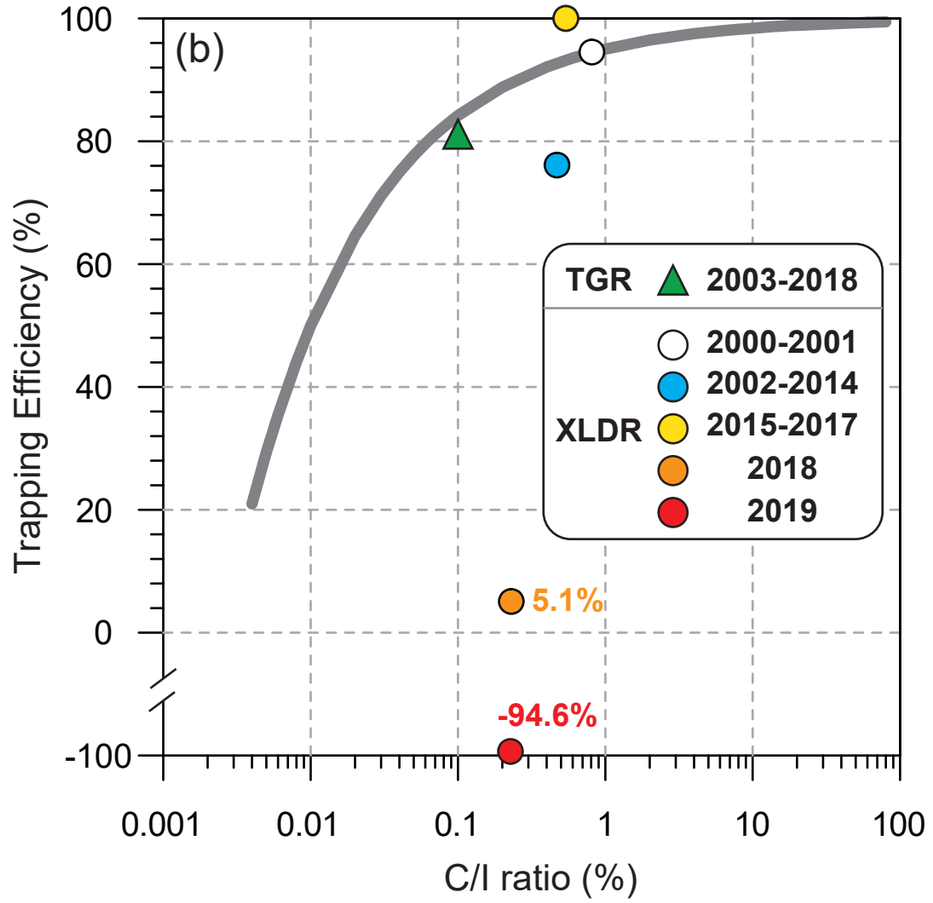
(b)
Trapping Efficiency (%)
C/I ratio (%)
TGR
2003-2018
2000-2001
2002-2014
XLDR
2015-2017
2018
2019
5.1%
-94.6%